FACTS device modelling in the harmonic domain

Christopher Donald Collins

A thesis presented for the degree of
Doctor of Philosophy
in
Electrical and Electronic Engineering
at the
University of Canterbury,
Christchurch, New Zealand.

April 2006

ABSTRACT

This thesis describes a novel harmonic domain approach for assessing the steady state performance of Flexible AC Transmission System (FACTS) devices. Existing harmonic analysis techniques are reviewed and used as the basis for a novel iterative harmonic domain model for PWM FACTS devices. The unified Newton formulation adopted uses a combination of positive frequency real valued harmonic and three-phase fundamental frequency power-flow mismatches to characterise a PWM converter system. A dc side mismatch formulation is employed in order to reduce the solution size, something only possible because of the hard switched nature of PWM converters. This computationally efficient formulation permits the study of generalised systems containing multiple FACTS devices.

This modular PWM converter block is applied to series, shunt and multi-converter FACTS topologies, with a variety of basic control schemes. Using a three-phase power-flow initialisation and a fixed harmonic Jacobian provides robust convergence to a solution consistent with time domain simulation. By including the power-flow variables in the full harmonic solution the model avoids unnecessary assumptions regarding a fixed (or linearised) operating point, fully modelling system imbalance and the associated non-characteristic harmonics.

The capability of the proposed technique is illustrated by considering a range of harmonic interaction mechanisms, both within and between FACTS devices. In particular, the impact of transmission network modelling and operating point variation is investigated with reference to ac and dc side harmonic interaction. The minor role harmonic distortion and over-modulation play in the PWM switching process is finally considered with reference to the associated reduction in system linearity.

ACKNOWLEDGEMENTS

The completion of this thesis marks the end of a major portion of my life, and at this stage I would like to acknowledge those people who have played an important part in my time at the University of Canterbury.

Firstly, I would like to thank my supervisors Associate Professor Neville Watson and Dr Alan Wood for their support, advice and encouragement. Thank you Neville, you and your family have been a real blessing. Alan, what would I have done without those quick questions which inevitably turned into afternoon long discussions, many thanks. A special thanks must also go to Dr Graeme Bathurst, for his patient correspondence and assistance early on in this research.

My thanks also goes to all my colleagues in Room 310 for their friendship and refreshing conversation over the past three years; Dr Dave Hume, Dr Yonghe Liu, Dr Zaid Mohamed, Dr John Schonberger, Geoff Love, Kent Yu, Bernard Perera, Suman Poudel, Dave Rentoul, Cynthia Liu, Jiak San Tan, Nikki Newham and Simon Bell.

Finally, I would like to acknowledge the financial support I received through the University of Canterbury Doctoral Scholarship, and Transpower NZ (Ltd).

CONTENTS

LIST OF FIGURES

LIST OF TABLES

GLOSSARY

Abbreviations

CSC	Current Sourced Converter
DVR	Dynamic Voltage Restorer
EMTDC	Electro Magnetic Transient Direct Current
FACTS	Flexible AC Transmission Systems
FFT	Fast Fourier Transform
GTO	Gate Turn Off thyristor
Hard Switched	Self-commutated
HDA	Harmonic Domain Analysis
HP	High Pass
HVdc	High Voltage direct current
IGBT	Insulated Gate Bi-polar Transistor
IGCT	Integrated Gate Commutated Thyristor
IPFC	Inter-line Power Flow Controller
PCC	Point of Common Coupling
PLL	Phase Locked Loop
PI	Proportional-Integral controller
PQ	Power-flow busbar where the real and reactive power are specified
PSCAD	Power System Computer Aided Design - interface for EMTDC
pu	per-unit
PV	Power-flow busbar where the real power and voltage magnitude are specified
PWM	Pulse Width Modulation
RLC	Resistance,Inductance and Capacitance network
SSSC	Static Synchronous Series Compensator
SVC	Static Var Compensator
STATCOM	Static Compensator
TCR	Thyristor Controlled Reactor
TCSC	Thyristor Controlled Series Capacitor
THD	Total Harmonic Distortion
UPFC	Unified Power Flow Controller

VSC	Voltage Sourced Converter

Notation (where X is a generic variable or quantity)

$[X]$	Matrix form of X
$\mathbf{X}$	Vector form of X
$\Re\{X\}$	Real part of X
$\Im\{X\}$	Imaginary part of X
X^T	Matrix transpose of X
X^*	Conjugate of X
$\|X\|$, $\angle X$	Magnitude, angle of X
ΔX	Change in X
$W \otimes X$	W convolved with X in the frequency domain
$X_{a/b/c}$	Phase $a/b/c$ quantity
X_+	Positive frequency phasor or Positive sequence component
X_-	Negative frequency phasor or Negative sequence component
X_0	Zero sequence component
X_{0Hz}	dc term
$X_{ac/dc}$	ac/dc quantity
$X_{d/q}$	d/q-axis quantity
$X_{pri/sec}$	Primary/secondary transformer quantity
$X_{se/sh}$	Variable refers to the series/shunt converter
X^{Sch}	Scheduled value of X
Y, Z	Admittance, impedance
V, I	Voltage, current

Symbols

C	dc side Capacitor
h,k	h^{th},k^{th} harmonic
j	Complex operator
J_i	Jacobian at iteration i
m_{dc}	dc component of the modulation index
$m_{1:nh}$	Ripple component of the distorted modulation index
$M(X)$	Mismatch vector or distorted Modulating index at angle X
nh	Highest harmonic of interest
N_p	Number of PWM pulses
P	Real power
Q	Imaginary power

R_{dc}	dc side resistor used to approximate converters losses
S	Positive frequency PWM switching spectrum
S_{node}	Power at a node, $S = P + jQ$
V_{conv}	ac converter terminal voltage (three-phase)
X_i	Solution variables at the i^{th} iteration
X_{Con}	Harmonic control variables
X_{Harm}	Harmonic solution variables (electrical)
X_{PF}	Power-flow variables
α_{dc}	dc component of the PWM phase angle
$\alpha_{1:nh}$	Ripple component of the PWM phase angle
α,β	Modulating angle for a shunt/series connected converter
δ	Fundamental frequency voltage angle
θ	Fundamental frequency current angle
ψ	PWM switching instant
$\psi_{ON/OFF}$	Vector of on/off PWM switching instants

Chapter 1

INTRODUCTION

1.1 GENERAL

The increasing prevalence of Flexible AC Transmission System (FACTS) devices reflects the modern power market and prevailing regulatory environment, an environment focused on increasing levels of plant utilisation. The control capabilities inherent to FACTS devices can help facilitate this increased utilisation of existing transmission networks, providing an attractive alternative to transmission system upgrades. FACTS devices derive this enhanced controllability using switching converters, which in addition to providing a controllable interface act as both a source and modulator of harmonic distortion.

FACTS devices are therefore in essence both a part of the power quality problem and a part of its solution. They provide the control capability necessary to solve transient and steady-state voltage stability issues while introducing steady-state waveform distortion. Distortion which in turn propagates through the power system has an adverse impact on losses, telecommunication interference, filter and machine over-heating, and increased current levels.

Computer simulation plays an important role both in evaluating this distortion, and mitigating any impact on power quality. However, the distributed nature of FACTS devices and the associated interaction with other system components makes accurate system level modelling difficult. Primarily, the models need to incorporate a full representation of the non-linear time-variant converters, without compromising on the scale and complexity of the system representation. This thesis details the development of an efficient analysis technique for steady-state PWM distortion which balances solution speed and accuracy.

1.2 THESIS OBJECTIVES

To date research into harmonic domain techniques for modelling waveform distortion has focused on low pulse number line commutated devices; however the harmonic domain is equally applicable to more advanced switching topologies with higher switching frequencies. Undertaking system level harmonic domain analysis of FACTS devices containing these advanced topologies is the primary focus of this thesis.

From a harmonic perspective, hard switched PWM converters are a simple extension of line commutated converters. The lack of commutation permitting significant simplifications to the solution framework. This thesis details one such framework, tailored to provide an efficient modular solution for hard switched converters. Integral to this objective is the application and validation of this technique for a variety of series, shunt and hybrid connected FACTS devices.

While numerous authors have presented individual FACTS models, comprehensive system level studies involving the interaction of multiple FACTS devices have not yet been undertaken. Investigating these phenomena forms the secondary objective for this thesis. The investigation will focus on the relationship between these interactions and the system operating point, imbalance, phase coupling and frequency dependence; with the aim of assessing both the impact of multiple FACTS devices and what type of harmonic assessment techniques are most appropriate.

1.3 THESIS OUTLINE

Chapter 2 provides a brief review of existing harmonic simulation techniques and FACTS device technology. The applicability of these harmonic analysis techniques to FACTS devices is then assessed before the models specifications, necessary to undertake accurate simulation, are finally detailed.

Chapter 3 describes the harmonic domain model used to characterise single level PWM FACTS devices. This representation is based around the switching converter transfers which are characterised using a positive frequency convolutional approach. The modular converter representation is used in conjunction with control blocks and a linear system representation to provide a thorough and versatile model, which can be applied to a range of FACTS connection topologies (including multi-converter devices).

Chapter 4 outlines how the harmonic domain models presented in Chapter 3 can be applied to a unified iterative Newton solution. First the choice of solution variables is discussed, before the associated mismatch equations are formulated as a function of these variables. While these mismatches can be broadly divided into those associated with the power-flow (operating point) or the harmonic solution, they do no act in isolation. The coupling being incorporated within the unified system Jacobian; the derivation and structure of which is also considered.

Chapter 5 presents the MATLAB implementation and the validation of the proposed model. The chapter compares the results obtained for a 5-busbar test system containing two FACTS devices with a commercial time domain simulation package, PSCAD/EMTDC. The convergence characteristics and Jacobian properties are also considered with reference to solution speed and FACTS device interaction. Finally the relationship between the linear harmonic solution and the non-linear operating point is discussed.

Chapter 6 develops more advanced test systems which highlight the principle mechanisms for ac and dc side harmonic interaction. To undertake ac side interaction studies the 5-busbar test system is adjusted to incorporate transmission system imbalance, phase coupling and frequency

dependence. Further for dc side analysis, the Static Synchronous Series Compensator (SSSC) and Static Compensator (STATCOM) are migrated together to form a Unified Power Flow Controller (UPFC). Both cases take advantage of the explicit inclusion of harmonic couplings in the solution, which allows device interaction to be visualised with the system Jacobian.

Chapter 7 considers the important role FACTS device control systems play in the harmonic solution; both in terms of the operating point and the transfer of harmonic distortion through the controller. This type of switching instant variation is the major source of converter non-linearity, and the principle reason why a non-linear formulation is adopted.

Chapter 8 summarises the research described by this thesis. The capability and limitations of the proposed model are considered, before possible extensions and the future direction of this research are discussed.

Chapter 2

HARMONIC SOLUTION TECHNIQUES AND THEIR APPLICABILITY TO FACTS DEVICES

2.1 INTRODUCTION

The generation, propagation and modelling of non-power frequency currents within power systems has been, and continues to be, a topic of significant research. Traditionally this research has focused on line commutated power converters, the largest source of harmonic currents, however a variety of other harmonic sources do exist in modern power systems. Of particular interest is the proliferation of smaller hard switched converters using advanced switching topologies, a more recent focus of harmonic analysis research.

Both converter types can, under idealised operating conditions, be described using classic closed form equations based on Fourier analysis Kimbark[1], Arrillaga[2] and Mohan[3]. The resulting integer harmonics are classed as characteristic harmonics; these harmonics, whilst dominant, are unfortunately not alone as idealised conditions rarely prevail. The presence of transmission network asymmetry, saturated transformers, synchronous and induction machines all impact on converter performance, leading to the generation of additional non-characteristic integer harmonics.

The presence of these non-ideal phenomena limits the applicability of simplistic closed form representations, therefore numerous harmonic techniques have been proposed to account for these effects. These converter representations, which range in both complexity and efficiency, can be divided into two general categories:

1. Time Domain techniques; while often thorough, are computationally intensive and must approximate the frequency dependence of the ac network.

2. Harmonic (or frequency) domain techniques; these offer a concise (and hence efficient) steady-state representation, yet often use linear approximations, and simplistic control representations.

2.2 HARMONIC ANALYSIS TECHNIQUES

2.2.1 Time domain techniques

Well established time domain modelling techniques, using numerical integration of differential equations (Dommel [4] and Woodford [5]) are by their nature very applicable to time variant converter systems. These techniques, which are widely available in general purpose software packages, are used extensively for power system analysis. While typically employed for transient simulation these techniques can be used to perform harmonic analysis. This is undertaken by simulating until a steady-state operating point is reached and then using the Fourier transform to obtain the frequency domain components. The practicability of this technique is limited by the computational effort required to reach an accurate steady-state operating point. Switching converters combine very long and very short time constants, resulting in a 'stiff' system which necessitates short time-step long run simulations, increasing the computational burden of finding a steady-state operating point. Methods involving boundary problem analysis [6] have been developed to accelerate this convergence to the steady-state solution.

Time domain techniques typically incorporate modular control blocks, capable of easily and accurately incorporating a variety of control schemes, making time domain simulation particularly suited to control and transient studies. In contrast the limitations of time domain simulation become apparent when considering system-wide power quality issues, which require more than idealised system equivalents. Realistic system equivalents need to account for the frequency dependence of generators, transformers, transmission lines and loads. While this is feasible in the time domain, take for example the accurate transmission line representation used in PSCAD/EMTDC [7], the present lack of appropriate harmonic models for generators, transformers and loads limit the harmonic modelling capability of the time domain. Even if appropriate models are available their inclusion further degrades computational efficiency, making the simulation of large systems difficult. Alternative methods involving the reduction of large systems to a series of equivalent RLC branches [8] also exist, providing a more efficient (yet less direct) alternative.

2.2.2 Harmonic domain techniques

The harmonic (or frequency) domain, in contrast to time domain techniques, is by definition a steady-state form of harmonic analysis based on representing converters in terms of their harmonic spectra. Converters are therefore viewed as harmonic modulators, the transfers characteristic of which can be defined using a range of techniques based on Fourier analysis [9]. The resultant models having a broader scope and significantly improved efficiency when compared with equivalent time domain techniques.

Further, the harmonic domain has the advantage of being capable of easily accommodating frequency dependent components in the system admittance. A range of harmonic domain equiv-

alents already existing for common system components. The harmonic domain does not however to date have the modular control blocks which are available to time domain techniques. While this type of analysis is not precluded from the harmonic domain, it is more difficult and less intuitive than the time domain equivalent.

A large number of harmonic domain converter models have been presented in literature, these models being broadly divisible into two groups: iterative non-linear formulations, and linearised approaches. Both approaches have been shown to provide satisfactory results given their respective limitations are taken into account. The difference between the two techniques is best illustrated for HVdc systems. These converters while being non-linear and time-variant exhibit a linear harmonic transfer characteristics in the absence of control or commutation variation [10]. The merits of both techniques are immediately apparent, linearised techniques taking advantage of an approximately fixed operating point to provide a fast solution, while iterative techniques compromise speed in order to fully model small operating point variations and the associated non-linearity. The situation for hard-switched PWM converter models is similar, with the exception of the lack of commutation which makes all harmonic domain non-linearity a function of the operating point.

Harmonic phasor transfers

The frequency coupling and phase dependence inherent to switching converters is best illustrated by considering the modulation of a sinusoidal quantity by a converter. This is the dual of multiplying two sinusoids in the time domain and results in the generation of sum and difference frequencies. The summed frequency terms having a phase angle directly related to the phase angle of the modulating signal, while the difference frequencies phase is related to the conjugate of the modulating signal:

$$\sin\left(m\omega_0 t+\delta_m\right)\sin\left(n\omega_0 t+\partial_n\right)=\frac{1}{2}\underbrace{\cos\left[\left(m-n\right)\omega_0 t+\delta_m-\delta_n\right]}_{conjugated}-\frac{1}{2}\underbrace{\cos\left[\left(m+n\right)\omega_0 t+\delta_m+\delta_n\right]}_{direct} \tag{2.1}$$

This frequency coupling and phase angle dependence can be modelled using a matrix, where each element corresponds to a linear frequency transfer between two electrical quantities (each of which is represented by a harmonic phasor containing Fourier series coefficients). When applied to non-linear analysis this transfer matrix is incorporated within the Jacobian matrix (the linearisation used to update variables within an iterative Newton solution), whereas for linearised analysis it is typically referred to as the frequency (or harmonic) coupling (or transfer) matrix.

Either way the harmonic transfers should account for the phase angle dependence of the conjugated (difference frequency) terms [10, 11]. This dependence requires the inclusion of the

conjugated negative frequency terms, leading to the common complex conjugate notation [12],

$$\begin{bmatrix} \Delta I_+ \\ \Delta I_- \end{bmatrix} = \begin{bmatrix} Y_1 & Y_2 \\ Y_1^* & Y_2^* \end{bmatrix} \begin{bmatrix} \Delta V_+ \\ \Delta V_- \end{bmatrix} \tag{2.2}$$

since $I_- = I_+^*$ for a real valued waveform [13], this can be re-written using complex positive frequency phasors as:

$$\Delta I_+ = Y_1 \Delta V_+ + Y_2 \Delta V_+^* \tag{2.3}$$

Which when decomposed into real and imaginary components this yields,

$$I_r + jI_i = (Y_{1r} + jY_{1i})(V_r + jV_i) + (Y_{2r} + jY_{2i})(V_r - jV_i) \tag{2.4}$$

$$I_r = (Y_{1r}V_r - Y_{1i}V_i) + (Y_{2r}V_r + Y_{2i}V_i) \tag{2.5}$$

$$I_i = (Y_{1r}V_i + Y_{1i}V_r) + (-Y_{2r}V_i + Y_{2i}V_r) \tag{2.6}$$

or in matrix form:

$$\begin{bmatrix} \Delta I_r \\ \Delta I_i \end{bmatrix} = \begin{bmatrix} Y_{1r} + Y_{2r} & Y_{2i} - Y_{1i} \\ Y_{1i} + Y_{2i} & Y_{1r} - Y_{2r} \end{bmatrix} \begin{bmatrix} \Delta V_r \\ \Delta V_i \end{bmatrix} \tag{2.7}$$

This positive frequency real valued tensor linearisation (Equation 2.7) was used by Smith [10] as a computationally efficient equivalent of the complex conjugate notation (Equation 2.2). While the positive frequency real valued decomposition is equivalent to complex conjugate notation, it is less elegant. The resultant harmonic linearisation is no longer a Toeplitz matrix, but rather has a lattice structure where the reverse diagonal components correspond to the negative frequency conjugated terms.

Direct / linearised harmonic analysis

The most basic application of harmonic phasor analysis is direct harmonic analysis, where harmonic current injections are assumed to be independent of the terminal conditions at the non-linear device. This technique uses the operating point, generated with a power-flow, to calculate fixed harmonic current injections using a simplified closed form harmonic model. The resultant injections propagate through the system admittance, allowing a direct solution according to:

$$[I_{node}] = [Y_{sys}]\,[V_{node}] \tag{2.8}$$

This technique represents the converter as a fixed harmonic current source (Figure 2.1(a)), ignoring both operating point and terminal voltage variation. An improvement on this technique is the incorporation of a linearisation of the converter impedance and harmonic transfers. This leads to either a Norton or Thevenin representation (Figure 2.1(b) and 2.1(c)). Linearised models have been proposed for both line commutated and hard switched devices, these models being either experimentally [14] or analytically derived [15]-[20] and ranging in complexity from

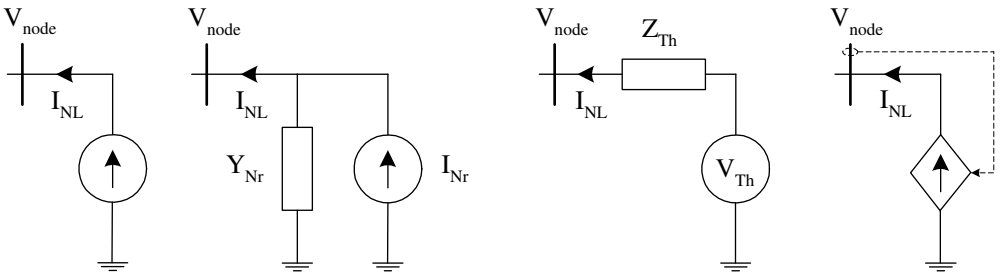

(a) Ideal current source

(b) Norton equivalent

(c) Thevenin Equivalent

(d) Dependant current source

Figure 2.1 Non-linear device representations

methods which ignore the impact of control schemes through to thorough models incorporating small signal firing and commutation angle variation. Nonetheless the accuracy of these schemes is limited by the assumption of a fixed operating point, unaffected by harmonic distortion. These techniques are not the focus of this thesis.

Iterative techniques

The presence of harmonic current injections in a non-ideal power system leads to the generation of harmonic voltage distortion. If the harmonic current injections are non-linearly sensitive to this voltage distortion then an iterative solution is required for accurate harmonic assessment. Two iterative techniques are predominantly used in the literature for this type of analysis: Gauss-Seidel (fixed point iteration) and the Newton method.

The first reported application of the Gauss-Seidel (or fixed point) iterative technique to harmonic analysis was for an HVdc converter by Reeve and Baron [21]. This technique used the present estimate of the nodal voltages (V_{node_i}) to calculate the harmonic current injections (I_{NL_i}), which are then applied to the system admittance (Y_{sys}) to provide a new estimate of the nodal voltages ($V_{node_{i+1}}$). This can be stated mathematically as:

$$I_{NL_i} = f\left(V_{node_i}\right) \tag{2.9}$$

$$V_{node_{i+1}} = \left[Y_{sys}\right]^{-1} I_{NL_i} \tag{2.10}$$

The technique was further developed by Yacamini [22] and Eggleston [23], the critical convergence difficulties being addressed by Callaghan [24], who reported that the techniques' poor convergence properties in highly distorted systems could be improved by including the converter linearisation in the nodal analysis. This was achieved using a Norton equivalent circuit (Figure 2.1(b)) rather than an ideal current source representation (Figure 2.1(a)). This principle has since been extended to include matched reactance pairs by Carbone [25] and Carpinelli [26].

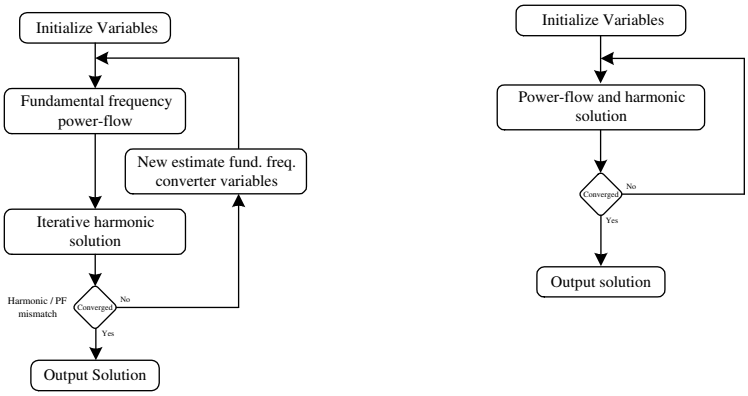

(a) Sequential (b) Simultaneous

Figure 2.2 Iterative Newton solutions

The alternative Newton technique, first used in a single-phase harmonic solution by Heydt [27], characterises the system using a mismatch between the converter currents (I_{NL_i}) and system nodal currents (I_{node_i}). The resulting mismatch (M_i) is then used in conjunction with a system Jacobian (J_i) to update the nodal voltages (ΔV_{node_i}) such that the mismatch vector tends to zero, and convergence is achieved:

$$I_{NL_i} = f\left(V_{node_i}\right) \tag{2.11}$$

$$I_{node_i} = \left[Y_{sys}\right] V_{node_i} \tag{2.12}$$

$$M_i = I_{NL_i} - I_{node_i} = \left[J_i\right] \Delta V_{node_i} \tag{2.13}$$

$$V_{node_{i+1}} = V_{node_i} - \Delta V_{node_i} \tag{2.14}$$

Acha [11] developed a three-phase non-linear transformer model using this solution technique. The model used Norton equivalents and the complex conjugate harmonic formulation, the resulting solution technique was named Harmonic Domain Analysis. This type of analysis has been subsequently developed to model a Thyristor Controlled Reactor (TCR) [28, 29] and more advanced transformer configurations [30, 31, 32]. This complex variable formulation does however lead to difficulties integrating control and power-flow components to the harmonic model, leading to the use of sequential or double iterative techniques [32]. Double iterative referring to use of two iterative solutions, one for the operating point and another for the harmonic solution nested inside a mismatch between the two solutions (Figure 2.2(a)). This type of analysis was also proposed by Valcarcel and Mayordomo for unbalanced converter systems [33].

However, if a full Newton solution is desired the non-linearity of the harmonic device must be linearised and incorporated within the power-flow loop, and vice versa. This is not necessarily trivial and can be avoided by using a unified or simultaneous solution (Figure 2.2(b)). Smith [10] achieved this for a 12-pulse HVdc rectifier using real valued positive frequency harmonic analysis. The model representing non-linear harmonic sources with dependent current sources

(Figure 2.1(d)), which is mathematically equivalent to using Norton equivalent given a Newton solution [34]. This simultaneous solution technique was extended by Dinh [35] to unit connected HVdc rectifiers, and then further by Bathurst [34] who internalised the solution of converter switching angles, making the model significantly more modular.

2.2.3 Extended harmonic analysis

A recent trend in harmonic research blurs the classical distinction between steady-state and transient analysis by incorporating time varying 'dynamic' harmonic phasors. This principle, first proposed for resonant power electronic studies by Sanders [36], describes time-domain electrical quantities using a time variant Fourier series of the form:

$$x(\tau) = \sum_{k=-\infty}^{\infty} X_k(t)\, e^{jk\omega_s\tau} \tag{2.15}$$

Where $X_k(t)$ are the time evolving Fourier series components calculated by passing a sliding window (of period T) over the time domain waveform $x(\tau)$. The k^{th} coefficient is calculated using the 'averaging' method:

$$X_k(t) = \frac{1}{T}\int_{t-T}^{t} x(\tau) e^{-jk\omega_s\tau} d\tau \tag{2.16}$$

This principle has been extended to multi-phase systems, an example being the Thyristor Controlled Series Capacitor (TCSC) and UPFC models proposed by Stankovic [37]. These models use the averaging approach to calculate the fundamental frequency Fourier coefficients, which are then applied to transient analysis. Given the assumption that ac and dc quantities can be represented by fundamental frequency or dc coefficients respectively it is somewhat questionable whether this type of analysis is truly harmonic. However Rico [38] has used the same principle in conjunction with PWM switching functions to represent a STATCOM in isolation excluding operating point variation. The resultant state space, coined the extended harmonic domain or the harmonic state space, being capable of both transient and steady-state analysis. Given the aim of investigating steady-state device interaction, this type of analysis is not the focus of this thesis.

2.3 APPLICABILITY TO FACTS DEVICES

While harmonic analysis techniques have matured significantly, there still exists a major bias toward line commutated converters, and relatively small simplified test systems. The distributed nature of FACTS devices and the move towards higher switching frequencies challenges this bias. This thesis extends detailed steady-state harmonic analysis to systems containing multiple PWM FACTS devices.

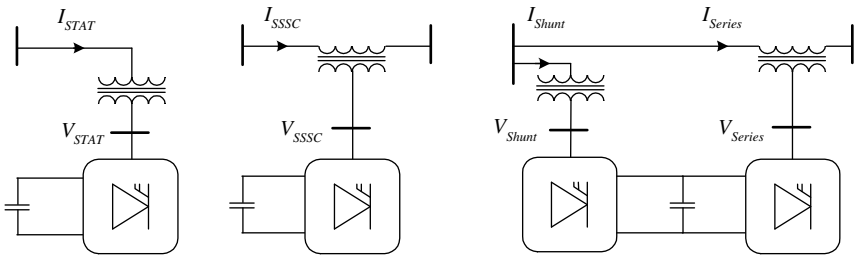

(a) STATCOM (b) SSSC (c) UPFC

Figure 2.3 VSC FACTS devices under consideration

2.3.1 FACTS devices

The term FACTS, first coined by Hingorani [39, 40, 41], refers to the application of switching converters to increase the flexibility of traditional power system equipment. This is achieved by using switching converters as a controllable interface between two power system terminals. A variety of combinations using this principle exist, providing a wide range of compensation and control possibilities. Early devices were based on line commutated switching topologies (Static Var Compensator (SVC) and TCSC) providing limited control flexibility, more advanced systems (STATCOM, SSSC, Dynamic Voltage Regulator (DVR), UPFC and Interline Power Flow Controller (IPFC)) being based on the turn off capability of modern semiconductor switches, which provides enhanced control capabilities.

The analysis described in this thesis is focused on FACTS devices containing hard-switched PWM bridges, the resulting converter representation being applicable to a variety of connection configurations. These are typically voltage sourced converters using some form of dc voltage source (typically a capacitor) to provide a variable ac voltage source which is capable of both steady-state reactive power compensation and transient real/reactive power compensation. Three common connection configurations are considered: shunt, series and hybrid. Examples of these are shown in Figure 2.3.

2.3.2 Harmonic modelling of FACTS devices

A large variety of analysis techniques have been proposed to analyze FACTS devices. The vast majority of these models concentrate on transient behaviour using time domain techniques [42]-[49], these have limited applicability to harmonic analysis. Of the harmonic domain models proposed, the most thorough have been developed for low pulse number converters: Ricos' Newton based TCR model [28], further developed by Lima [29], and Woods' linearised STATCOM [50] are good examples.

While harmonic domain models for PWM FACTS devices do exist they are focused on taking advantage of the entirely linear harmonic transfer characteristic of hard switched converters.

Madrigal [19] for example assumes a fixed operating point (specified separately in a power-flow) and then uses a linearised Thevenin equivalent to model a single level PWM STATCOM. Likewise, for the unbalanced PWM model proposed by Saniter [20] which has subsequently been developed to include linearised firing instant variation [51], yet still depends on an externally specified operating point. In essence existing work has concentrated on the near linear aspects of PWM behaviour, rather than the operating point which is the most significant source of non-linearity.

In contrast iterative techniques can incorporate operating point variation and the interaction between the harmonic and fundamental frequency solutions, maintaining generality. The cost being a loss in computational efficiency, the magnitude of which is minimised if the Jacobian is not recalculated.

2.3.3 Model specification

This thesis details a novel extension to the iterative harmonic solution framework proposed by Smith [10]; first for individual shunt/series FACTS devices and then to multiple converter systems. The aim is a comprehensive steady-state analysis technique for FACTS devices, the associated controllers and system components. To achieve this a generalised formulation capable of considering the likely harmonic generation mechanisms is proposed, as detailed below:

1. Iterative: A non-linear representation avoids unnecessary assumptions regarding the operating point, making the model capable of analyzing heavily distorted systems where the harmonic and fundamental frequency solutions are not isolated.

2. Three-phase: Since system unbalance is the primary cause of non-characteristic harmonic distortion a three-phase formulation is critical.

3. Robust and efficient: A unified Newton is specified in order to provide reliable and efficient convergence, a requirement for realistically sized test systems.

4. Modular: By maintaining a modular structure for the PWM converter, the model will be capable of being reconfigured for a range of FACTS devices:

   (a) Shunt: STATCOM

   (b) Series: SSSC, DVR

   (c) Hybrid: UPFC, IPFC

5. Scalable: In order to understand the impact of having multiple FACTS devices interacting with each other the model must be scalable to larger more complex systems.

6. Control aspects: Harmonic generation is heavily dependent on the operating point of the converter, as such the model should consider both the operating point, and the impact harmonics have on this operating point.

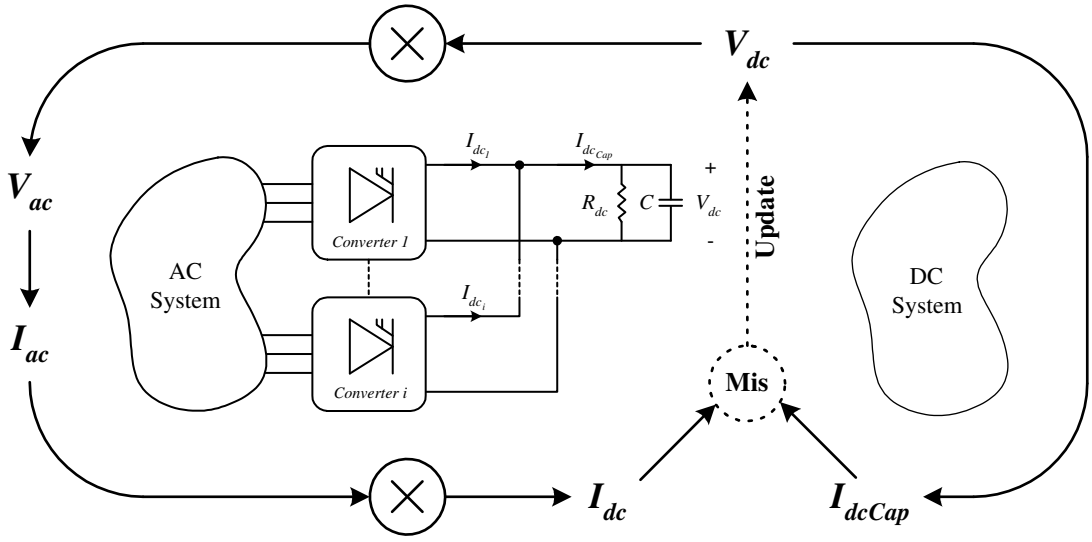

Figure 2.4 A diagrammatic overview of the proposed iterative solution technique

7. Realistic test systems: For full analysis of FACTS devices it is necessary to realistically model the remainder of the system. Therefore the formulation should be capable of including models of relevant system components, any phase coupling and non-linear frequency dependence.

2.3.4 Model summary

This specification is satisfied by the iterative solution outlined in Figure 2.4. Given the hard switched nature of PWM devices each converter can be characterised (at harmonic frequencies) using a single terminal quantity, in this case the dc voltage harmonics. This quantity is initially estimated and then iteratively updated via a dc current mismatch until convergence is achieved. The component models and the associated mismatches are described in two steps; first Chapter 3 develops the appropriate harmonic domain models, before Chapter 4 focuses on the application of these models to a Newton solution. The resultant technique uses convolution ($\otimes$ in Figure 2.4) to describe the $ac \leftrightarrow dc$ harmonic transfers for each converter. These transfers form the basis of the dc current mismatch, which concisely characterises PWM FACTS devices in the harmonic domain.

Chapter 3

FACTS DEVICE MODELLING IN THE HARMONIC DOMAIN

3.1 INTRODUCTION

The control capabilities which FACTS devices possess are primarily derived from the switching converters they are based on. This controllable interface, in addition to providing fundamental frequency and transient control, acts as both a source and modulator of harmonic distortion. The PWM converter and the associated control block are therefore the central component of any FACTS device harmonic representation. Since these blocks couple harmonic frequencies they are naturally non-linear in the time domain. However the extent of this non-linearity is significantly reduced in the harmonic (or frequency) domain [10], making harmonic domain analysis a concise solution format.

Chapter 3 outlines how FACTS devices can be represented in the harmonic domain, describing the hard switched converter transfers (Section 3.2), the connection configuration (Section 3.3) and the associated control scheme (Section 3.4). These components define an isolated FACTS device at harmonic frequencies. Finally, in order to permit the generalised harmonic domain modelling of systems containing multiple FACTS devices, these representations are combined with a linear network equivalent (Section 3.5).

These harmonic domain models form the basis of non-linear solution proposed in Chapter 4. The proposed formulation integrates the near linear PWM harmonic transfers with a power-flow model describing the operating point. To achieve this the PWM transfer model proposed in this Chapter is reformulated into fundamental and harmonic frequency mismatches, which are then solved using an iterative Newton solution.

3.1.1 Underlying assumptions and definitions

In order to derive the harmonic domain PWM model the following assumptions / definitions have been made:

Phase angle reference: Given the complex nature of the electrical quantities represented it is necessary to define an arbitrary phase reference. This reference would typically be derived from an ac terminal quantity (using a phase locked loop, PLL); however given the assumption

of a perfect PLL this reference can be placed anywhere within the system. The slack generator busbar has therefore been defined as the zero angle reference, all firing angles being described relative to this reference point. This does not preclude full analysis of the PLL, whose error could be linearised or incorporated as an additional term in the switching instant solution.

Harmonic phasors: Complex valued positive frequency harmonic phasors have been used to define sinusoidally varying quantities within this thesis. The time domain equivalent of these phasors, which rotate in an anti-clockwise direction, are defined as the sine referenced imaginary component.

Network linearity: The harmonic performance of any converter based device is heavily dependant on the ac system to which it is connected, as such the ac network must be represented. However, fully modelling the entire ac network in a non-linear fashion at harmonic frequencies would result in a massive increase in the number of solution variables. In order to maintain an efficient formulation it is advantageous to assume that the ac network behaves in a linear time invariant fashion (at harmonic frequencies), greatly reducing the number of solution variables. This assumption limits coupling between harmonic frequencies to components specified by the mismatch equations.

Idealised switching: The semiconductor switching devices used in the converter bridges are assumed to perform in an ideal fashion, having zero ON state and an infinite OFF state resistance. This simplifies the switching function derivation, while still permitting switching losses to be represented as a component of the series connection impedance.

Per unit system: All power system quantities have been incorporated on a per unit (pu) basis, decreasing the chance of matrix conditioning problems and reducing the internal complexity of the formulation.

3.2 A PWM CONVERTER MODEL

The primary component of any FACTS device is the switching bridge and a wide variety of converter configurations have been proposed to carry out the controllable interface function. These configurations range from simplistic single level line commutated configurations (6, 12 pulse etc.), through single level hard switched PWM, to advanced multi-level multi-switch configurations.

Assuming the devices are hard switched (self-commutated), any arbitrary configuration can be approximated within the harmonic domain using an $ac \leftrightarrow dc$ transfer function which is predominantly a function of the control variables. As such a generic formulation is proposed, this permits a range of converter configurations to be incorporated via the transfer function. For illustrative purposes only the stereotypical six switch three-phase PWM bridge is considered within this thesis (Figure 3.1).

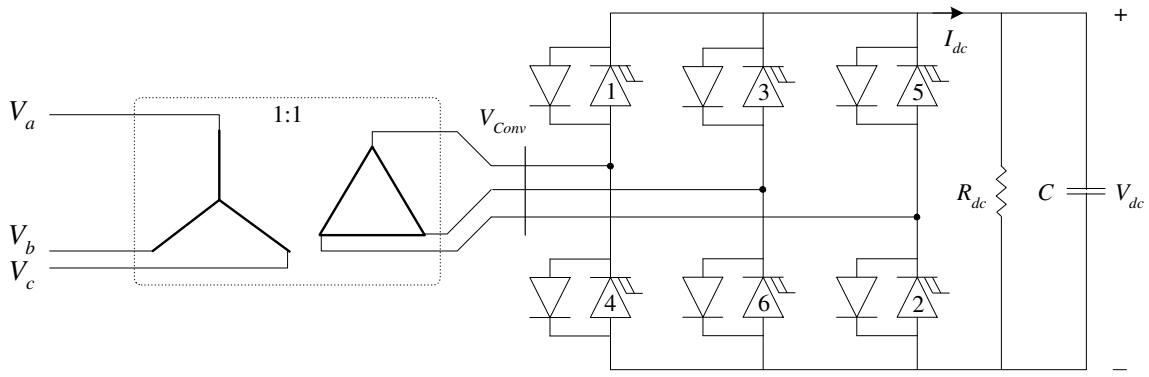

Figure 3.1 A three-phase PWM converter and connection transformer

3.2.1 Ideal PWM transfers by convolution

The convolutional approach proposed by Smith [10] for line commutated devices is equally applicable to hard switched converters. In fact, from a computational perspective, the only difference between a 6-pulse and a PWM waveform is the number of piecewise linear components which need to be summated. As such an arbitrary steady-state waveform can be obtained from a sum of linear expressions, each multiplied by a pulse train (or switching function) corresponding to the period over which they are valid. For a single level PWM converter only one linear expression is required (e.g. the dc voltage or an ac phase current), this expression being multiplied by a pulse train corresponding to each pair of PWM switching instants. The total waveform equating to the summation of these time domain multiplications.

PWM switching instant calculation

The boundaries for these square pulse sampling functions are defined by the PWM modulation scheme used. For simplicity this thesis concentrates on a basic single level PWM control scheme [3], although the principles presented are equally relevant to more advanced control schemes. To facilitate this the proposed solution format internalises the switching instant solution, permitting advanced modulation schemes (selective harmonic elimination, multi-level etc.) to be substituted without affecting the main Newton solution. As a result the main Newton solution uses the control quantities (e.g. the modulation index and angle) as solution variables rather than the switching instants themselves, which are calculated in a separate single variable iterative solution nested within the main loop.

The basic hard switched scheme implemented within this thesis describes the switching instants as the intersection of a triangular carrier (V_{tri}, of frequency f_s) with the modulating sinusoid (of magnitude M and phase angle A)[1]. Under ideal steady state operating conditions the triangular

[1]While the work described in this thesis assumes the modulating sinusoid is an integer multiple of the system

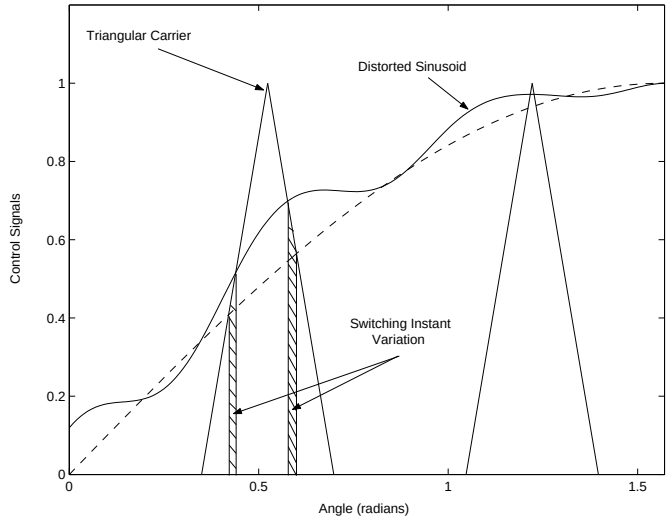

Figure 3.2 Switching instant variation resulting from control signal distortion, in this case modulation index ripple

carrier, typically generated from a PLL, can be assumed to perfectly track the system frequency. Similarly the modulating signal can be assumed to be a fundamental frequency sinusoid. However the presence of harmonic distortion at the point of common coupling (PCC) affects both of these assumptions.

While the PLL is assumed to be immune to harmonic distortion the feedback path is not idealised, hence both control variables (the magnitude, M, and phase, A, of the modulating signals) are represented as distorted harmonic phasor quantities. The ripple on these signals being derived from the transfer through the feedback path, as discussed in Section 3.4. The resultant distorted modulating sinusoid and the ideal triangular carrier define the switching angles, as illustrated in Figure 3.2. Each switching angle (ψ) is solved using a single variable Newton-Raphson formulation,

$$\psi_{(i+1)} = \psi_i - \frac{F(\psi_i)}{\left(\frac{dF(\psi_i)}{d\psi_i}\right)} \tag{3.1}$$

for the i^{th} iterative step, and where the mismatch ($F(\psi)$) is defined in terms of the distorted modulating function and the triangular carrier,

$$F(\psi) = \Im\left\{\left(M(\psi)\angle \mathrm{A}(\psi)\right)\mathrm{e}^{j\psi}\right\} - V_{tri}(\psi) = 0 \tag{3.2}$$

(or base) frequency, the model can be extended to non-harmonic modulating functions. This is achieved by reducing the base frequency (not the system frequency) until the modulating function is a harmonic of the new base frequency. The associated increase in the size of the Jacobian can be minimised by applying the 'adaptive' harmonic analysis techniques proposed by Bathurst [52].

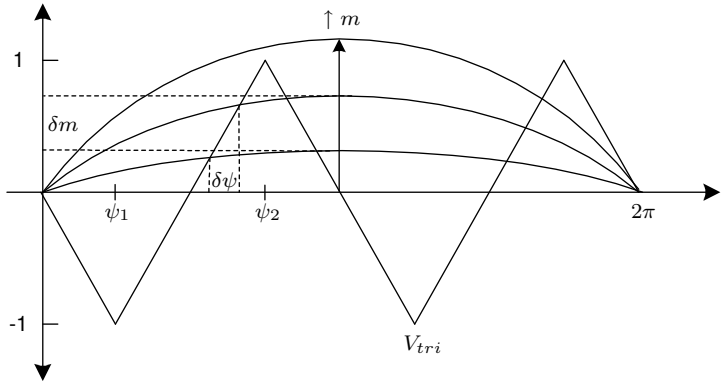

Figure 3.3 Un-defined $\frac{\delta\psi}{\delta m}$ resulting from PWM over-modulation

and $M(\psi)$ and $\mathrm{A}(\psi)$ have been modulated by the harmonic ripple components.

$$M(\psi) = \Im\left\{m_{dc} + \sum_{h=1}^{nh} m_h e^{jh\psi}\right\} \tag{3.3}$$

$$\mathrm{A}(\psi) = \Im\left\{\alpha_{dc} + \sum_{h=1}^{nh} \alpha_h e^{jh\psi}\right\} \tag{3.4}$$

This definition of the distorted modulating signal differs from the typical approach taken for linearised models, where a small signal distortion (at harmonic h) is added to the modulating signal (Equation 3.5). In contrast the proposed model represents control distortion as the multiplication of sinusoids (Equation 3.6). This representation more closely replicates realistic methods of generating the modulating sinusoid, which are often based on modulating two almost dc control variables.

$$Mod_a = m_{dc}\sin(\omega t + \alpha_{dc}) + \underbrace{m_h \sin(h\omega t + \alpha_h)}_{Distortion} \tag{3.5}$$

$$Mod_a = \left(m_{dc} + \underbrace{|m_h|\sin(h\omega t + \angle m_h)}_{Distortion}\right)\sin\left(\omega t + \left(\alpha_{dc} + \underbrace{|\alpha_h|\sin(h\omega t + \angle\alpha_h)}_{Distortion}\right)\right) \tag{3.6}$$

Typically all of the three phase modulating signals have the same magnitude (m_{dc}) and a phase angle offset by $\alpha_{dc} - \frac{2\pi}{3}$ or $\alpha_{dc} - \frac{4\pi}{3}$, hence only one vector containing nh harmonic phasors is required for each of the two converter control variables. The dc component is derived from the fundamental frequency power-flow, while the ripple is derived from the harmonic solution. All three modulating signals are compared against the same triangular carrier signal which is synchronised to the a-phase modulating signal, which given the perfect PLL is itself synchronised to the remote slack busbar phase angle reference.

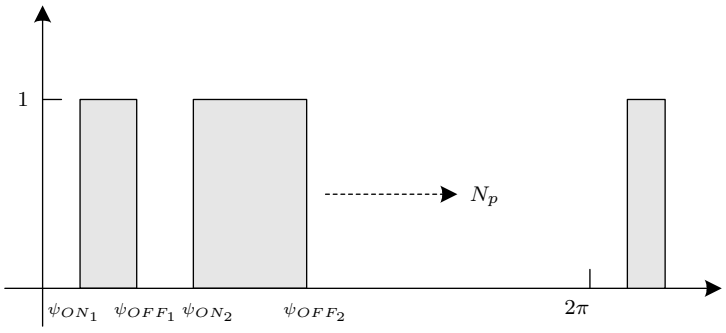

Figure 3.4 Square pulse sampling function

PWM over-modulation

If the modulation index remains within $0 \leq m < |V_{tri}|$ this modulation scheme results in a pair of switching angles for each of the N_p periods of the triangular carrier. The location of these angles can be described over the interval ($\psi_1 : \psi_2$ in Figure 3.3) as a function of the modulating signal (Mod_a). This relationship does not hold in the generalised case when over-modulation may be present. Over-modulation, where the magnitude of the modulating signal exceeds that of the triangle carrier ($m > |V_{tri}|$), reduces the number of switching pulses, since each segment of the triangular carrier does not necessarily intersect with the modulating function.

Since the switching angles are included implicitly within the solution (i.e. they are not solution variables), this situation does not affect the switching spectrum derivation. The difficultly this situation poses lies in how the reduction in the number of switching instants causes a discontinuity in switching angles ($\frac{\delta\psi}{\delta m}$), and hence the resultant PWM spectrum ($\frac{\delta S}{\delta m}$). These step changes make analytic derivation of the system Jacobian more difficult, this is considered in Section 4.5.

Harmonic domain convolution

In the time domain each converter transfer can be represented by the multiplication of the PWM switching pulses with an electrical terminal quantity. The harmonic domain equivalent of this piecewise linear time domain multiplication is convolution; where each converter transfer is represented by a convolution of the PWM switching spectrum with the spectrum of a terminal variable. In order to calculate these transfers the PWM switching spectra must be defined. This is achieved by summing the individual spectra of all N_p switching pulses, where each pulse is bounded by an ON (ψ_{ON_p}) and OFF (ψ_{OFF_p}) angle (see Figure 3.4).

Given that only the first nh harmonics of the piecewise linear waveform are of interest, the switching function can be bandlimited to $2nh$, while the sampled waveform itself is bandlimited to nh. The h^{th} harmonic of the PWM spectra corresponding to a per phase PWM switching

function can therefore be described using Fourier analysis,

$$S_h = \sum_{p=1}^{N_p} \frac{j}{2\pi} \left(\psi_{OFF_p} - \psi_{ON_p}\right) \ , h = 0 \tag{3.7}$$

$$S_h = \sum_{p=1}^{N_p} \frac{\left(e^{jh\psi_{OFF_p}} - e^{jh\psi_{ON_p}}\right)^*}{h\pi} \ , h \neq 0 \tag{3.8}$$

where the OFF (ψ_{OFF_p}) angle must occur after the associated ON (ψ_{ON_p}) angle.

The convolution itself is defined using the conjugate operator (replacing the requirement for negative frequency harmonics), leading to the following definition which describes the convolution of a PWM switching spectrum (S) with a generic bandlimited signal (F) [53]. The k^{th} harmonic of the resulting spectra being:

$$(F \otimes S)_k = \frac{j}{2}\left[-2F_0S_0 + \sum_{q=0}^{nh} F_q S_q^*\right], k = 0 \tag{3.9}$$

$$(F \otimes S)_k = \frac{j}{2}\left[\sum_{q=0}^{nh}\left(F_q S_{(q+k)}^*\right)^* - \sum_{q=0}^{k} F_q S_{(k-q)}^* + \sum_{q=k}^{nh} F_q S_{(q-k)}^*\right], k > 0 \tag{3.10}$$

AC/DC transfers

Using these results the ac terminal voltage for a PWM converter can be described as the frequency domain convolution of the dc terminal voltage and the appropriate PWM switching function. A single-phase bandlimited ($nh = 100$) time domain example of this process is shown in Figure 3.5.

$$V_{Conv_{ph}} = V_{dc} \otimes S_{ph} \tag{3.11}$$

Conversely the dc side current can be described as the sum over all three phases of the ac side current convolved with the associated per phase switching function, according to Equation 3.12. Figure 3.6 illustrates this principle (in the time domain) for the first term in the summation.

$$I_{dc} = \sum_{ph=1}^{3} I_{Conv_{ph}} \otimes S_{ph} \tag{3.12}$$

3.2.2 Connection transformer

Typically a transformer is included as an electromagnetic interface between the converter and the ac system; it acts as both a voltage step down and a current smoothing reactor. Here this transformer is assumed to be a linear on-tap star-delta connection, any associated imbalance being represented via the transformer reactance and resistance. The lack of commutation also removes any necessity of separating the connection reactance and resistance with a fictitious

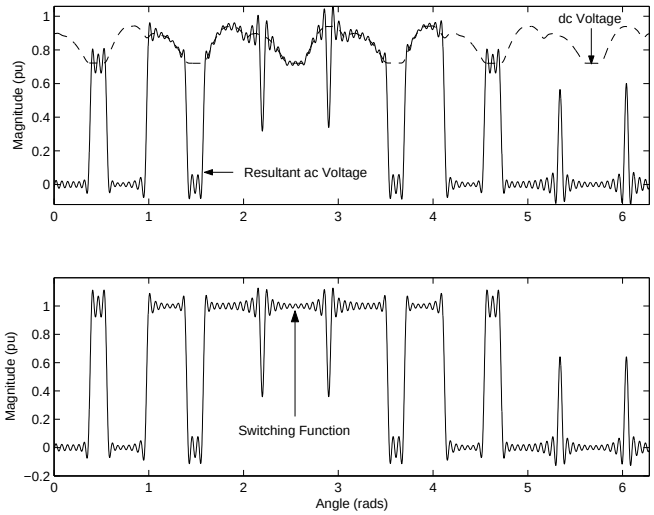

Figure 3.5 ac Voltage formulation by convolution

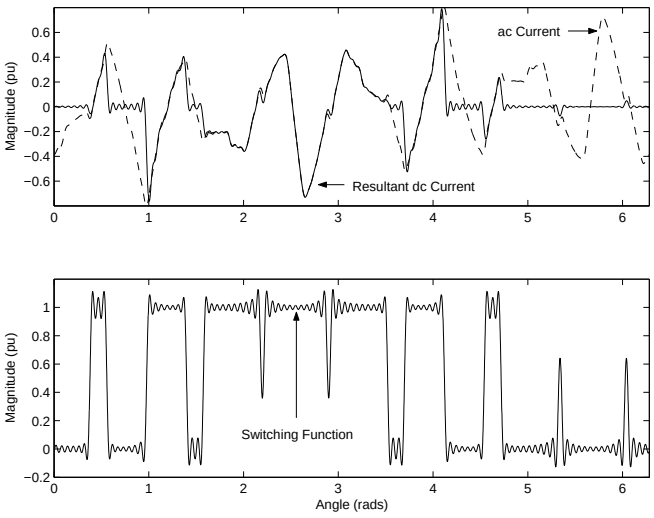

Figure 3.6 dc Current formulation by convolution

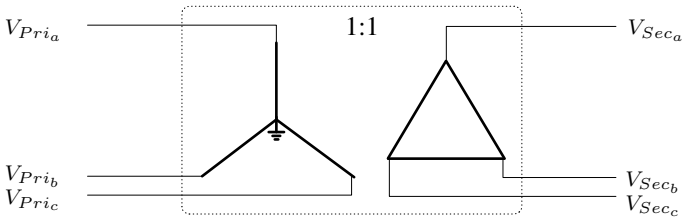

(a) A star-delta connection

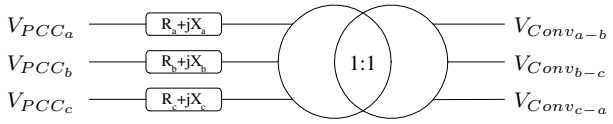

(b) Transformer equivalent

Figure 3.7 Connection transformer representation

busbar (this improves model convergence with line commutated devices [34]), permitting the simple representation presented in Figure 3.7. The transformer reactance and resistance are both referred to the primary side of an ideal (non-saturated) 1:1 transformer.

This transformer connection results in a 30° phase shifted PWM waveform (derived from the difference between the secondary side harmonic phasors). The phase shifted waveform is applied to the ac system harmonic admittance according to the procedure outlined in Section 3.3.

3.2.3 Switching losses and snubbers

The previously described analysis has assumed ideal switching devices, however PWM schemes typically employ semiconductor switches (IGBT, IGCT, GTO etc.) with less than ideal characteristics. Yang [54] proposes a two pronged approximation to the analysis of these highly non-linear turn on, turn off and on state losses. This approach models harmonic and switching losses within the power-flow using a shunt dc side resistor (for harmonic losses) and a series ac side resistance (for switching losses). Both of these principles can be extended to the proposed unified solution. Since harmonics are explicitly modelled it is only necessary to approximate their impact on the power-flow (operating point), this is achieved via a dc side resistance (R_{dc} in Figure 3.1). The impact of switching losses could likewise be incorporated within the power-flow as an additional series connection resistance, however this loss mechanism was not a major issue when validating results against PSCAD/EMTDC.

The evaluation of switching losses is further complicated by the presence of snubber circuits which while commonly used in real world situations have not been incorporated in the harmonic solution. Any additional losses attributed to the snubber circuits could be lumped with the

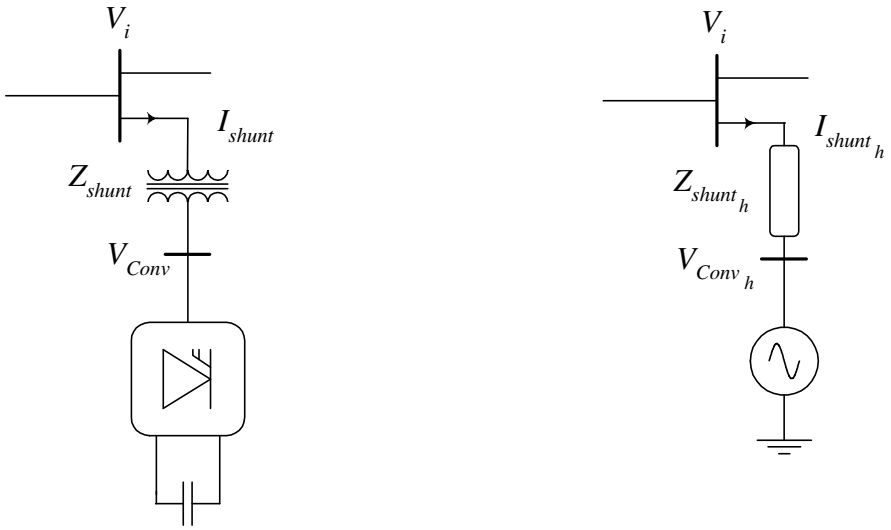

(a) Shunt connection

(b) Harmonic equivalent at harmonic h

Figure 3.8 Shunt connection representation (single line diagram)

switching losses; the accurate assessment of these losses would require additional analysis not included within this thesis.

3.3 FACTS CONNECTION MODELLING

The generalised PWM converter bridge presented can be configured to represent a range of FACTS devices, with a variety of ac and dc side topologies. Each topology can be decomposed on the ac side into a combination of shunt and series converter elements all of which share a voltage sourced dc busbar. The converter model acting as an interface block between two linear admittances representing the ac and dc systems.

3.3.1 AC side interface

The ac component of this interface is based around star-grounded harmonic voltage and current sources, simplifying any issues regarding over specification (cut sets and loops) of the system. The harmonic voltage and current sources introducing shunt and series connected distortion respectively. The choice of representation is both a function of the mismatch location used for the iterative solution (see Section 4.2) and admittance structure used to model the ac system.

Shunt Devices

For iterative solutions it is typical to choose the least distorted quantities as the solution variables. Given the proposed mismatches are defined on the dc side (to minimise the number of

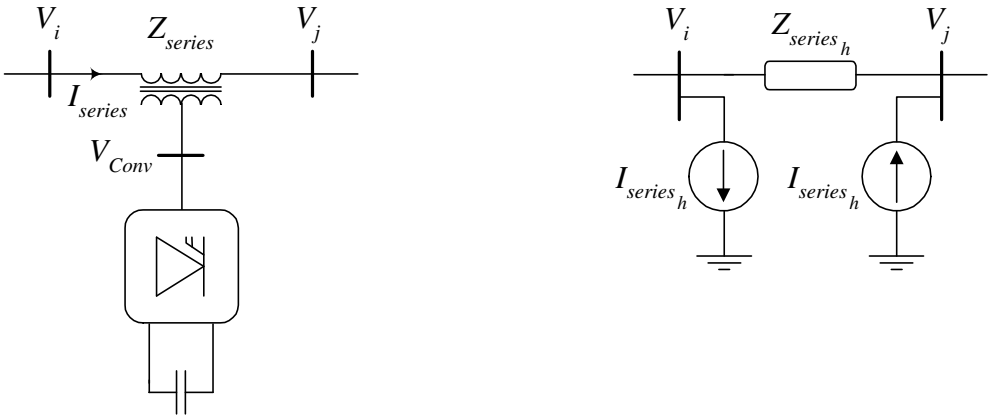

(a) Series connection

(b) Harmonic equivalent at harmonic h

Figure 3.9 Series connection representation (single line diagram)

solution variables) and voltage sourced conversion is assumed, the best choice of variable is the dc voltage. This choice makes it convenient to represent the ac side of a shunt connected converter using voltage sources; primarily since the only processing required to generate the phase voltages is the PWM $dc \leftrightarrow ac$ transfer. In contrast a shunt current injection representation [55] would require an additional conversion step or a different choice of variables, both of which would affect computational efficiency.

The voltage source representation is also very easy to incorporate within linear harmonic analysis, all that is required is an additional voltage defined busbar connected through the transformer impedance to the PCC (see Figure 3.8). The voltage on the new busbar being equal to the converters ac terminal voltage (e.g. $V_{Conv_{a-b}} = V_{Conv_a} - V_{Conv_b}$), as defined in Section 3.2.

Series Devices

The same logic applies to series connected converters, with the dc side voltage making an appropriate solution variable, however the series connection poses issues for the ac admittance formulation. The ac admittance is structured for shunt connected sources, making it more straightforward to convert each series voltage source into a pair of opposing shunt current sources (Figure 3.9). Each current source injecting or sinking a current equivalent to the impact of a series voltage source, as defined in Equation 3.13. This representation maintains the generality of the solution format, allowing combinations of shunt and series converters to be easily incorporated with the ac system.

$$\mathbf{I_{Series}} = \frac{\mathbf{V_{Conv}}}{\mathbf{Z_{series}}} \tag{3.13}$$

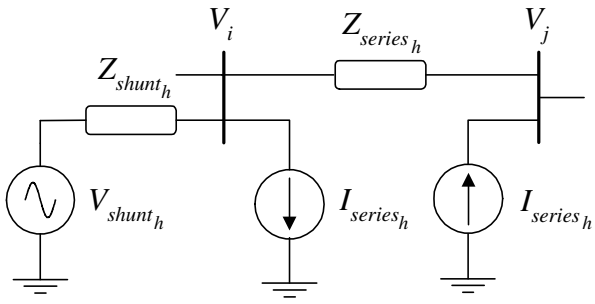

Figure 3.10 A harmonic voltage/current source UPFC model (single line diagram)

Hybrid Connections

The shunt and series converter blocks can be combined to model more advanced connection schemes such as the UPFC and IPFC. This representation can be generalised to any FACTS scheme which is composed of series and/or shunt PWM converters with either individual or shared dc buses. The principle has been applied to a UPFC as an example of how the technique accounts for the ac side interaction of multi-converter devices, as outlined in Figure 3.10.

3.3.2 DC side interface

The dc side of either converter configuration is treated in the same fashion. Each converter presenting a current source connected to the dc system admittance. These currents are used to form the harmonic system mismatches, which incorporate the dc side admittance and any dc side coupling between converters (for multi-converter devices). These mismatches are discussed in Section 4.4.

3.4 CONTROL ASPECTS

Modern FACTS devices utilise a wide variety of increasingly complex control schemes, the vast majority of which are aimed at fundamental frequency and transient response optimisation. Due to the limited control bandwidth, authors often isolate the harmonic and control (or operating point) solutions. While this assumption, that good control loop design can fully isolate the harmonic solution from the operating point, is applicable to specific situations it does not provide a generalised solution method.

In order to maintain generality, the impact of operating point variation (i.e. harmonics affecting the operating point) and harmonic propagation through the control loop are incorporated within the proposed solution. These two mechanisms are addressed separately, the operating point variation within the power-flow (Section 3.4.1) and harmonic propagation within the harmonic solution (Section 3.4.2). This separation effectively permits an infinite dc controller gain,

resulting in the correct operating point, without the associated numerical difficulties of incorporating zero frequency control components within the harmonic matrices (the PI controller has a pole at zero frequency).

While a massive variety of control techniques could be modelled (to differing extents) in HDA, this thesis focuses on common (and basic) voltage, current and power regulation schemes which are not necessarily optimised for transient response. These control schemes are succinctly included using a combination of two control blocks; one based on fundamental frequency real/reactive power flows and the other a single variable PI control loop.

3.4.1 Fundamental frequency component

Since most FACTS controllers are principally aimed at regulating fundamental frequency quantities, the most significant control aspect is the component associated with fundamental frequency. This component is dealt with in the power-flow section of the model using classic mismatches between a set-point and the current value. These mismatches can be used in isolation, given the assumption of 'pseudo fundamental' control quantities, or as the dc component of a distorted control mismatch. The first option improves efficiency when modelling large systems with multiple FACTS devices, the second being more appropriate for detailed analysis of a single device.

Real and reactive power control schemes

The assumption that the harmonics do not propagate through the controller is particularly applicable to control schemes which regulate real or reactive power since these quantities are predominantly a function of fundamental frequency quantities. The limited bandwidth of metering transducers and the requirement that both harmonic voltage and current must be present at the same harmonic to generate real or reactive power, make the assumption of harmonic isolation fair in all but the most distorted systems. Given this assumption fundamental frequency real/reactive control schemes can be implemented entirely within the power-flow solution block. For example the series element of a UPFC, controlled to regulate both the positive sequence real and reactive power being transferred through an adjacent transmission system is represented using two simple mismatches:

$$0 = P^{+}_{Line} - P_{Order} \tag{3.14}$$

$$0 = Q^{+}_{Line} - Q_{Order} \tag{3.15}$$

Since single converter FACTS devices are limited to reactive power compensation (in the steady-state), the associated STATCOM and SSSC reactive power control schemes can be modelled using a single Q mismatch.

Voltage and current control schemes

While voltage and current quantities are often more distorted than power quantities it is sometimes useful to make the somewhat questionable assumption that these quantities too can be isolated from the harmonic solution. This is done primarily because incorporating harmonic propagation through the controller requires significantly more computational effort.

For phase angle control schemes the power-flow mismatches state that the positive sequence voltage at the PCC (or current through the converter) must equate to the corresponding voltage (or current) order, while the magnitude of the modulating index (m_{dc}) must equate to the fixed modulating index order (m_{Order}). The second modulating index mismatches can be replaced by a dc voltage mismatch in regulated dc busbar schemes.

For a STATCOM, with an optional droop characteristic (X_{Droop}):

$$0 = V^{+}_{PCC} - V_{Order} + X_{Droop} I^{+}_{STAT} \tag{3.16}$$

$$0 = m_{dc} - m_{Order} \tag{3.17}$$

For an SSSC:

$$0 = I^{+}_{SSSC} - I_{Order} \tag{3.18}$$

$$0 = m_{dc} - m_{Order} \tag{3.19}$$

3.4.2 Distorted control feedback

If the measurement point is heavily distorted, or the converter controller is aimed at fast transient response (hence requiring wider control bandwidth), it is necessary to assess the impact of harmonic propagation through the controller. This can be achieved by incorporating the frequency response of the controller within the harmonic solution. The proposed formulation, while capable of incorporating any linear (or linearised) controller, is described here with reference to a basic PI feedback loop (Figure 3.11). While extremely simple this demonstrates how this mechanism can impact the fundamental and harmonic frequency solutions. If a non-linear control scheme were to be included the number and location of the control mismatches (described in Section 4.4.4) would need to be adjusted.

These control loops are typically used to adjust the phase (α) and/or magnitude (m) of the PWM modulating function in order to regulate an ac or dc quantity. The basic example given here regulates an ac quantity using phase angle control, which indirectly adjusts the the magnitude of the converter's terminal voltage. This basic principle is applied to more advanced schemes in later chapters, obviously the *dq* transformation can be omitted for control schemes based on dc quantities (e.g. regulated dc busbar systems).

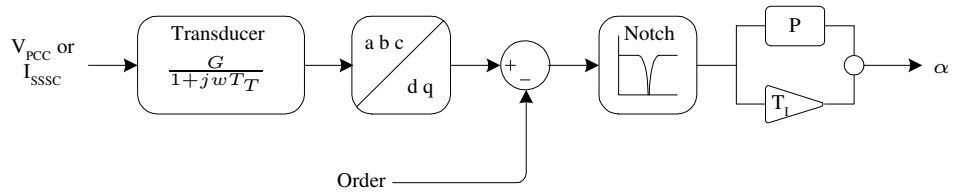

Figure 3.11 Single variable voltage (or current) controller

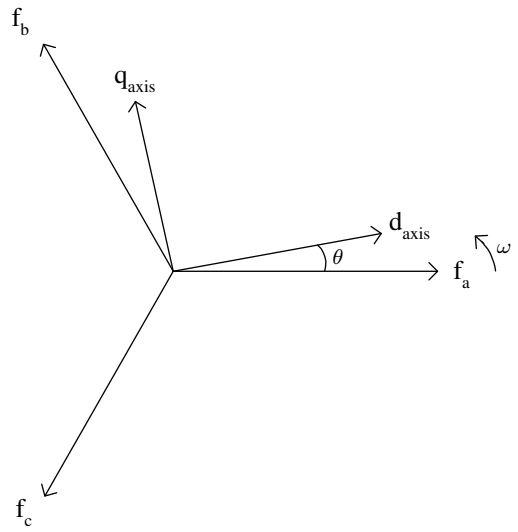

Figure 3.12 *dq* Transformation definition

dq Transformation in the harmonic domain

Since control schemes (and the associated variables) operating under steady-state conditions are nominally based on dc values it is necessary to measure ac quantities within a rotating frame of reference such as the *dq* transformation. The *dq* transformation is defined by the time domain multiplication of a measured ac value with a sinusoidal reference, see Figure 3.12 and Equation 3.20.

$$\begin{bmatrix} f_d \\ f_q \\ f_0 \end{bmatrix} = \frac{2}{3} \begin{bmatrix} \cos\theta & \cos\left(\theta - 2\pi/3\right) & \cos\left(\theta - 4\pi/3\right) \\ -\sin\theta & -\sin\left(\theta - 2\pi/3\right) & -\sin\left(\theta - 4\pi/3\right) \\ 1/2 & 1/2 & 1/2 \end{bmatrix} \begin{bmatrix} f_a \\ f_b \\ f_c \end{bmatrix} \tag{3.20}$$

This time domain transformation is to a large extent the dual of converter rectification, the only difference being that the modulation function is a perfect sinusoid rather than a PWM approximation. The *dq* transformation can therefore be undertaken in the frequency domain by convolving the 3-phase terminal voltage (or converter current) with three balanced fundamental

frequency sinusoids (Equation 3.21), derived from the PLL (which is assumed to be ideal);

$$f_d = \frac{2}{3}\sum_{ph}\left[f_{ph}F_{Trans}\right] \otimes \begin{bmatrix} 1\angle f_{ph} & 0 & ... & 0 \end{bmatrix}^T \tag{3.21}$$

where F_{Trans} accounts for the transducers frequency response, approximated using a single pole filter.

$$F_{Trans_k} = \frac{G}{1 + jk\omega T_T} \tag{3.22}$$

The resultant estimate of the positive sequence value contains both a dc value and a small harmonic ripple, the magnitude of which is primarily dependent on system imbalance.

DC Control component

The scaled dc part of the direct component (f_d), which corresponds to the positive sequence voltage (or current), is used by the power-flow block, as per Section 3.4.1. The positive sequence voltage (or current) estimate being compared with the control order generating a mismatch which defines the dc value for the firing angle (α_{dc}). Since the *dq* transform uses an ideal fundamental frequency sine reference, the dc component of the positive sequence estimate is only a function of the fundamental frequency voltage or current, no harmonic distortion being modulated by the *dq* transform to dc.

Harmonic transfers through the controller

While the dc component of the measured signal is immune from harmonic distortion, the harmonic ripple in the direct component is a function of both the fundamental frequency imbalance and any harmonic distortion present. This ripple is reflected in a distorted PWM modulation signal via the control loop. The controller itself is modelled using linear control analysis, the frequency response being defined by the multiplication of the notch filter and PI controller transfer functions. The notch filter is necessary since some degree of system imbalance is unavoidable, which causes the positive sequence estimate from the *dq* transform to contain a second harmonic ripple component. The resultant transfer function is:

$$\alpha_k = \left(\frac{G\left[1 + \left(\frac{jk\omega}{\omega_n}\right)^2\right]}{1 + 2\zeta\left(\frac{jk\omega}{\omega_n}\right) + \left(\frac{jk\omega}{\omega_n}\right)^2}\right)\left(P + \frac{1}{jk\omega T_I}\right) f_{d_k} \tag{3.23}$$

3.5 LINEAR SYSTEM COMPONENTS

The vast majority of a power system can, when operated in unsaturated regions, be reasonably approximated as a network of linear electrical components. This assumption allows converter

(a) RLC tuned shunt filter

(b) Second order HP filter

Figure 3.13 Single line diagram of the filter types modelled

interaction to be solved using direct three-phase harmonic analysis, the system being characterised by a linear harmonic admittance matrix. This permits the straight forward application of linearised models available in literature (see Densem [56]).

The linear systems includes phase imbalance, phase to phase coupling, and frequency dependence but does not contribute any linearised harmonic transfers. The models described here have been deliberately reduced to an elementary level; making it possible to replicate a test system exactly within the corresponding time domain simulation used for validation. The proposed technique is in no way limited to using these basic RLC equivalents exclusively.

3.5.1 Shunt: Loads and filters

From a harmonic perspective the nature of shunt components varies greatly, from filters (the harmonic profile of which is well defined) to ac system loads (typically defined in terms of the real and reactive power absorbtion at fundamental frequency). At harmonic frequencies both blocks are modelled in essentially the same fashion using a grounded-star RLC branch.

The proposed model is capable of modelling basic RL, RC and filter branches or of using a harmonic profile specified by an external file. Two basic passive filters are included: the tuned RLC 3.13(a) and the second order high-pass 3.13(b). Load busbars are treated at harmonic frequencies as a fixed RL branches; to accommodate this PQ defined buses are transformed to an equivalent branch sized to match the load power at the nominal fundamental frequency voltage. Loads can also be specified as a RL branches at both fundamental and harmonic frequencies, an option particularly useful for validation with PSCAD/EMTDC (which lacks appropriate constant power loads).

3.5.2 Equivalent-pi: Transmission lines and transformers

Both transformers and transmission lines can be concisely represented using an equivalent-pi model, the data for which is frequency dependent and calculated prior to the main solution.

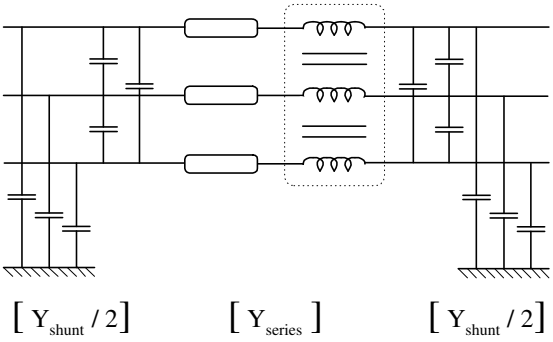

Figure 3.14 Three-phase equivalent-pi circuit for transmission lines

Transmission lines are particularly critical because of the significant levels of both phase coupling and impedance imbalance at harmonic frequencies, neither of which are cancelled at harmonic frequencies by transposition [57]. The transmission line data is typically generated using line images and Carson's correction series [58], or taken directly from the PSCAD/EMTDC transmission line representation [7], see Appendix C. Either way all transmission lines are incorporated using a three-phase equivalent-pi circuit, as shown in Figure 3.14.

Transformers can also be modelled using an equivalent-pi which incorporates phase coupling and frequency dependence, however in order to ease validation issues they are modelled using three single phase transformers. Each of these is modelled as a basic series admittance branch, permitting straight forward validation with the single phase transformer used in PSCAD/EMTDC.

3.6 CONCLUSIONS

This chapter has presented the basis for an iterative harmonic domain model for FACTS devices using single level three-phase PWM bridges. The model is based on the concise representation of PWM converters using a positive frequency spectra, coupled with basic control and system component models. The non-linear aspects of these relationships, particularly with respect to control, dictate an iterative solution. The formulation of which is described in Chapter 4.

Chapter 4

A UNIFIED SOLUTION TECHNIQUE

4.1 INTRODUCTION

This chapter presents a generalised iterative solution framework appropriate for the analysis of PWM FACTS devices, the harmonic domain representation of which was described in Chapter 3. The proposed Newton solution incorporates both the fundamental and harmonic frequency variables within a single ('unified') iterative loop; a structure which avoids convergence difficulties associated with sequential approaches [9]. The technique, outlined in Figure 4.1, is composed of three major blocks: variable initialisation, Jacobian formulation, and finally the iterative solution which includes both the power-flow and harmonic mismatches.

The Newton method has been shown by numerous authors [11, 10, 34] to provide rapid and robust convergence for harmonic domain solutions. The technique is based on the non-linear system being described by a set of mismatch equations ($M(X_i)$). These mismatches are a function of the solution variables (X_i) which are iteratively updated using a matrix of partial derivatives (the Jacobian, J) until the mismatch vector is sufficiently close to zero and the solution is deemed

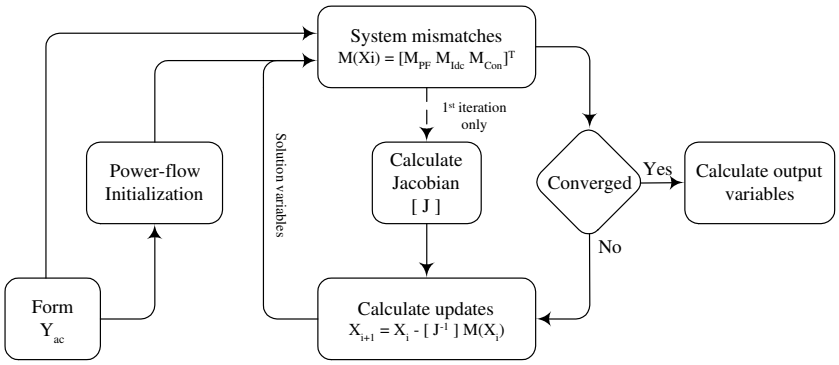

Figure 4.1 The iterative solution process

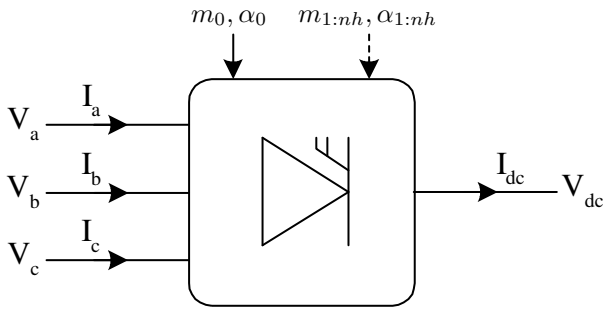

Figure 4.2 Converter control, ac and dc ports

to have converged:

$$M(X_i) = J_i \Delta X_i \tag{4.1}$$

$$\Delta X_i = J_i^{-1} M(X_i) \tag{4.2}$$

$$X_{i+1} = X_i - \Delta X_i \tag{4.3}$$

The system mismatch vector is formed by concatenating the power-flow, harmonic and control mismatches each of which is described as a function of the associated solution variables.

$$M\left(X_{PF}, X_{Harm(1:nh)}, X_{Con(1:nh)}\right) = \begin{bmatrix} M_{PF} \\ M_{Idc(1:nh)} \\ M_{Con(1:nh)} \end{bmatrix} \tag{4.4}$$

This interdependence between the operating point and harmonic solutions (system and controls) underlies the requirement for an iterative solution. The formulation is described by first justifying and initialising the solution variables (Section 4.2), after which the derivation of the power-flow and harmonic mismatches is detailed (Sections 4.3 & 4.4). Finally, the structure and calculation of the system Jacobian is presented (Section 4.5).

4.2 SOLUTION VARIABLE SELECTION AND INITIALISATION

4.2.1 Harmonic solution variable selection

Previous work conducted in the harmonic domain [11, 10, 34] has focused on line commutated devices, these devices possess a transfer characteristic which is highly dependent on the terminal conditions. This has resulted in models which characterise each converter using both the ac (typically positive and negative sequence components) and dc terminal quantities as solution variables, as shown in Figure 4.2.

While this formulation could be applied to hard-switched PWM devices, it is not an optimal

Table 4.1 Solution variable selection

ac side	dc side	$\alpha_{1:nh}$	α_{dc}	No. of Complex Variables
dc Control				
✓	✓		✓	$4nh + PF$
✓			✓	$3nh + PF$
	✓		✓	$nh + PF$
dc + harmonic Control				
✓	✓		✓	$4nh + PF$
✓			✓	$3nh + PF$
	✓	✓	✓	$2nh + PF$

solution in terms of computational efficiency. Since the ac to dc harmonic transfer characteristic of a PWM converter is fully defined by the control signals (m, α) the ac and dc terminal quantities are a linear function of each other and the switching function (itself non-linearly dependent on the control signals). This result permits a PWM converter to be described at harmonic frequencies by the control signals (a function of the power-flow) and either the three-phase ac terminals or the single dc terminal quantities.

However, the control signals are not always an exclusive function of the fundamental frequency power-flow variables, complicating the choice of variables. Harmonic transfers through the controller make the PWM transfer a function of the distorted terminal (ac and/or dc) conditions. It is therefore necessary to include additional solution variables, which reflect any terminal conditions being measured by the control scheme.

These two cases are considered separately, the solution variables being selected in order to maximise computational efficiency in both cases. Table 4.1 summarises how the following principles can be applied to phase angle controlled SSSC.

DC control variables

When an idealised controller (i.e. one immune to harmonic distortion) is assumed the PWM converter harmonic transfers become a function of the power-flow exclusively, making it unnecessary to include all terminal quantities as harmonic solution variables. Computationally efficient simulation being a primary goal of harmonic domain analysis, it is therefore advantageous to describe each converter solely in terms of dc terminal quantities. This reduces the number of solution variables required for a converter by a factor of three. This factor is further improved for multiple converter configurations such as the UPFC where the a,b and c phases for both the series and shunt terminals can be reduced to a single dc terminal mismatch.

DC and harmonic control variables

Since the terminal conditions surrounding FACTS devices are typically distorted any non-ideal measurement and control block will respond to non-fundamental frequency electrical quantities. As such the controller will become a function of both the three-phase ac and the dc harmonic

terminal conditions (assuming a regulated dc busbar scheme is used); its output containing a portion of the terminal distortion present. Including all these quantities as solution variables would cause a massive increase in the number of harmonic mismatches and the size of the Jacobian, reducing computational efficiency.

The reduction in efficiency can be lessened by choosing the control ripple signals as the additional extra harmonic variables, rather than the ac terminal values. This is possible since (for simplistic PI controllers) each control block is dependent on a single harmonic vector variable (e.g. I^+, V^+, P, Q etc.), making it more efficient to choose the ac side solution variable after the measurement block (e.g. dq transformation, P or Q calculation). Each PI controller can therefore be characterised by a distorted control signal (e.g. α or m) updated with a positive sequence mismatch [1].

When used in combination with the previously described dc variable formulation a wide variety of basic ac and dc control schemes can be incorporated without the associated large increase in the number of solution variables / mismatches.

4.2.2 Solution variable initialisation

To achieve reliable convergence it is critical that the solution variables are suitably initialised, in particular the fundamental frequency operating point for each PWM converter. While it is possible to initialise the system with a flat voltage profile and no harmonic distortion and then solve the system using the full solution immediately, this is highly inefficient since each full iteration is computationally intensive.

The solution variables are therefore initialised using the three-phase power-flow solved with no harmonics included. When convergence is achieved the harmonic solution is added with all harmonics initialised to zero. This point typically generates an adequate estimate of the full Jacobian; making it unnecessary to re-calculate the Jacobian at subsequent iterations, while still achieving satisfactory convergence.

4.3 POWER-FLOW SOLUTION

The harmonic performance of a converter is extremely dependent on the operating point of the system to which it is connected, this necessitates the incorporation of fundamental frequency operating point variation within the solution. A basic three-phase power-flow, the predominant tool for this type of analysis, is used to fulfill this requirement.

Traditional PQ (load), PV (generator) and Slack buses are used in conjunction with a three-phase adaptation of Canizares positive sequence FACTS device power-flow models [59] to represent the

[1] If the control scheme regulates both positive and negative sequence ac quantities it becomes necessary to include two harmonic control vectors of length nh, one for each sequence component. This makes it more straightforward, and equally as efficient, to use the three ac terminals as the solution variables.

fundamental frequency backbone of the system. The three-phase formulation is a requirement since non-characteristic harmonics are generated primarily as a result of unbalanced terminal conditions.

4.3.1 Load and generator mismatches

The small illustrative test systems used within this thesis use star grounded transformer, load and generator connections. This connection effectively isolates each phase of a load (or generator), avoiding power-flow convergence issues resulting from the zero sequence blocking effect of ungrounded star or delta connections. The formulation, which still permits imbalance and phase coupling (e.g. transmission circuits), results in the classic load and generator mismatches.

For the a-phase of a PQ load:

$$M_{PQ} = \begin{bmatrix} P_a^{Sch} - P_a \\ Q_a^{Sch} - Q_a \end{bmatrix} \tag{4.5}$$

For the a-phase of a PV generator:

$$M_{PV} = \begin{bmatrix} P_a^{Sch} - P_a \end{bmatrix} \tag{4.6}$$

where the real and reactive power at the i^{th} a-phase busbar are defined as:

$$P_{i_a} = \sum_{ph=a}^{c} \sum_{j=1}^{n} |V_{i_a}| \left|V_{j_{ph}}\right| \left|Y_{i_a j_{ph}}\right| \cos\left(\angle Y_{i_a j_{ph}} - \delta_{i_a} + \delta_{j_{ph}}\right) \tag{4.7}$$

$$Q_{i_a} = -\sum_{ph=a}^{c} \sum_{j=1}^{n} |V_{i_a}| \left|V_{j_{ph}}\right| \left|Y_{i_a j_{ph}}\right| \sin\left(\angle Y_{i_a j_{ph}} - \delta_{i_a} + \delta_{j_{ph}}\right) \tag{4.8}$$

The fully defined slack busbar acts as a generic three-phase voltage source; typically employed as the voltage source component of the Thevenin system equivalent.

4.3.2 FACTS power-flow mismatches

Under steady-state fundamental frequency conditions FACTS devices are normally modelled with a controllable voltage source connected to the ac system via the inductance of the connection transformer. The combination is either producing or absorbing real or reactive power. As such each FACTS device can be included within the system power-flow by defining the power transfer across the connection transformer and ensuring the power balance is maintained. This balance equates the ac terminal real power with the dc side power and device losses, maintaining a steady dc capacitor voltage [59]. Device losses are modelled as a series transformer connection loss (R) and a shunt dc side resistor (R_{dc}) sized to account for converter losses.

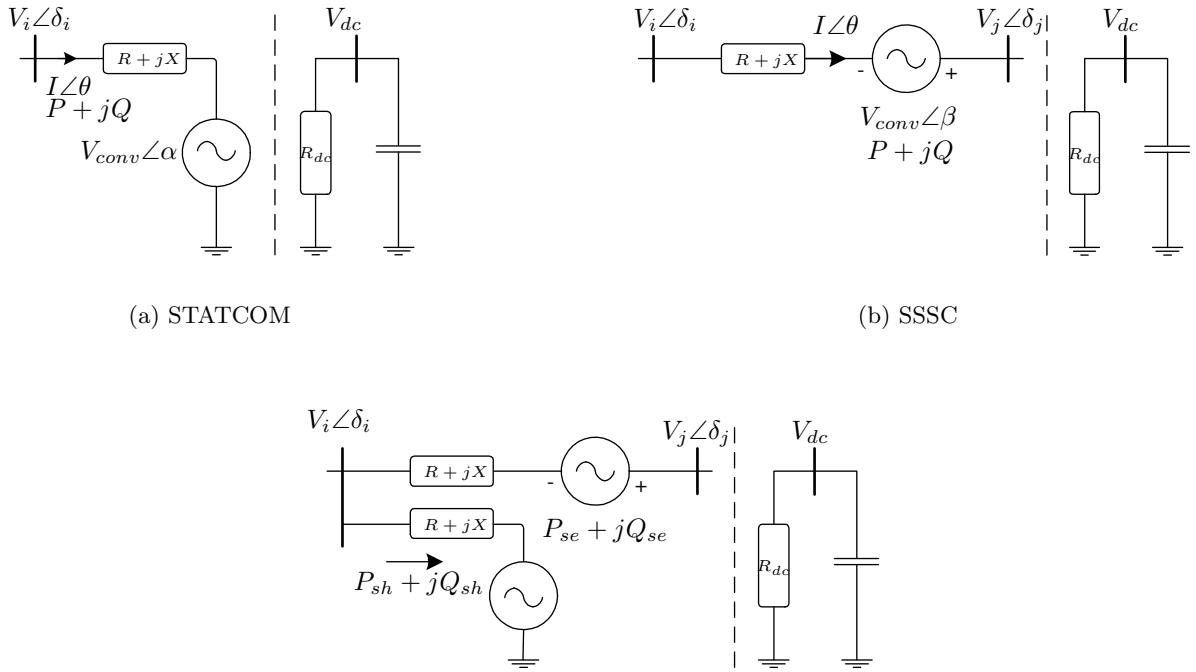

(a) STATCOM

(b) SSSC

(c) UPFC

Figure 4.3 Power-flow equivalents for FACTS devices (single line diagrams)

STATCOM representation

Figure 4.3(a) presents the fundamental frequency solution variables used to represent the shunt connected STATCOM. The control scheme and the associated mismatches (described in Section 3.4) have been omitted. As such the real and reactive power in each phase can be described using the following mismatches,

$$M_{STATCOM_a} = \begin{bmatrix} P - V_i I \cos(\delta_i - \theta) \\ Q - V_i I \sin(\delta_i - \theta) \\ P - V_i^2 G + V_{conv} V_i G \cos(\delta_i - \alpha) \\ \quad + V_{conv} V_i B \sin(\delta_i - \alpha) \\ Q + V_i^2 B - V_{conv} V_i B \cos(\delta_i - \alpha) \\ \quad + V_{conv} V_i G \sin(\delta_i - \alpha) \end{bmatrix} \tag{4.9}$$

where $G + jB = (R + jX)^{-1}$ refers to the transformer connection admittance. Three sets of these per phase mismatches are used in conjunction with the real power balance mismatch to model each STATCOM. Since, in the steady state, a STATCOM cannot produce or absorb real power the power balance mismatch equates the device losses with the incoming real power:

$$M_{Bal} = \left[\sum_{p=a,b,c} P^p - \sum_{p=a,b,c} R_t^p I_p^2 - \left(\frac{V_{dc}^2}{R_{dc}} \right) \right] \tag{4.10}$$

SSSC representation

The per phase power mismatches for a series connected SSSC (see Figure 4.3(b)) can be described in a similar fashion to the STATCOM. The only significant difference is the requirement for an additional set of PQ terminal mismatches,

$$M_{SSSC_a} = \begin{bmatrix} P_i - V_i I \cos(\delta_i - \theta) \\ Q_i - V_i I \sin(\delta_i - \theta) \\ P_j + V_j I \cos(\delta_j - \theta) \\ Q_j + V_j I \sin(\delta_j - \theta) \\ P - (P_i + P_j) \\ Q - (Q_i + Q_j) \\ P - V^2 G + V_{conv} V G \cos(\delta - \beta) \\ \quad + V_{conv} V B \sin(\delta - \beta) \\ Q + V^2 B - V_{conv} V B \cos(\delta - \beta) \\ \quad + V_{conv} V G \sin(\delta - \beta) \end{bmatrix} \tag{4.11}$$

where $V\angle\delta$ refers to the voltage difference between the ac terminal voltages V_i and V_j. The power balance mismatch (Equation 4.10) remains unchanged for the SSSC.

UPFC representation

Given the hybrid nature of the UPFC (Figure 4.3(c)) it is modelled using a combination of the shunt and series representations (Equations 4.9 and 4.11). However the power balance mismatch must be generalised in order to permit real power transfers between the series and shunt connections. This results in the following additional mismatches.

$$M_{Bal} = \begin{bmatrix} (P_{sh} + P_{se}) - (P_i + P_j) \\ (Q_{sh} + Q_{se}) - (Q_i + Q_j) \\ \sum\limits_{p=a,b,c} \left(P^p_{sh} + P^p_{se}\right) - \sum\limits_{p=a,b,c} \left(R^p_{sh}(I^p_{sh})^2 + R^p_{se}(I^p_{se})^2\right) - \left(\frac{V^2_{dc}}{R_{dc}}\right) \end{bmatrix} \tag{4.12}$$

4.3.3 Power-flow dependence on harmonic solution variables

This power-flow representation is typically used in an isolated fashion, the impact of harmonics being ignored. While this assumption is often adequate for fundamental frequency studies, it is not strictly correct, nor is it appropriate for detailed harmonic studies. Since switching converters can modulate harmonic frequency components at the dc terminal to fundamental frequency ac quantities (and vice versa) the series or shunt voltage source equivalents become a function of both fundamental and harmonic frequency variables.

Equations 4.9 and 4.11 have been included in a generalised fashion which can accommodate either type of representation. The series or shunt voltage source (V_{conv}) can be defined as a

function of the power-flow variables,

$$V_{conv} = k_{PWM} m_{dc} V_{dc(0Hz)} \angle \alpha_{dc} \tag{4.13}$$

where k_{PWM} is a constant relating the dc and ac voltage. It can also be defined as a function of the dc voltage (V_{dc} including harmonics) and the switching function (itself a function of the control variables).

$$V_{conv_{ph}} = S_{ph}(\alpha, m) \otimes V_{dc_{1:nh}} \tag{4.14}$$

The fundamental frequency version is used for variable initialisation, while the convolutional approach is adopted for the full harmonic solution.

4.4 HARMONIC SOLUTION

In contrast to the fundamental frequency power-flow, the majority of the harmonic system is assumed to behave in a linear fashion, acting as a linear admittance over which non-linear harmonic injections can interact. As such the harmonic mismatches are dependent on the ac and dc system admittances, the operating point and the harmonic solution variables.

4.4.1 Linear ac system analysis

The ac system acts as the medium over which FACTS devices interact, making the ac system impedance an integral part of the harmonic mismatches. Given the assumption that the remainder of the ac system behaves in a linear fashion (at a given operating point), it is relatively straightforward to incorporate using nodal analysis. This reduces the ac system to a harmonic admittance matrix of the following form,

$$\begin{bmatrix} I_1 \\ I_2 \end{bmatrix} = \begin{bmatrix} Y_{11} + Y_{12} & -Y_{12} \\ -Y_{12} & Y_{22} + Y_{12} \end{bmatrix} \begin{bmatrix} V_1 \\ V_2 \end{bmatrix} \tag{4.15}$$

where each branch of the equivalent-pi admittance (see Figure 3.14) is calculated or read from an appropriate data file (for frequency dependent components) at all harmonics up to nh. The full formation replicates Equation 4.15 for all three phases, including any phase to phase coupling terms.

Since significant non-linear harmonic injections are only present at a small proportion of the system nodes it is advantageous to eliminate passive busbars, improving computational efficiency. Passive busbars are defined as linear busbars with no harmonic injection present, an example being PQ busses, which are non-linear at fundamental frequency, but are represented as a fixed impedance at harmonic frequencies. The resultant reduced system only contains the non-linear FACTS harmonic injection busses, which are linked by equivalent impedances, as illustrated for a two converter system system in Figure 4.4.

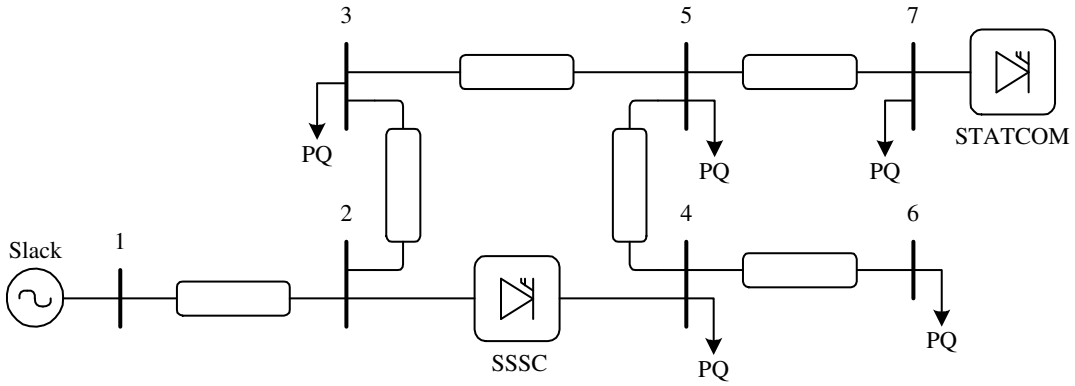

(a) Full system

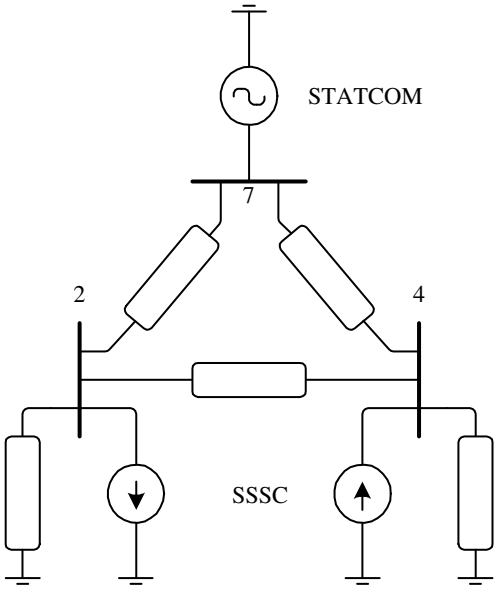

(b) Reduced harmonic equivalent

Figure 4.4 Harmonic reduction of a two converter system

This reduction process is implemented by partitioning the harmonic admittance according to the type of bus:

$\mathbf{I_{VSource}}$: ac current through an ideal voltage source, typically used as a system equivalent.

$\mathbf{V_{VSource}}$: ac voltage present at an ideal voltage source.

$\mathbf{I_{IHarm}}$: ac current injected by a harmonic current source, also used for PQ buses (injection set to zero).

$\mathbf{V_{IHarm}}$: ac voltage present at a current defined harmonic bus.

$\mathbf{I_{VHarm}}$: ac current through a harmonic voltage defined bus.

$\mathbf{V_{VHarm}}$: ac voltage present at a harmonic voltage source.

The resultant partitioned harmonic admittance is of the form:

$$\begin{bmatrix} I_{VSource} \\ I_{IHarm} \\ I_{VHarm} \end{bmatrix} = \begin{bmatrix} A & B & C \\ D & E & F \\ G & H & J \end{bmatrix} \times \begin{bmatrix} V_{VSource} \\ V_{IHarm} \\ V_{VHarm} \end{bmatrix} \tag{4.16}$$

By assuming that no voltage harmonics are present at the ideal voltage sources it is possible to derive equations 4.17 and 4.18. These describe the unknown harmonic current flows at the voltage defined busbars and the unknown voltages at the current defined busbars.

$$\mathbf{I}_{VHarm} = [HE^{-1}]\mathbf{I}_{IHarm} + [J - HE^{-1}F]\mathbf{V}_{VHarm} \tag{4.17}$$

$$\mathbf{V}_{IHarm} = [E^{-1}]\mathbf{I}_{IHarm} - [E^{-1}F]\mathbf{V}_{VHarm} \tag{4.18}$$

The three-phase shunt voltage vector (V_{VHarm}) representing shunt connected devices is derived from the dc voltage and the associated switching functions (Equation 3.11). Likewise, the current vector (I_{IHarm}) is formed by concatenating the opposing series injection vectors (which represent series connected devices, Equation 3.13), with any fixed current injections and a vector of zeros corresponding to PQ busbars.

Finally, since the proposed Newton solution is based on harmonic current mismatches it is necessary to convert the harmonic voltages present at each series connected ac terminal (V_{IHarm} or V_i and V_j from Fig. 4.3(b)) to an equivalent current. This is achieved using the transformer leakage impedance and converter voltage according to,

$$\begin{aligned} \mathbf{I_{series}} &= [\mathbf{V_i} - (\mathbf{V_j} - \mathbf{V_{conv}})] \times \left(\tfrac{1}{\mathbf{Z_{series}}}\right) \\ \mathbf{I_{series}} &= [\mathbf{V_i} - \mathbf{V_j} + \mathbf{V_{conv}}] \times \mathbf{Y_{series}} \end{aligned} \tag{4.19}$$

where the harmonic phasors V_i and V_j are a per phase decomposition of V_{IHarm}. In contrast shunt connected sources do not require any additional conversion; the ac harmonic current at each shunt terminal busbar being a direct decomposition of I_{VHarm}, the result from Equation 4.17.

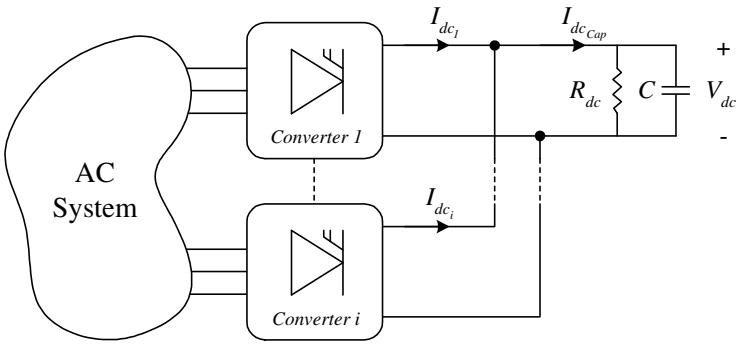

Figure 4.5 dc Side configuration of multiple converter FACTS devices

4.4.2 Modelling dc connection configurations

The harmonic performance of FACTS devices is not only a function of the ac terminal conditions, but also the connection type and amount of distortion present on the dc side. The dc side is typically composed of an energy storage device which is sized to provide either a relatively smooth dc voltage or current. This thesis focuses on the predominant voltage sourced technology, however the analysis techniques described are equally valid for current sourced devices.

While some specialised FACTS devices (e.g. DVR) make use of an energy source which can supply real power for transient voltage depressions, the majority use capacitor banks which only supply steady-state reactive compensation. This common dc capacitor bank configuration has been applied to the models described within this thesis. If the capacitor was replaced with a semi-constant long term storage device this could still be modelled using the harmonic impedance of the storage device.

Figure 4.5 presents the simplified dc side representation used for each FACTS device. All dc side capacitors have been lumped into a single equivalent capacitance, which is then connected in shunt to any number of PWM converters. Each converter contributes a dc current phasor (I_{dc_i}) derived from the convolved sum of the three-phase ac shunt or series currents (via Equation 3.12), taking care to account for the star-delta connection transformer. The sum of these currents defines the dc capacitor ripple. For example a STATCOM or SSSC would have a single converter connected to the capacitor, whereas a UPFC would have two and an IPFC as many as required.

4.4.3 Harmonic mismatches

This section details how the previously described harmonic analysis is used to formulate the real-valued harmonic mismatch equations. When used in conjunction with a three-phase power-flow these characterise a power system containing FACTS devices.

The type of dc harmonic solution variable used (the terminal voltage or current) is dependent on the FACTS device under consideration; devices using a VSC being best described in terms

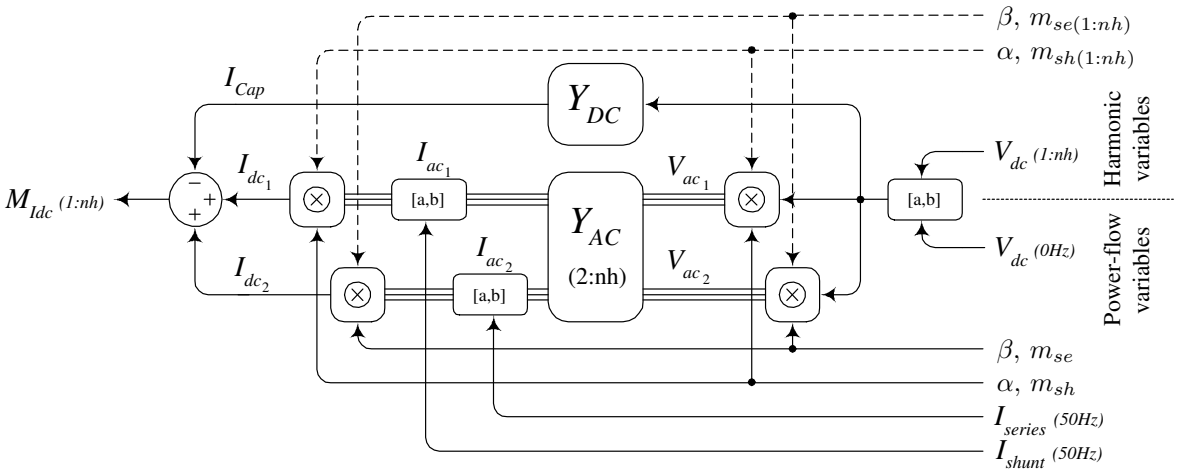

Figure 4.6 Harmonic current mismatches: dependence on the harmonic and power-flow variables

of the less distorted dc busbar voltage. Similarly, the dc terminal current is the best choice of solution variable for CSC devices. Since the FACTS devices considered within this thesis are VSC based, all harmonic solutions are formed in terms of dc voltages, updated via a dc terminal current mismatch.

The terminal mismatch is formed by applying KCL to the positive terminal of the dc bus, effectively forming a mismatch between the converter (I_{dc_i}) and capacitor (I_{Cap}) currents,

$$\mathbf{M_{Idc_h}} = \mathbf{I_{Cap_h}}(\mathbf{V_{dc}}, \mathbf{Y_{dc}}) - \sum_i \left[\mathbf{I_{dc_{i_h}}}(\mathbf{V_{dc}}, \mathbf{Y_{ac}}, \mathbf{X_{Con}}, \mathbf{X_{PF}})\right] \tag{4.20}$$

where the subscript i refers to one of any number of parallel dc connected converters and I_{Cap} is defined in terms of the dc voltage and admittance.

$$\mathbf{I_{Cap}} = [Y_{dc}]\,\mathbf{V_{dc}} \tag{4.21}$$

The complete formulation reflects both the ac and dc system admittance, while also incorporating the dependence of the harmonic solution on fundamental frequency variables. Figure 4.6 outlines this dependence for a generic two converter FACTS device. Each dc terminal harmonic current (I_{dc_i}) is derived by applying the ac terminal voltages (found via convolution according to Equation 3.11) to the ac admittance, the resultant ac terminal currents are transferred back to the dc side (Equation 3.12) where they are used to formulate dc current mismatch against the capacitor current (I_{Cap}). The capacitor current is defined by the dc side voltage and the capacitive admittance. Each of these transfers (or convolutions, $\otimes$) are dependant on the fundamental frequency electrical quantities, the dc controls, and the optional argument for control signal ripple.

Given the real valued Newton structure proposed, the complex harmonic current mismatches are finally decomposed into the associated real and imaginary components. Likewise the harmonic frequency solution variables (the dc voltage and control signal harmonics) are stored and updated in their associated quadrature components.

4.4.4 Control mismatches

PWM converter schemes are typically simulated using a perfect sinusoidal modulating function, the corresponding α and m values being perfect dc and included within the power-flow. These schemes do not require additional harmonic control mismatches (which at least double the size of the system Jacobian) making them concise and efficient. However the increasing use of FACTS devices for transient compensation, which requires increased control bandwidths, makes the assumptions associated with these techniques more questionable.

The proposed formulation can incorporate control distortion, the harmonic ripple in α and/or m being used as the harmonic variable. The associated harmonic control mismatch used to update this ripple is formulated between the dq transform of the ac quantity under control and the input to the corresponding PI controller. The resultant mismatches differ depending on the type of FACTS device and control scheme modelled; therefore as an illustration the approach is outlined for a basic SSSC with phase angle control.

Fundamental Frequency

For this basic positive sequence current (I^{+}_{SSSC}) regulation scheme the dc component of angle of the modulating signal (α) is varied to charge or discharge the dc capacitor, and hence have a secondary effect on the series voltage injection. The magnitude of this series voltage regulating the series current according to the following power-flow mismatch:

$$M_{Con_{50Hz}} = \begin{bmatrix} I^{+}_{SSSC} - I_{Order} \\ m_{dc} - m_{Order} \end{bmatrix} \tag{4.22}$$

The magnitude of the modulating signal has been fixed for this simplistic implementation.

Harmonic Frequencies

The control voltage mismatch used to define the harmonic ripple on each control variable (in this case only one, α) is formulated in a similar fashion to the dc current harmonic mismatches. The present estimate of the dc busbar voltage and control signals (both including harmonic distortion) being used to generate the ac terminal voltages, which are in turn applied to the ac admittance generating the ac control parameter (I_{SSSC} in this case). This distorted signal is then transformed into dq co-ordinates, where the direct component is compared with the

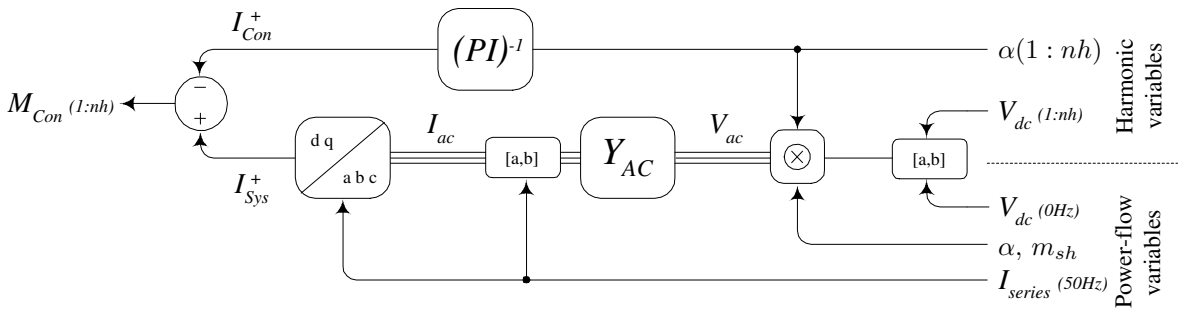

Figure 4.7 Harmonic control mismatches: dependence on the harmonic and power-flow variables

input to the control block, derived from the control variable ripple and the inverse PI control characteristic.

$$\mathbf{M_{Con_h}} = \mathbf{I^d_{Sys_h}}(\mathbf{V_{dc}}, \mathbf{X_{Con}}, \mathbf{X_{PF}}) - \mathbf{I^d_{Con_h}}(\mathbf{X_{Con}}, \mathbf{PI}) \tag{4.23}$$

$I^d_{Sys_h}$ refers to the positive sequence estimate (via the dq transform) of the series current, and $I^d_{Con_h}$ is the same quantity calculated via the PI controller block. Figure 4.7 outlines this process, highlighting the interdependence with the power-flow variables. Note how the phase angle reference for the dq transformation is idealised, and hence provided by the power-flow rather than via a PLL (for which the angle reference would be a function of the harmonic variables).

4.5 SYSTEM JACOBIAN FORMULATION

The final critical component of the harmonic solution system is the system Jacobian, a matrix of partial derivatives representing the case specific linearisation for a system. This linearisation is both relatively complex to derive analytically and computationally expensive to derive numerically, making it the critical determinant of the models flexibility and efficiency.

4.5.1 Jacobian derivation

While analytic derivation of the system Jacobian has been shown to be an efficient and practical method for HVdc converters [10, 34] it is not necessarily as applicable to PWM converters. PWM converters differ from 6 or 12 pulse line commutated devices in that the number of switching instants can vary with the operating point. Over-modulation (where the magnitude of m exceeds that of V_{tri}) leads to a reduction in the number of switching instants and a discontinuity in $\frac{\delta\psi}{\delta m}$, making analytic Jacobian derivation more difficult.

In contrast numerical derivation of the Jacobian, while computationally expensive, can be easily applied to generalised PWM systems containing multiple switching frequencies and modulation

indices. Further, numerical derivation of the Jacobian is straightforward to formulate, can be extended in a modular fashion, and is robust. A numerical Jacobian is calculated by simply sequentially perturbing each of the solution variables, and observing the change in the resultant mismatch vector. This difference vector is then divided by the magnitude of the perturbation, generating one column of the Jacobian. In order for this approximation to be valid the perturbation must be small enough such that:

$$J = \frac{\delta F}{\delta x} \approx \frac{F\left(x + \Delta x\right) - F\left(x\right)}{\Delta x} \tag{4.24}$$

Numerical derivation has therefore been adopted so as to maintain generality at the cost of computational efficiency. A perturbation magnitude of 10^{-6} pu has been applied to the fundamental frequency (distortion free) operating point; this technique has been shown experimentally to provide a satisfactory estimate of the full harmonic Jacobian.

4.5.2 Jacobian structure

Block structure: dc control variables

Regardless of its derivation, the structure of the Jacobian is defined by the test system and the choice of solution variables. Each variable is related to a column of dependent mismatches by the Jacobian. For a basic fundamental frequency controller this structure is relatively simple, the unified solution being defined in terms of the power-flow variables (X_{PF}) and a single dc voltage phasor (V_{dc}) for each FACTS device.

The resulting Jacobian therefore contains a power-flow block ($\frac{\delta M_{PF}}{\delta X_{PF}}$), diagonal harmonic blocks for each FACTS device ($\frac{\delta M_{I_{dci}}}{\delta V_{dci}}$), and off-diagonal mutual coupling blocks. Each of these harmonic blocks has a lattice structure corresponding to converter frequency transfers, themselves function of the PWM switching frequency. As such the Jacobian for a system containing two FACTS devices is of the form of Equation 4.25, a numerically derived example being included in Figure 4.8(a).

$$\begin{bmatrix} M_{PF} \\ M_{I_{dc1}} \\ M_{I_{dc2}} \end{bmatrix} = \begin{bmatrix} \frac{\delta M_{PF}}{\delta X_{PF}} & \frac{\delta M_{PF}}{\delta V_{dc1}} & \frac{\delta M_{PF}}{\delta V_{dc2}} \\ \frac{\delta M_{I_{dc1}}}{\delta X_{PF}} & \frac{\delta M_{I_{dc1}}}{\delta V_{dc1}} & \frac{\delta M_{I_{dc1}}}{\delta V_{dc2}} \\ \frac{\delta M_{I_{dc2}}}{\delta X_{PF}} & \frac{\delta M_{I_{dc2}}}{\delta V_{dc1}} & \frac{\delta M_{I_{dc2}}}{\delta V_{dc2}} \end{bmatrix} \begin{bmatrix} \Delta X_{PF} \\ \Delta V_{dc1} \\ \Delta V_{dc2} \end{bmatrix} \tag{4.25}$$

The real and imaginary component of each dc voltage harmonic (and the associated mismatch) are treated as separate solution variables. The real valued Jacobian elements relating these variables are therefore 2×2 tensors [10], having the form of Equation 4.26.

$$\begin{bmatrix} \Re(M_{Idc}) \\ \Im(M_{Idc}) \end{bmatrix} = \begin{bmatrix} J_{11} & J_{12} \\ J_{21} & J_{22} \end{bmatrix} \cdot \begin{bmatrix} \Delta\Re(V_{dc}) \\ \Delta\Im(V_{dc}) \end{bmatrix} \tag{4.26}$$

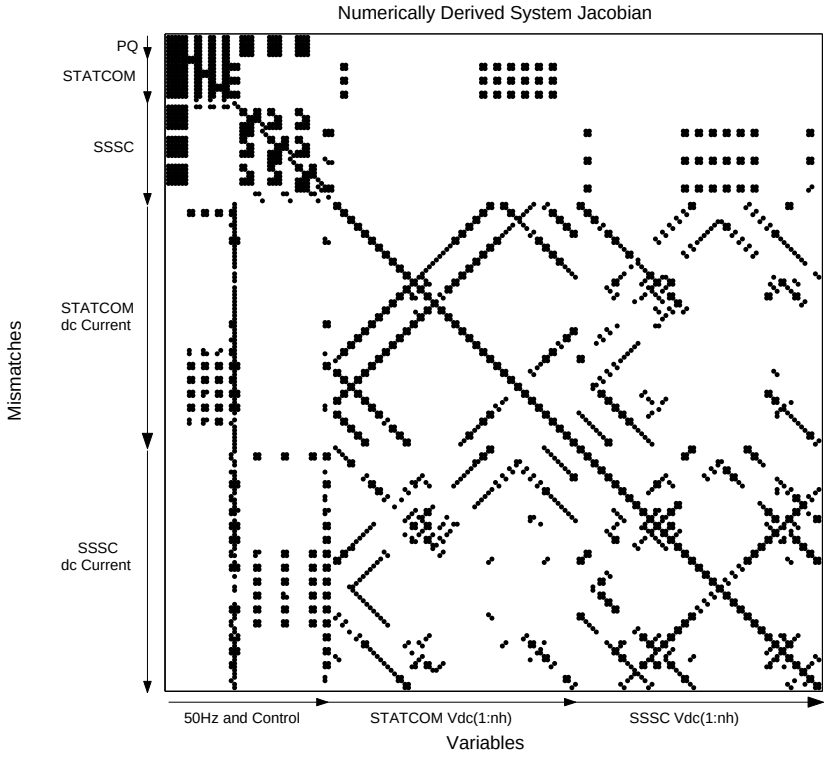

(a) System Jacobian for a two converter system with dc control variables

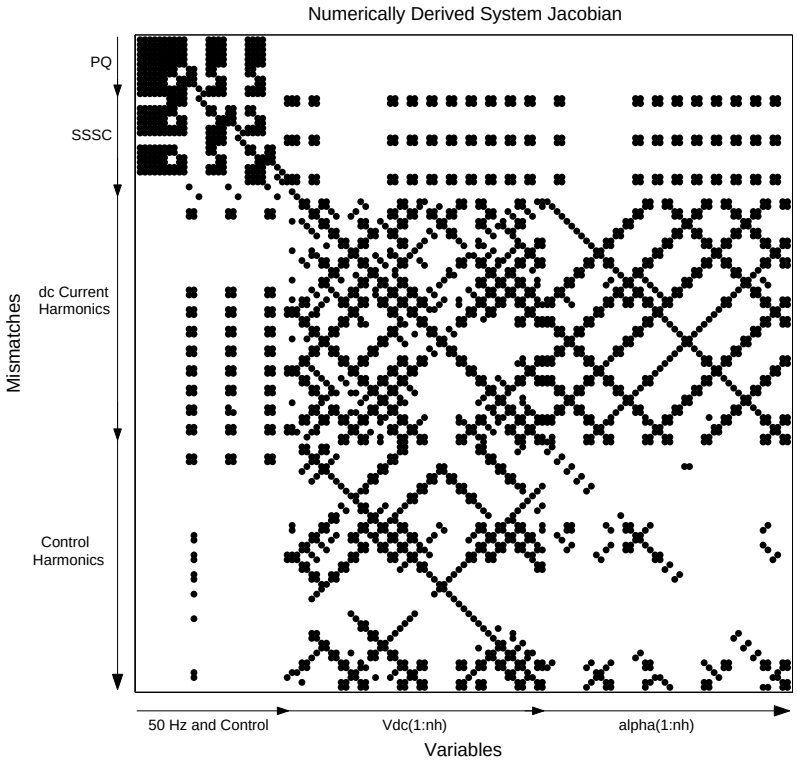

(b) System Jacobian for an SSSC with a distorted firing angle

Figure 4.8 Example system Jacobian matrices, $nh = 25$

Block structure: harmonic control transfers

The addition of harmonic control variables has a significant impact on the solution format; the converter transfer characteristic no longer being fully defined by the fundamental frequency operating point. As a result additional control variables (and the associated mismatches) must be incorporated within the Jacobian. Each FACTS device therefore contributes four harmonic blocks (each containing $2nh \times 2nh$ elements) corresponding to the system harmonics, controls, and any interactions between these (Equation 4.27).

$$\begin{bmatrix} M_{PF} \\ M_{I_{dc}} \\ M_{Con_h} \end{bmatrix} = \begin{bmatrix} \frac{\delta M_{PF}}{\delta X_{PF}} & \frac{\delta M_{PF}}{\delta V_{dc}} & \frac{\delta M_{PF}}{\delta \alpha_h} \\ \frac{\delta M_{I_{dc}}}{\delta X_{PF}} & \frac{\delta M_{I_{dc}}}{\delta V_{dc}} & \frac{\delta M_{I_{dc}}}{\delta \alpha_h} \\ \frac{\delta M_{Con_h}}{\delta X_{PF}} & \frac{\delta M_{Con_h}}{\delta V_{dc}} & \frac{\delta M_{Con_h}}{\delta \alpha_h} \end{bmatrix} \begin{bmatrix} \Delta X_{PF} \\ \Delta V_{dc} \\ \Delta \alpha_h \end{bmatrix} \tag{4.27}$$

In Equation 4.27 α_h refers to the harmonic component of a generic control variable (or variables). Figure 4.8(b) highlights this structure for a phase angle controlled SSSC; where the dc voltage and phase angle ripple are used as the harmonic solution variables.

4.5.3 Reducing computational expense

Calculating a Jacobian numerically requires $n + 1$ sequential perturbations and evaluations of the mismatch equations, where n is the total number of solution variables. From a computational perspective this is the most expensive process in the iterative scheme. In a full Newton solution this process and the associated matrix inversion is repeated at each iteration, however re-calculation is often unnecessary since the Jacobian does not necessarily change significantly between iterations. Keeping the Jacobian fixed when the solution is converging rapidly reduces the computational effort significantly. Hence during the power-flow initialisation the partial (power-flow alone) Jacobian is only recalculated when the rate of convergence (Equation 4.28) is less than a predetermined limit.

$$\Lambda_i = 1 - \frac{\sum M_i}{\sum M_{(i-1)}} \tag{4.28}$$

The full harmonic Jacobian is first derived after the fundamental frequency operating point has been found with the power-flow. This estimate of the linearisation is typically satisfactory for robust convergence and does not need to be updated at each iteration. This simplification is possible since while harmonics do affect the operating point they only do so to a small extent.

Further, since the Jacobian is typically sparse, the storage requirements can be reduced using sparse matrix manipulation techniques. Removing Jacobian elements (below a given tolerance, typically $0.01pu$ within this thesis) makes the linearisation approximate and increases the number of iterations required for convergence. However the comparatively small amount of computation required for each iteration makes this efficiency loss negligible. This combination massively

reduces the amount of computation required to reach convergence since only the smaller power-flow Jacobian is recalculated, while the massive harmonic Jacobian is only formulated once and handled using sparse routines.

4.6 MODEL EXTENSION TO OTHER NON-LINEAR DEVICES

If under given operating conditions a system component is deemed to be unsatisfactorily approximated using linearised analysis, additional non-linear models could be incorporated within the proposed formulation. Each additional non-linear component would need to be defined as either a harmonic current or voltage source each of which would be a function of a further set of solution variables. The dc side FACTS formulation makes any combined representation somewhat less intuitive, since the system would be composed of a combination of ac and dc ports, but does not limit the addition of further ac side non-linear injections.

The additional accuracy which could be obtained by using more advanced component models needs to be balanced against the increase in computational expense and the accuracy of system data at harmonic frequencies. Given the lack of harmonic information pertaining to system loads and transmission lines it is uncertain whether the possible gain in accuracy merits the associated reduction in efficiency.

4.7 CONCLUSIONS

This chapter has presented a generalised harmonic domain algorithm capable of representing hard-switched FACTS devices and the associated electrical systems, according to the models described in Chapter 3. The formulation is based around a three-phase power-flow used in conjunction with a harmonic representation. The harmonic solution reduces the linear ac and dc systems to a dc side harmonic equivalent for each FACTS device. This cuts the number of solution variables and reduces the size and computational expense of deriving the system Jacobian. This principle is applicable to a variety of ac and dc connection topologies with multiple PWM converters, providing a comprehensive, yet efficient, harmonic representation.

Chapter 5

MODEL IMPLEMENTATION, VALIDATION AND PERFORMANCE

5.1 INTRODUCTION

This chapter presents the MATLAB implementation and validation for the proposed FACTS device models. The models are applied to a basic 5-busbar test system containing a series (SSSC) and shunt (STATCOM) connected PWM converter, the results being compared against time domain simulation. The test system (see Figure 5.1 and Appendix B.1) is composed of a deliberately over-simplified transmission network (a balanced series equivalent impedance), two fixed impedance loads and a balanced Thevenin equivalent system representation. This system avoids the modelling difficulties associated with the more advanced transmission representations (see Section 6.2.2), making accurate validation of the proposed PWM converter model more straightforward.

The computational efficiency aspects, which differentiate time and harmonic domain steady-state analysis are considered, both in terms of the solution speed and convergence properties. These properties are heavily dependent on the nature of the system Jacobian, which is explored both as a visual measure of variable interaction and with the aim of improving model efficiency. Finally the interaction between the operating point and the harmonic solution is discussed, with reference to the advantages and disadvantages of using linearised analysis.

5.2 MODEL IMPLEMENTATION

5.2.1 Harmonic domain model

The proposed Newton solution was implemented within the MATLAB environment which, even though it includes extra computational overheads, provides a versatile (if somewhat inefficient) range of matrix handling functions. Of particular importance to harmonic analysis are the sparse matrix handling and matrix inversion facilities which deal with the large harmonic admittance and Jacobian matrices.

The program is structured to first form the harmonic and power-flow admittance matrices in per phase and per unit terms, either from basic RLC branch data, or an external file containing harmonic admittance data. These matrices are then re-structured according to Section 4.4.1,

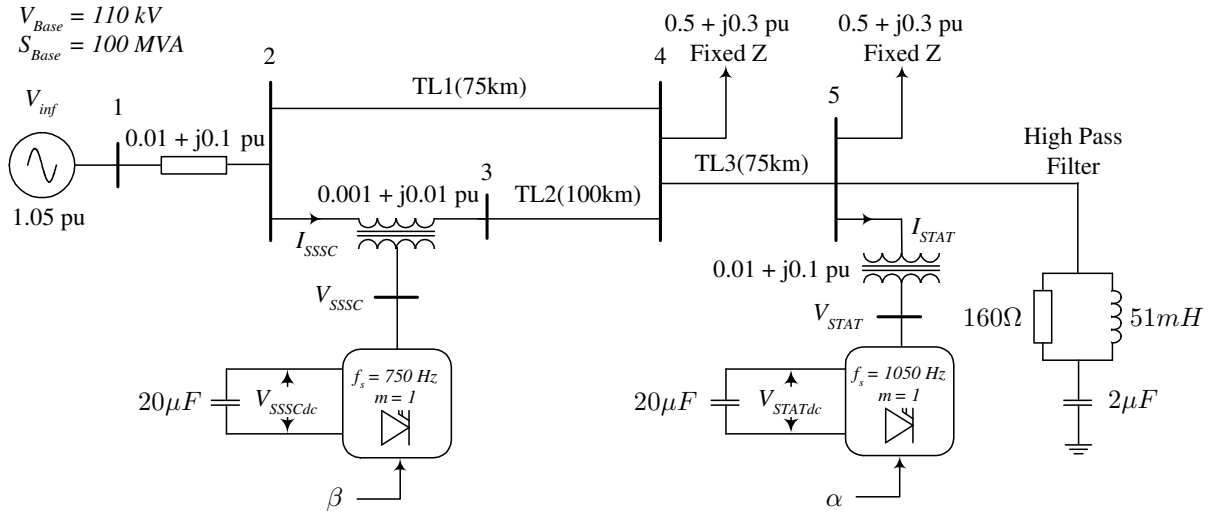

Figure 5.1 Single line diagram of the 5-busbar test system

including any associated matrix inversion. The full harmonic solution is then initialised by a three-phase power-flow, which is deemed to have converged when the 1-norm of the mismatch vector is less than 10^{-6}:

$$|M|_1 = \sum_{i=1}^{n} |M_i| \tag{5.1}$$

At this stage the full Jacobian is computed using numerical perturbation of the solution variable vector, and the mismatch function. The Jacobian is then inverted and used for the full harmonic solution, which is also deemed to have converged when the 1-norm of the mismatch vector is less than 10^{-6}. This effectively applies a universal convergence tolerance to a range of different magnitude mismatches, as such it does not guarantee the same level of convergence for all variables. This is not necessarily a disadvantage since it places more significance on larger harmonic terms, not wasting iterations on tiny harmonics of little consequence.

In order to generate typical output variables, such as ac terminal voltages and currents, post convergence processing is required. The dc formulation outputs each device's capacitor voltage, which is in turn transformed using the final operating point, the switching function and the system admittance to the desired ac output quantities.

5.2.2 PSCAD/EMTDC: Time domain model

In order to validate the accuracy of the harmonic domain model the results are compared with a suitable alternative approach, in this case time domain simulation [60]. The time domain is used as a benchmark, since it inherently incorporates both the system operating point and any associated waveform distortion. The primary difficulty with this approach is the long simulation lengths required to reach a steady-state solution while using what is essentially a transient

simulation package.

The steady-state time domain solution used for comparison was obtained using PSCAD/EMTDC, a commercial transient simulation package [7]. Each FACTS device is composed of a semi-ideal six switch GTO bridge (without snubbers) controlled using interpolated switching and a heavily filtered feedback network (hence dc control variables) [1]. Each FACTS device was interfaced to the ac system using three single-phase unsaturated transformers.

The time domain solution used a $5\mu s$ time step, a simulation length of $1s$ and snapshot startup to help overcome the computational burden of using such a small time step. All spectra are derived from the final $0.5s$ of data using an FFT, while all time domain waveforms correspond to the final cycle of the simulation.

5.3 VALIDATION AGAINST TIME DOMAIN SIMULATION

5.3.1 Balanced case

The balanced time (PSCAD) and harmonic (HDA) domain results computed compare very favourably, with both the operating point and harmonic solutions being practically identical. This similarity is best illustrated by the time domain comparison of the simulation results (Figure 5.2), which reflects the accuracy both at fundamental and harmonic frequencies. While small errors are apparent in regions containing a high $\frac{dV}{dt}$, these errors are primarily a result of harmonic phasor truncation. Errors of this type are a function of the highest harmonic of interest (nh).

When compared in the harmonic domain, with the dominant fundamental frequency terms removed, the results are equally satisfactory. Take for example the dc side voltage harmonics (Figure 5.3) and the ac terminal current harmonics which are derived from the dc voltage harmonics (Figure 5.4), which show that the time and harmonic domain results are practically identical. Note how the phase angle of extremely small magnitude harmonics is unreliable (e.g. the 30^{th} harmonic in Figure 5.3), this negligible effect is a result of the universal convergence criteria, truncated harmonic spectra and finite precision computation used all of which are biased against tiny harmonics. Further, the phase angle of a zero magnitude harmonic vector has little or no electrical significance.

Given the balanced nature of the ac system, each converter generates characteristic harmonics, that is harmonics which are derived directly from the switching function. As such ac side current distortion is present around multiples of the PWM switching frequency (f_s),

$$h_{distorted} = (jh_s \pm k) \ , j,k = 1,2,3,... \tag{5.2}$$

[1] Chapter 7 considers this critical control assumption in more depth.

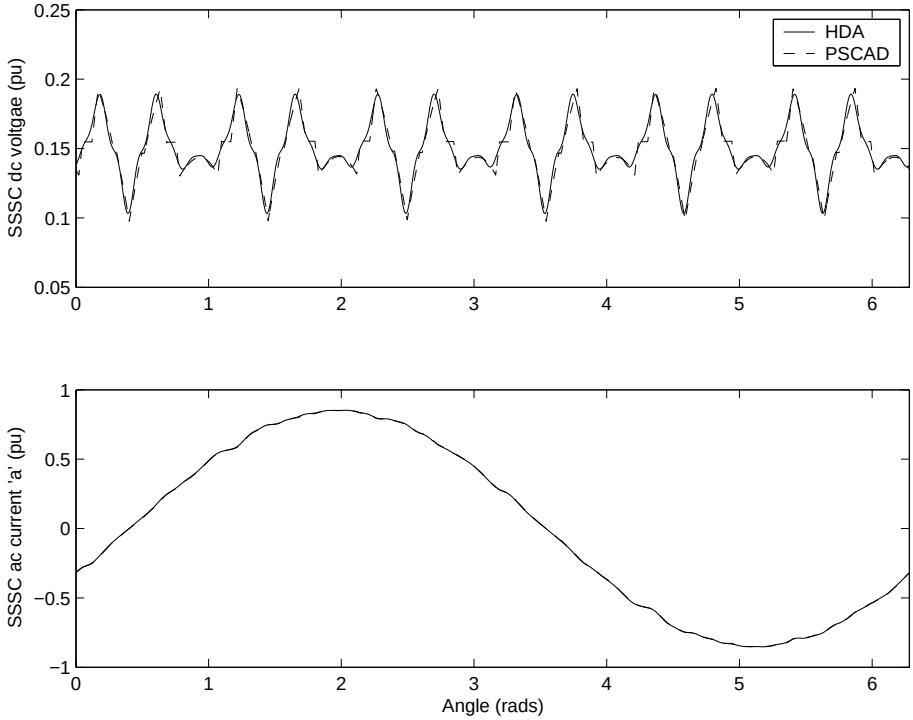

(a) SSSC results

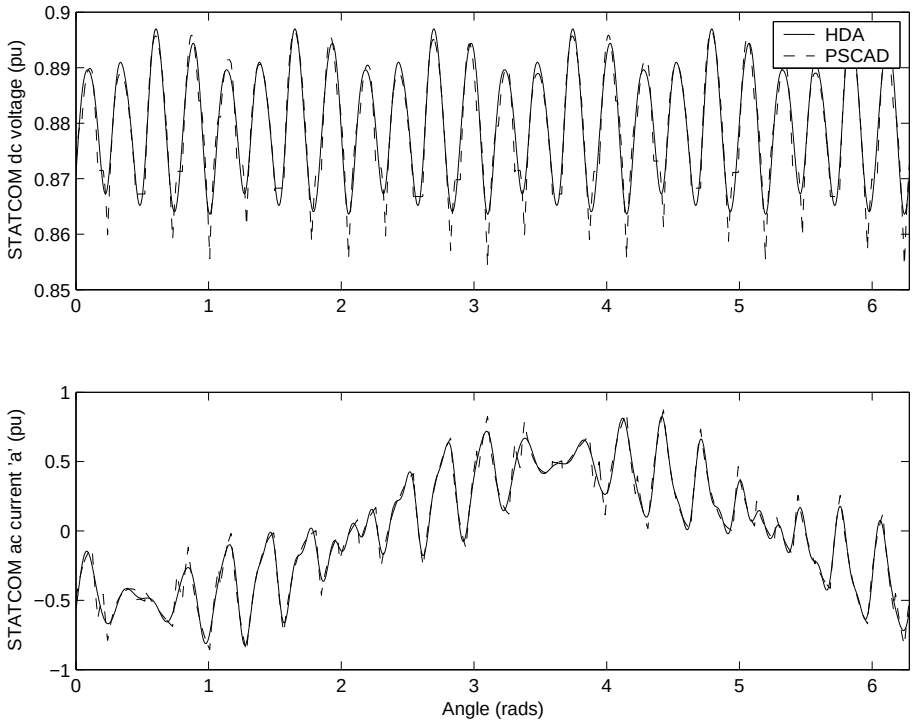

(b) STATCOM results

Figure 5.2 Time domain comparison for the balanced system

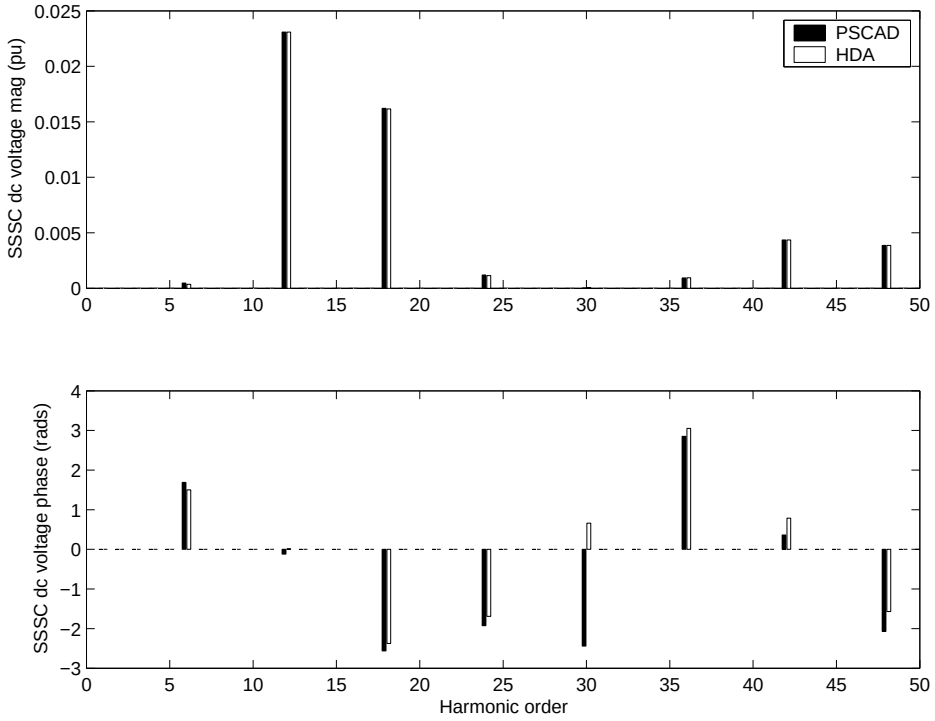

(a) SSSC results

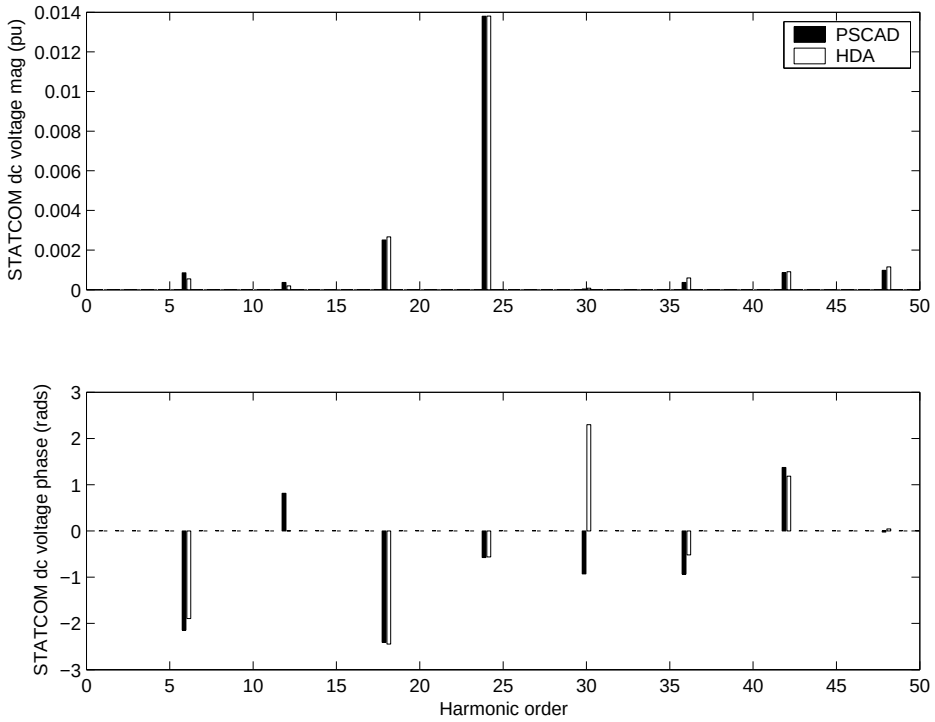

(b) STATCOM results

Figure 5.3 Harmonic domain comparison of the dc voltages for the balanced system

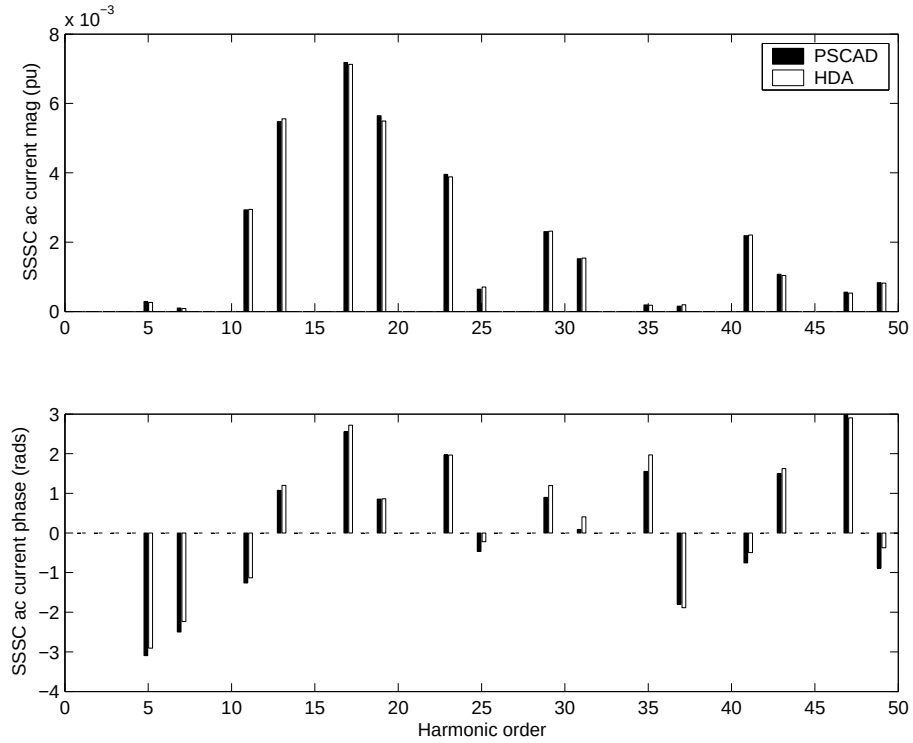

(a) SSSC results

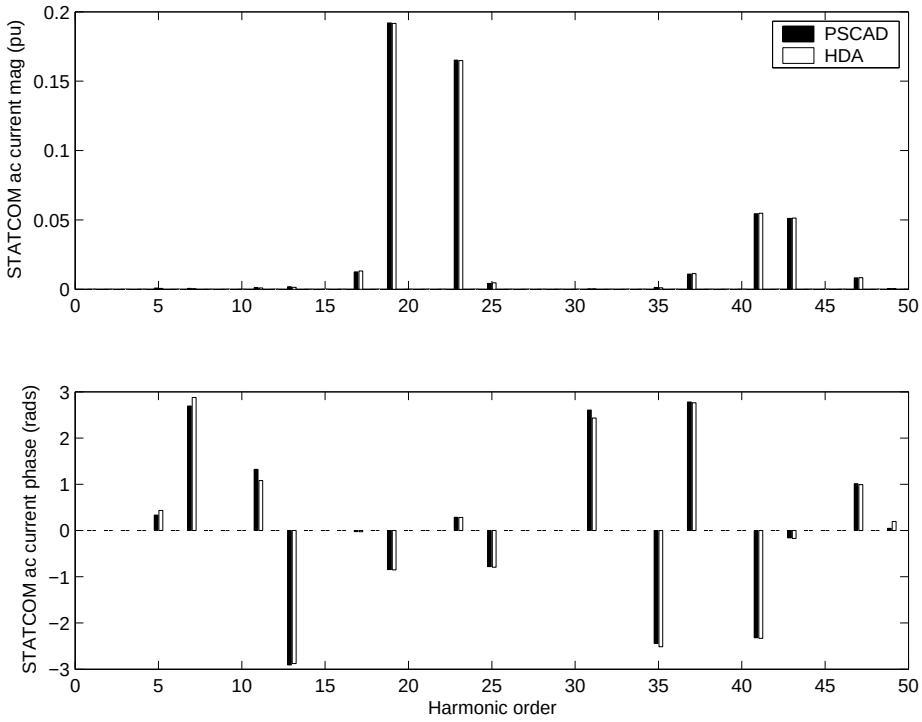

(b) STATCOM results

Figure 5.4 Harmonic domain comparison of the a-phase currents for the balanced system

where

$$h_s = \frac{f_s}{f_1}. \tag{5.3}$$

This is particularly evident in the ac current spectra for the STATCOM ($h_s = 21$), which has dominant terms at $h_s \pm 2$ and $2h_s \pm 1$ (i.e. 19^{th},23^{rd},41^{st} and 43^{rd} harmonics). These textbook characteristic spectra are complicated by the presence of the other converters' characteristic harmonics which are coupled, to differing extents, through the ac system. The magnitude of the interaction is a function of the converters' respective operating points, in this case the relatively small series injection ($V_{series} \sim 0.1pu$) does not rival the dominance of the shunt injection ($V_{shunt} \sim 1pu$). Hence the ac current spectra for the SSSC has large spectral components derived from the STATCOM's characteristic distortion, whereas the STATCOM current is almost exclusively a function of its own converter.

5.3.2 Unbalanced case

The presence of system imbalance leads to the generation of additional non-characteristic harmonics, these require either a three-phase or positive/negative sequence approach. To test the proposed method, which reflects a full three-phase formulation in the dc side variables, a grossly exaggerated imbalance in the leakage impedance of the connection transformer was included. This amounted to a 50% increase in the a-phase impedance for the STATCOM and the b-phase impedance for the SSSC. The result is a 5% negative sequence current imbalance at the STATCOM and a very small imbalance in the SSSC current (since the series transformer leakage impedance is small in comparison with the line impedances).

This imbalance does not result in any significant degradation in the quality of the match between the two simulation techniques, the time domain results still being almost indistinguishable (Figure 5.5). Likewise, the frequency domain comparison of the dc voltages shows good agreement (Figure 5.6). The dc voltage now contains a slew of small uncharacteristic harmonic terms and a large second harmonic component. This second harmonic component is reflected in the ac terminal currents as a third harmonic component, now present in both converters spectra (Figure 5.7).

5.4 MODEL PERFORMANCE

5.4.1 Convergence properties

While accurate agreement with PSCAD/EMTDC is important, this in itself does not advance harmonic analysis. Equally critical is the rate and manner in which convergence is achieved. In general, given appropriate power-flow initialisation, the proposed harmonic model reliably converges to a solution consistent with time domain simulation using PSCAD/EMTDC. The rate of convergence is dependent on the type of system being simulated, in particular the number

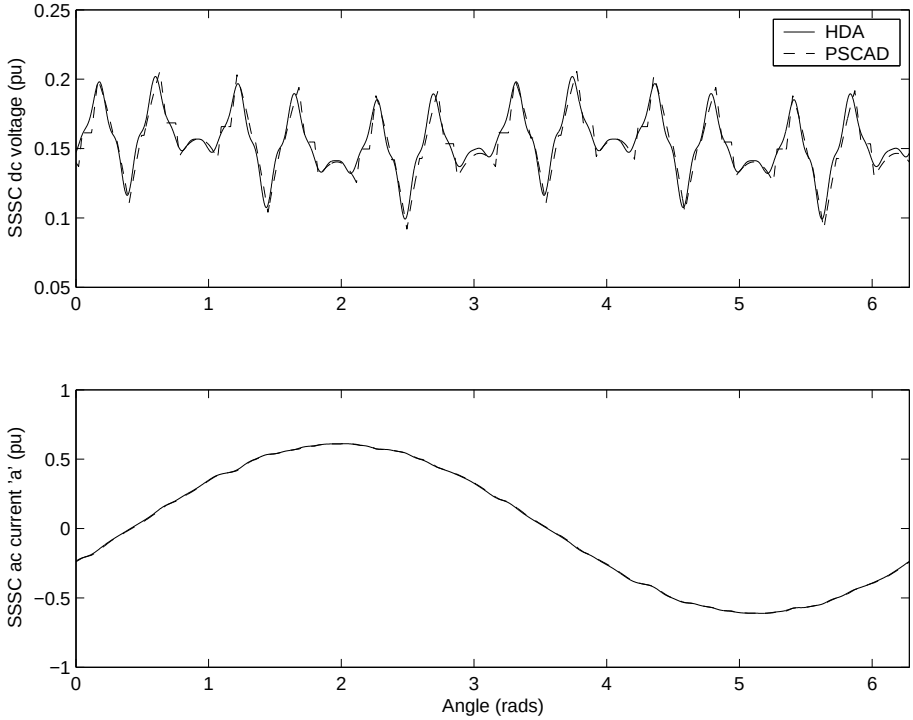

(a) SSSC results

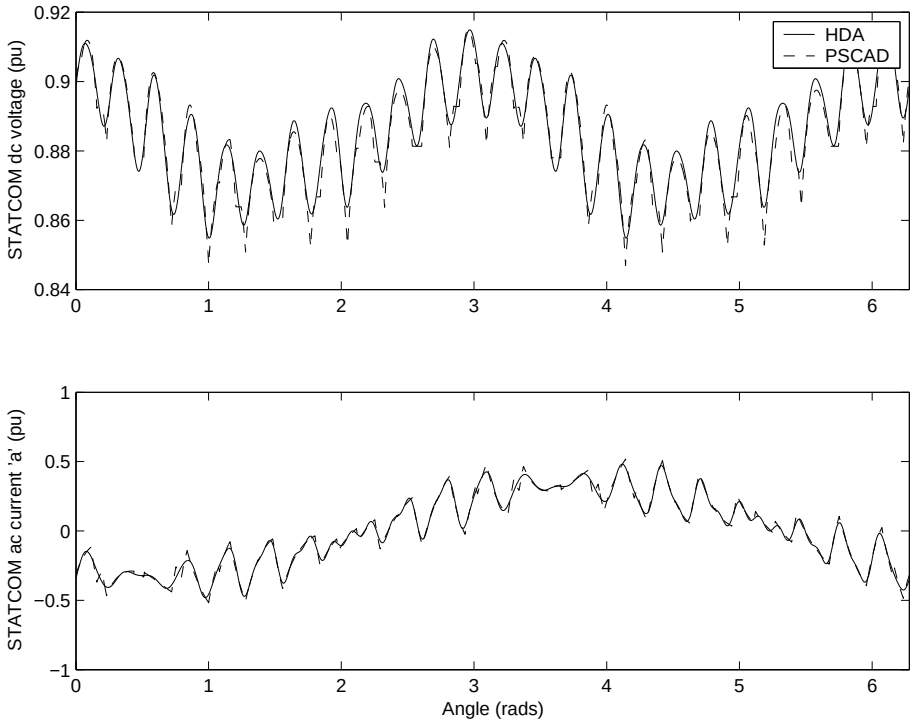

(b) STATCOM results

Figure 5.5 Time domain comparison for the unbalanced system

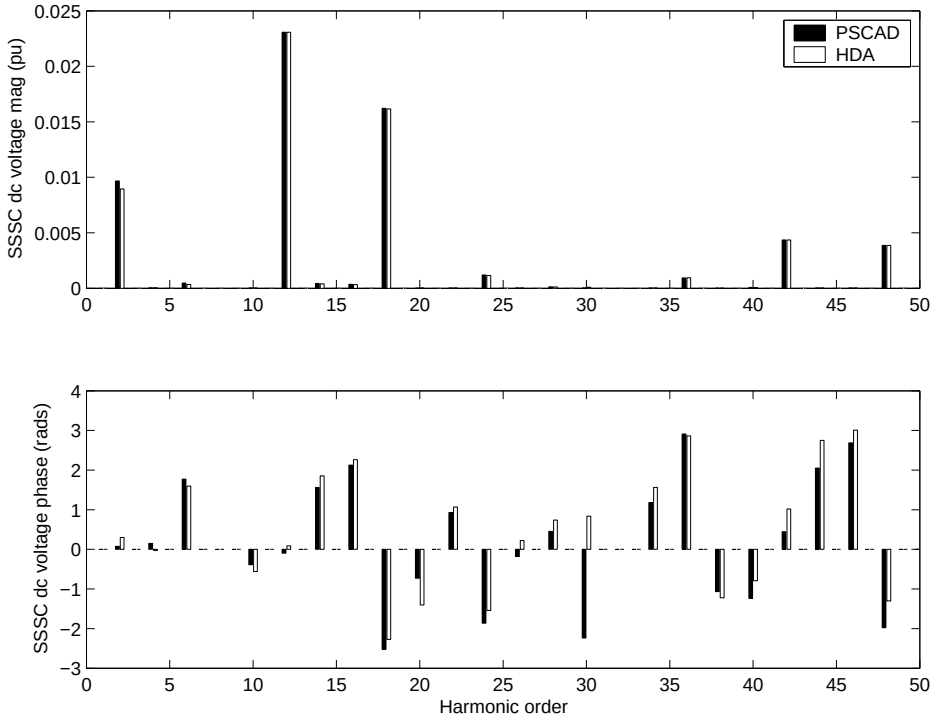

(a) SSSC results

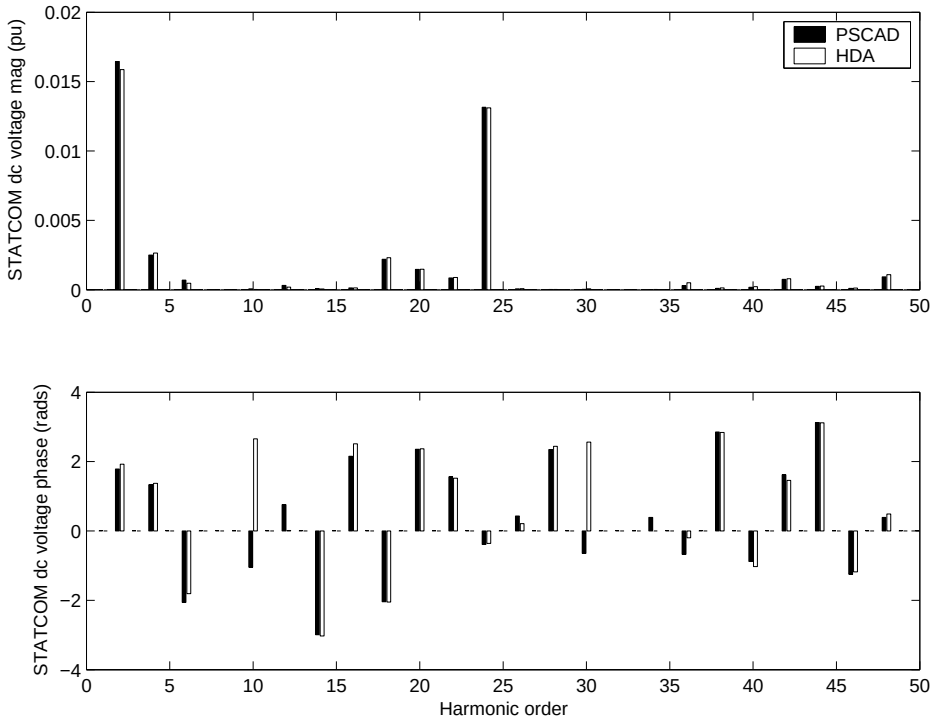

(b) STATCOM results

Figure 5.6 Harmonic domain comparison of the dc voltages for the unbalanced system

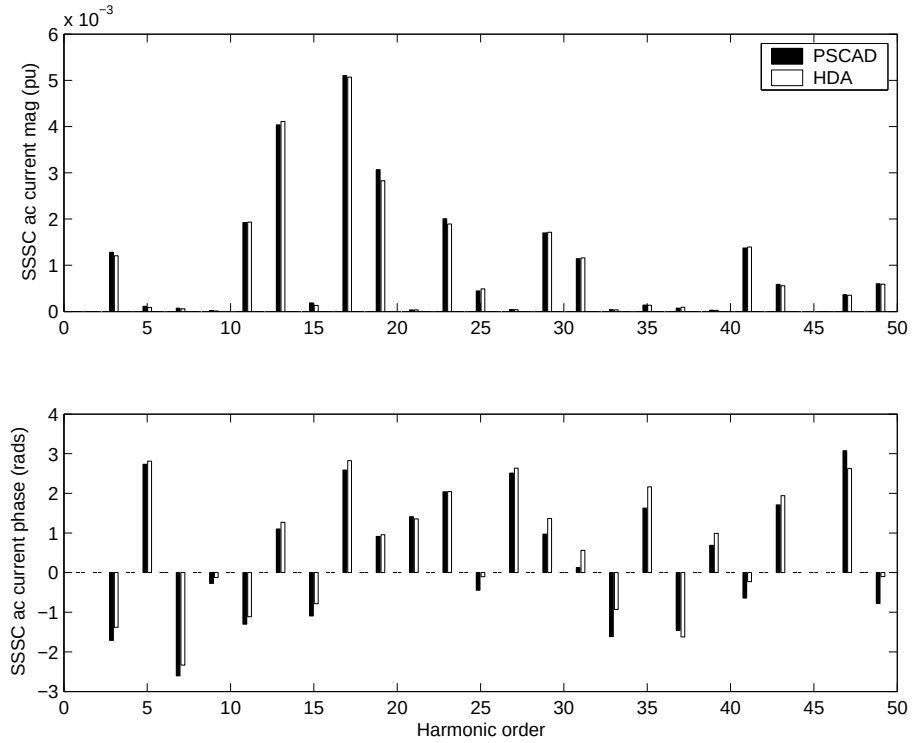

(a) SSSC results

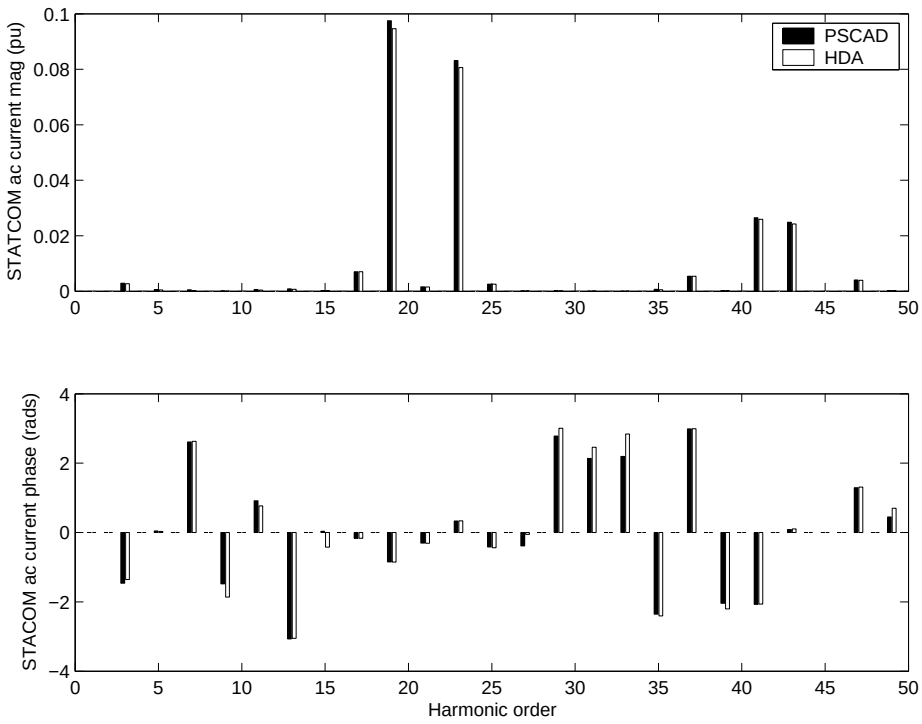

(b) STATCOM results

Figure 5.7 Harmonic domain comparison of the a-phase currents for the unbalanced system

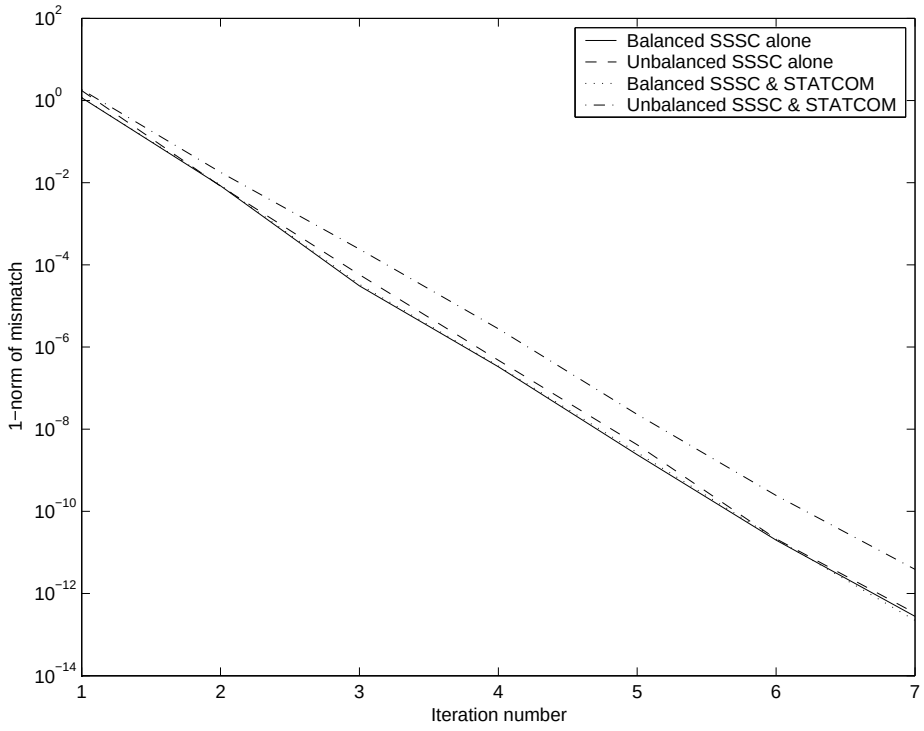

Figure 5.8 Model convergence using a full Newton solution

of converters and level of imbalance. The rate of convergence is considered for test systems containing one or two FACTS devices, operating under either balanced or unbalanced conditions.

All four cases converge very rapidly (approximately two orders of magnitude per iteration) when the full Jacobian is recalculated at every iteration (Figure 5.8). Little difference is observed between the rate of convergence for the first three cases, the unbalanced dual converter case converging slightly slower. However, since the Jacobian only needs to be an estimate of the linearisation it is unnecessarily wasteful to update it at each iteration, instead the model typically uses a fixed Jacobian. This results in a significantly slower rate of convergence for all test cases (Figure 5.9).

The rate of convergence using a fixed Jacobian differs markedly from simulations using a full Newton solution, each test system behaving distinctively. Initially the first three test systems converge at a similar rate to that achieved when updating the Jacobian, before the rate of convergence drops after two (balanced SSSC+STATCOM case) or three (single converter cases) iterations. The unbalanced two converter case never achieves rates of convergence similar to the those obtained when the Jacobian was updated, converging at a slower near constant rate. This illustrates how the knee point where the rate of convergence drops off occurs progressively earlier as the number of converters or the amount of system imbalance is increased. This reduction in the rate of convergence reflects an increase in the coupling between the non-linear power-flow mismatches and the linear harmonic transfers.

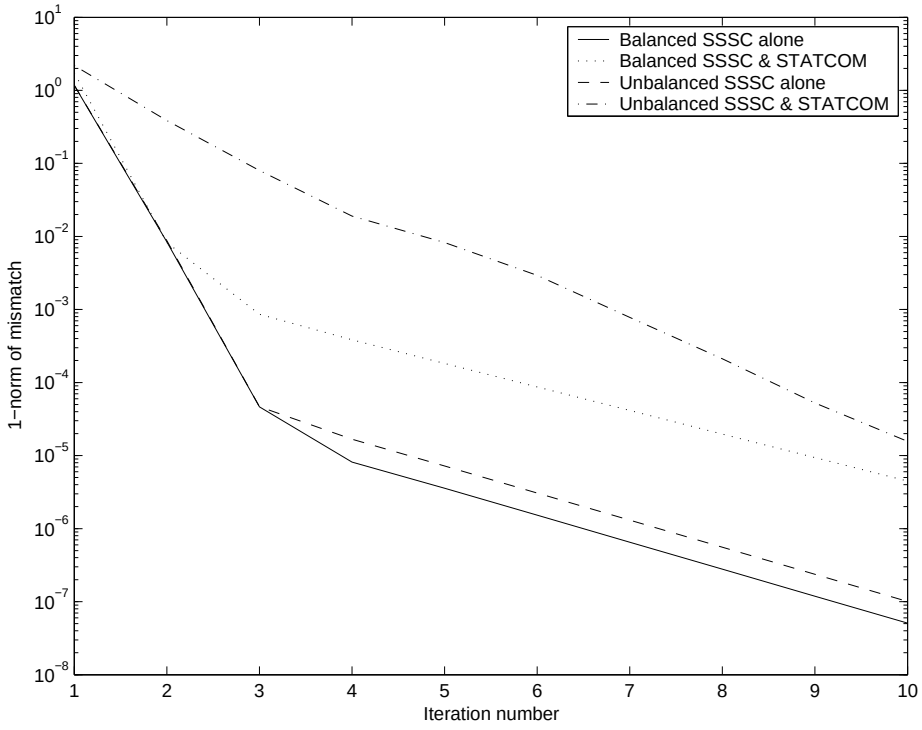

Figure 5.9 Model convergence using a fixed Jacobian

Simulation speed

While the rate of convergence does deteriorate for fixed Jacobian solutions it is still more efficient to use this deteriorating estimate of the Jacobian. This is because each iteration takes a fraction of the time required to recalculate the Jacobian, making it more efficient to use an increased number of less accurate iterations.

The entire iterative component of the solution therefore takes a comparatively small proportion of the full solution ($\sim 5\%$). The vast majority of each simulation is spent formulating the system admittance ($\sim 30\%$) and numerically deriving the full Jacobian once ($\sim 40\%$). Hence the size of these matrices is the primary influence on simulation speed. The number of elements in both matrices are a function of the highest harmonic of interest (nh). In addition, the Jacobian is also dependent on the number of converters while the admittance matrices are a function of the ac system size. Figure 5.10 summarises the effect these variables have on solution speed; all are solved using a fixed Jacobian and a $2.2GHz$ PC. For comparison the long run time domain simulation used for validation takes approximately $180s$ to reach a steady-state solution.

Interestingly while the solution time is approximately dependent on the highest harmonic of interest (nh) squared, it appears to be linearly dependent on the number of isolated FACTS device dc buses. This can be accounted for by the exceedingly sparse nature of the off-diagonal Jacobian terms for these simplified cases (see Figure 5.11), which leads to a less than square law increase in the number of significant Jacobian elements given a change in the number of

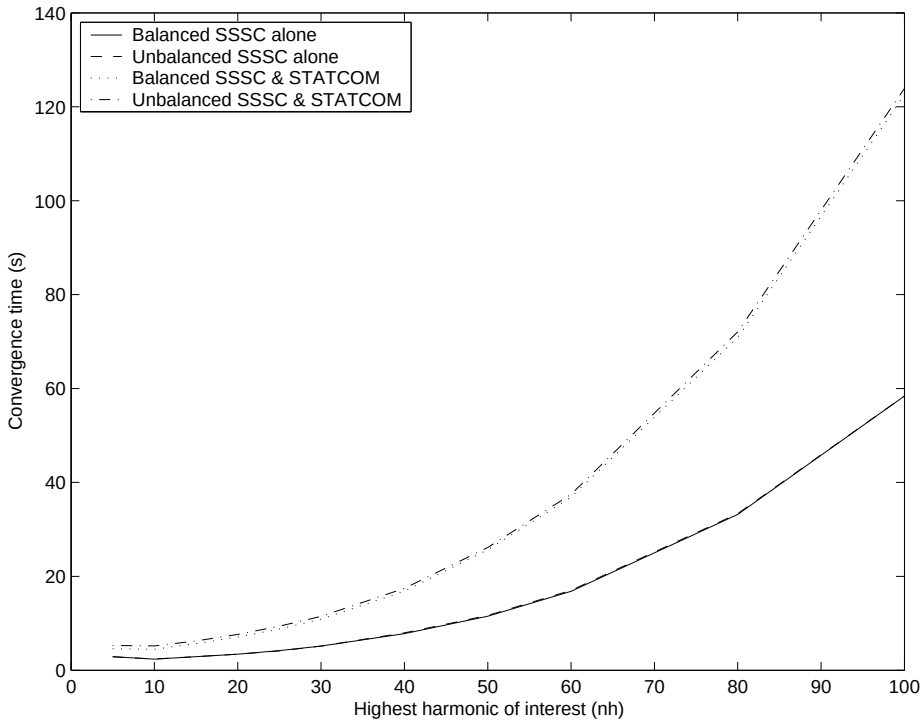

Figure 5.10 Solution speed using a 2.2GHz PC

converters.

System imbalance does not have a very significant impact on the solution time since the Jacobian inherently includes a full three-phase representation under both balanced and unbalanced cases. Any small differences are caused by the additional iterations required to reach convergence in unbalanced cases.

5.4.2 Jacobian characteristics

In addition to the critical role the Jacobian plays in the iterative solution process it also provides a visual measure of the dependence/sensitivity of the solution to particular system variables. The dc side mismatch formulation leads to a Jacobian structure that is different to previously described HVdc modelling techniques [10, 34] which explicitly incorporated ac side quantities. In the new formulation the dc harmonic block contains both the dc side admittance (on-diagonal) and the harmonic transfers (off-diagonal), these inherently incorporate the ac system admittance (Figure 5.11). This makes assessing the amount of interaction between FACTS devices straightforward, but makes visualising the impact of the ac system less intuitive.

The Jacobian is typically quite sparse ($\sim 95\%$); especially in simplistic test cases which do not have much inter-device harmonic interaction. Those terms which are significant can be broadly grouped according to their cause, of particular interest are the following blocks:

A & B Each FACTS device contributes the dominant diagonal harmonics terms, which corre-

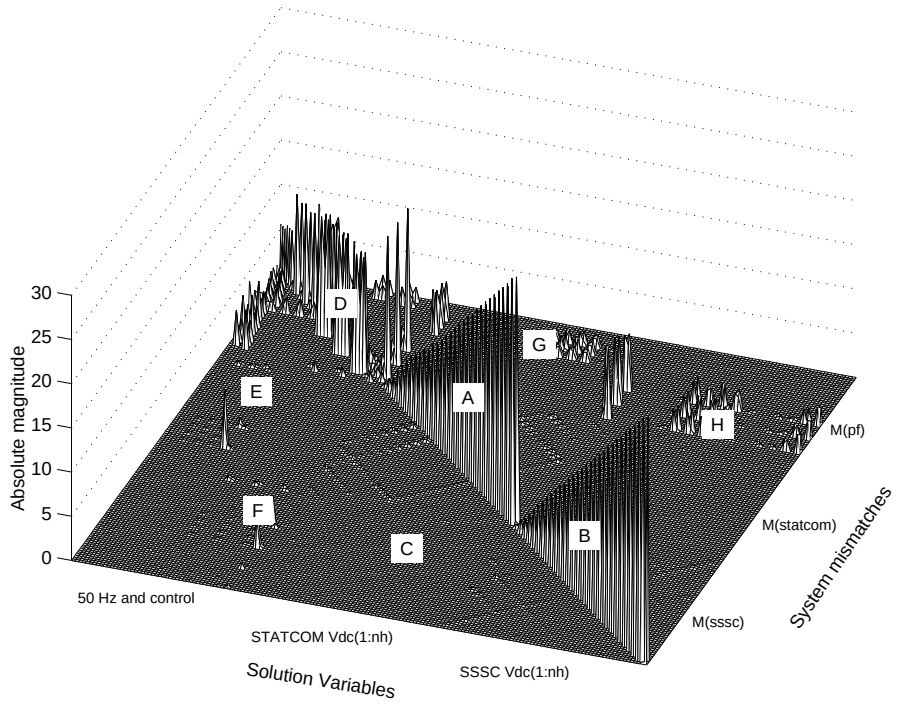

Figure 5.11 Numerically derived full Jacobian for the balanced two converter case, $nh = 30$

spond to the harmonic frequency admittance of the dc side capacitor. The linear ramp of terms marked as A relating to the STATCOM dc side capacitor, while B corresponds to the SSSC. Each capacitors' complex admittance leads to the 2×2 tensor at each frequency being dominated by the reverse diagonal terms (i.e. a real voltage transfers to an imaginary current).

C The remainder of the harmonic section of the Jacobian is composed of a harmonic lattice structure, which relates frequencies coupled by the switching converter. Figure 5.12 presents an expanded view of the double diagonal structure, spaced according to the converter switching frequency. Since the Jacobian reflects two transfers across the converter (see Figure 4.6) the lattice is spaced according to $h_s \pm 2$, $2h_s \pm 1$, $3h_s \pm 2, 4$, ... [3] multiplied by $dc \pm 1$, ... This leads to the first three lattices being placed at $h_s \pm 3$, $2h_s$ and $3h_s \pm 3$ respectively, for the balanced single level PWM converter with a switching harmonic of h_s and a modulation index of one.

D This block of large terms corresponds to the fundamental frequency power-flow. The relatively large magnitude of these components reflects the large difference in sensitivity between the fundamental and harmonic solutions. The harmonic terms are almost negligible in comparison with the power-flow. In addition to containing the largest terms, the power-flow block is also the most non-linear.

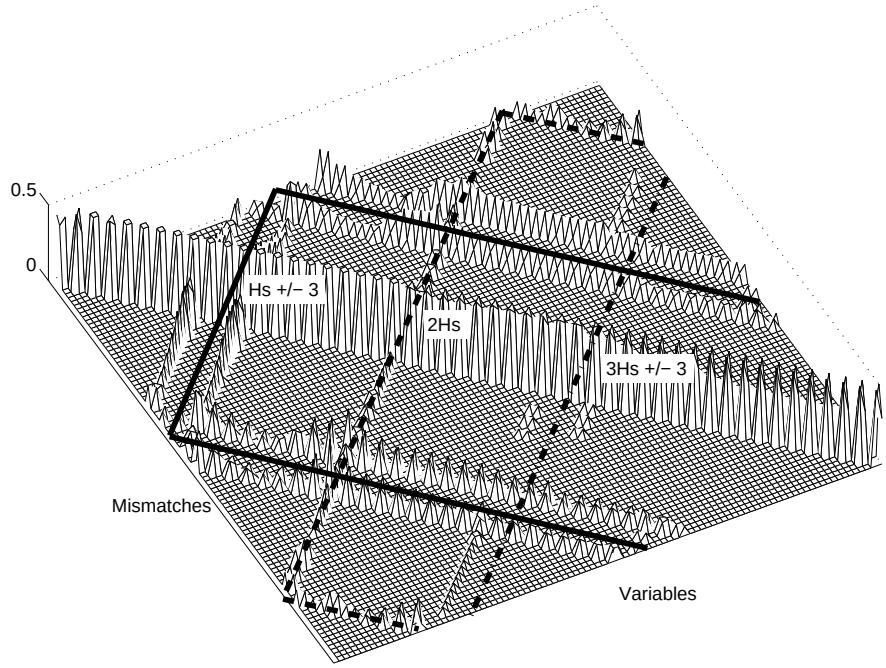

Figure 5.12 Enlargement of the harmonic lattice structure for the STATCOM, $nh = 50$

E & F These blocks reflect the sensitivity of the harmonic solutions to the operating point, in particular the terminal current for the STATCOM (E) and the SSSC series current (F). Larger terms corresponding to the modulation index and phase angle are also visible.

G & H The reverse is also true, blocks G & H reflecting how the power-flow and control mismatches are sensitive to harmonic solution variables. In this case the most sensitive variables are the real and reactive power at each FACTS terminal, both of which are a function of those dc voltage harmonics which are modulated down to fundamental frequency.

5.5 CAPACITOR SIZE, UNBALANCE, AND LINEARISED SOLUTIONS

While the proposed model behaves in a non-linear fashion taking 6-10 iterations to converge (see Figure 5.9), the harmonic portion of the solution is in fact linear given the assumption of a fixed operating point. A number of authors [18, 19, 20, 50] have taken advantage of this linearity to create computationally efficient linear small-signal converter models. However the accuracy of these techniques is not only limited by the magnitude of any applied distortion, but also by the accuracy of the operating point around which the converter system is linearised.

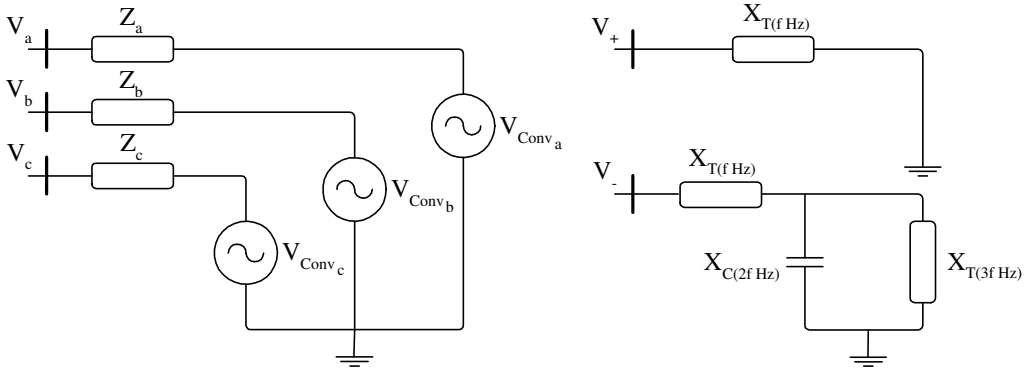

(a) Decoupled voltage source representation (b) Realistic sequence representation

Figure 5.13 PWM VSC FACTS representation in a three-phase power-flow

5.5.1 Operating point for linearisation

Describing the operating point for a switching converter is not necessarily trivial, since coupling between the fundamental and harmonic frequency variables complicates any definition. Madrigal [19] ignores these transfers using a classic power-flow definition for the operating point of the STATCOM. In contrast Hume [18] and Saniter [20] use an operating point generated with a long run time domain simulation using PSCAD/EMTDC. This technique, while extremely inefficient and redundant [2], improves accuracy by accounting for the effect of harmonic distortion on the operating point.

Neither approach is ideal, however if the realistic power-flow option is adopted it should account for the impact system unbalance has on converter harmonic sequence coupling. This is typically not the case, as common three-phase power-flow formulations for PWM VSC FACTS devices are based on the assumption of a ripple free dc voltage (e.g. Acha [63]). This results in the common three-phase decoupled voltage source equivalent (Figure 5.13(a)).

The limitations of this power-flow equivalent can be illustrated by considering the operating point shift observed for the 5-busbar test system. Tables 5.1 and 5.2 compare the operating point generated for initialisation (a 3-phase power-flow with perfect dc) with the final operating point calculated using the full harmonic Jacobian (this includes voltage source coupling resulting from dc ripple). For the balanced case the difference in operating point is negligible, reflecting how under balanced circumstances the assumption of ripple free dc is valid (at least at frequencies near fundamental). However the presence of sequence imbalance (exactly what three-phase power-flows are designed to analyze) causes a noticeable discrepancy in STATCOM terminal currents, questioning the validity of this assumption.

The difference in the unbalanced case reflects how the assumption of ripple-free dc isolates the

[2]Using a PSCAD/EMTDC generated operating point is redundant in that the harmonic system is solved twice, once in the time domain and once again in the linearised harmonic domain, making the harmonic domain solution unnecessary.

Table 5.1 Operating point variation: Balanced case

		STATCOM			
Solution	V_5^+	I_{STAT}^+	m	α	$V_{dc(0)}$
PF	$0.900\angle -27.32°$	$0.364\angle 55.43°$	1.0	$-27.83°$	0.8820
PF + HDA	$0.900\angle -27.32°$	$0.364\angle 55.48°$	1.0	$-27.80°$	0.8799
		SSSC			
	V_2^+	V_3^+ I_{SSSC}^+	m	α	$V_{dc(0)}$
PF	$1.000\angle -4.853°$	$1.055\angle 3.088°$ $0.600\angle -22.96°$	1.0	$67.49°$	0.1496
PF + HDA	$1.000\angle -4.848°$	$1.055\angle 3.094°$ $0.600\angle -22.95°$	1.0	$67.51°$	0.1507

Table 5.2 Operating point variation: Unbalanced case

		STATCOM			
Solution	$V_5^{a,b,c}$	$I_{STAT}^{a,b,c}$	m	α	$V_{dc(0)}$
PF	$0.889\angle -27.23°$	$0.347\angle 53.96°$			
	$0.905\angle -147.46°$	$0.373\angle -63.97°$	1.0	$-27.94°$	0.8880
	$0.905\angle -267.45°$	$0.374\angle -184.19°$			
PF + HDA	$0.887\angle -27.62°$	$0.350\angle 51.70°$			
	$0.901\angle -147.12°$	$0.359\angle -63.16°$	1.0	$-27.94°$	0.8861
	$0.912\angle -267.38°$	$0.385\angle -182.81°$			
		SSSC			
	$V_2^{a,b,c}$	$V_3^{a,b,c}$ $I_{SSSC}^{a,b,c}$	m	α	$V_{dc(0)}$
PF	$0.998\angle -4.81°$	$1.055\angle 3.17°$ $0.600\angle -23.49°$			
	$1.000\angle -124.87°$	$1.055\angle -117.06°$ $0.598\angle -142.75°$	1.0	$67.48°$	0.1504
	$1.000\angle -244.88°$	$1.056\angle -236.91°$ $0.602\angle -262.66°$			
PF + HDA	$0.998\angle -4.86°$	$1.058\angle 3.27°$ $0.610\angle -23.79°$			
	$1.000\angle -124.81°$	$1.055\angle -117.24°$ $0.590\angle -143.38°$	1.0	$67.49°$	0.1514
	$1.001\angle -244.89°$	$1.053\angle -236.81°$ $0.603\angle -261.70°$			

power-flow from the dc side harmonic admittance. This is not adequate in the presence of negative sequence currents since the converter couples the fundamental frequency imbalance to the dc side second harmonic, and then in turn back to the ac side third harmonic. Both of these harmonic transfers contribute to the negative sequence impedance presented by the converter: the dc capacitor at the second harmonic and the connection transformer at the third harmonic (Figure 5.13(b)). This makes the power-flow a function of two harmonic impedances; something which the decoupled three-phase voltage source equivalent does not account for. This reduces the accuracy of the operating point around which a system is linearised [3].

5.5.2 A linearised solution

While this difficultly can degrade low frequency accuracy the negligible shifts in the converter control variables (α and m), even in unbalanced cases, implies that the harmonic transfers for a converter can be satisfactorily characterised using a linearised model based on a basic power-flow operating point. This type of analysis can be illustrated by fixing the operating point after

[3]The proposed iterative solution avoids this inaccuracy by defining each voltage source as function of dc side ripple and converter switching function, see Section 4.3.3.

initialisation, and then using a single iteration of the harmonic solution. The harmonic solution obviously converges ($|Mismatch| \sim 10^{-10}$) since the harmonic solution in isolation is linear. The results are very satisfactory for the balanced case (Figure 5.14(a)), but contain an extremely large inaccuracy in low order harmonics for the unbalanced case (Figure 5.14(b)).

The degradation in the accuracy of the linearised results highlights the impact of using a fixed operating point which does not account for power/harmonic frequency inter-dependence. The magnitude of this error can be reduced by linearising the effect of harmonic distortion on the operating point. This type of linearisation [4] is adopted by Wood [50] and permits small-signal changes in the fundamental frequency operating point. Figure 5.15 demonstrates the improvement in accuracy which can be obtained using this type of technique, which is equivalent to a single full iteration of the Newton solution. The resultant dc spectra being satisfactory for the unbalanced case.

5.5.3 Capacitor size

The size of the dc side capacitor has a significant role in determining the amount of interaction which exists between the fundamental and harmonic solutions. Large capacitors reduce the dc second harmonic ripple and hence its impact on the negative sequence impedance of the converter. This makes the isolated power-flow/linearized approach more appropriate, even in unbalanced cases. For example, if the size of both dc capacitors in the unbalanced 5-busbar test system is increased by a factor of ten the linearised approach gives satisfactory results, even for the dc side second harmonic (Figure 5.16).

Unfortunately assessing when this assumption is valid is troublesome, particularly since the relationship between second harmonic dc ripple and capacitor size is complicated by low frequency system resonances. The first resonance occurs between the capacitor and the connection transformer at a frequency defined by their relative impedances transferred to the ac side. When this is applied to the STATCOM in the 5-busbar test system, the resultant resonance occurs at fundamental frequency when the capacitor is $13.9\mu F$. This resonance corresponds with the peak dc side second harmonic ripple (Figure 5.17).

5.6 CONCLUSIONS

Using the MATLAB environment, a practical harmonic domain representation for FACTS devices has been presented and successfully validated against time domain simulation. The nonlinear Newton formulation has been validated for a two converter test system which included shunt and series connected switching elements. The model accurately assesses the operating point and harmonic distortion present for both balanced and unbalanced cases. Satisfactory

[4] Obtaining this linearisation analytically is challenging, here it is obtained numerically for illustrative purposes.

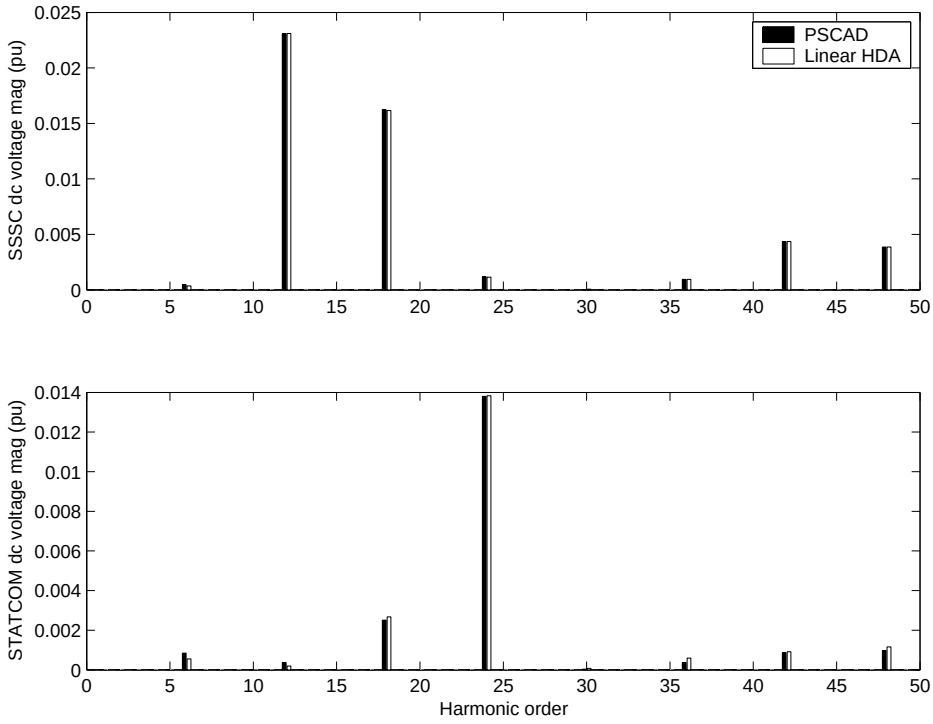

(a) Balanced results

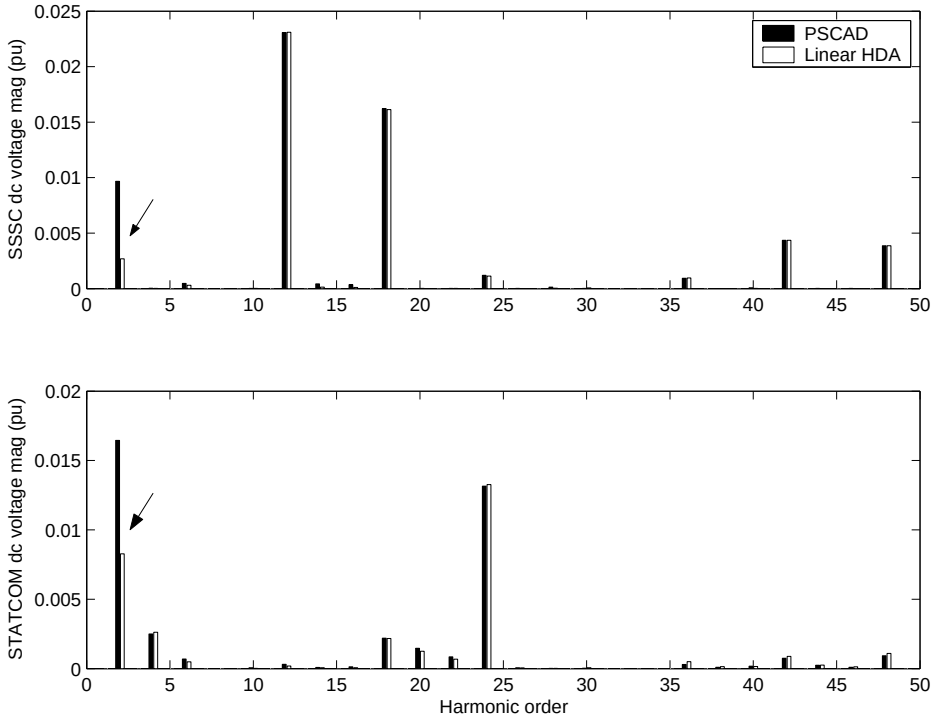

(b) Unbalanced results

Figure 5.14 Harmonic domain illustration of the limitations of a linearised harmonic solution based on a fixed operating point which neglects harmonic/power-flow interaction

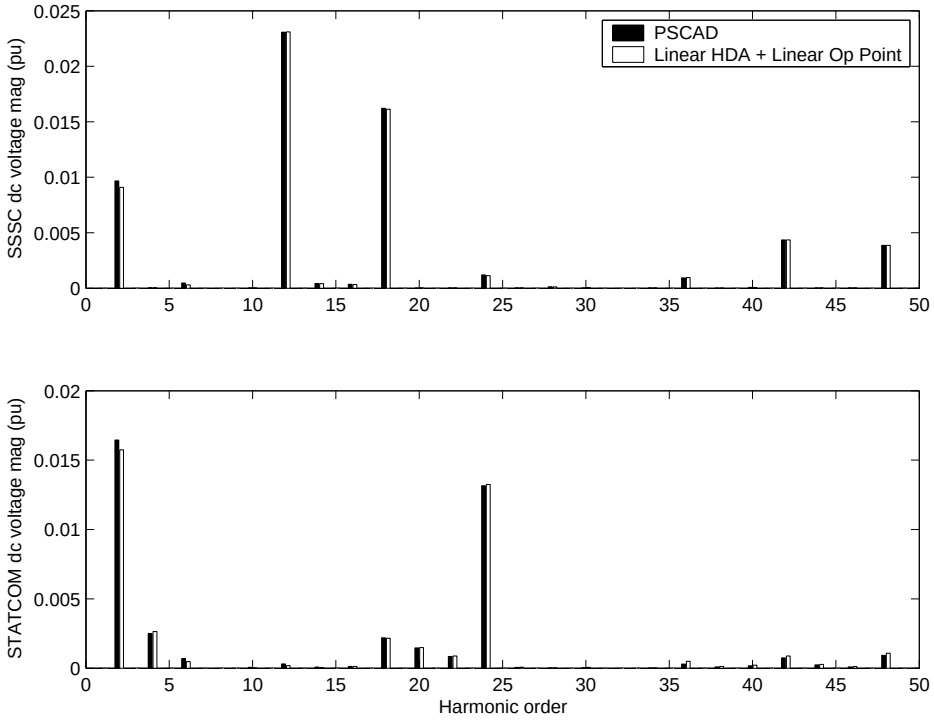

Figure 5.15 Accuracy improvement obtained, for the unbalanced case, using an operating point which is linearly dependent on the harmonic solution

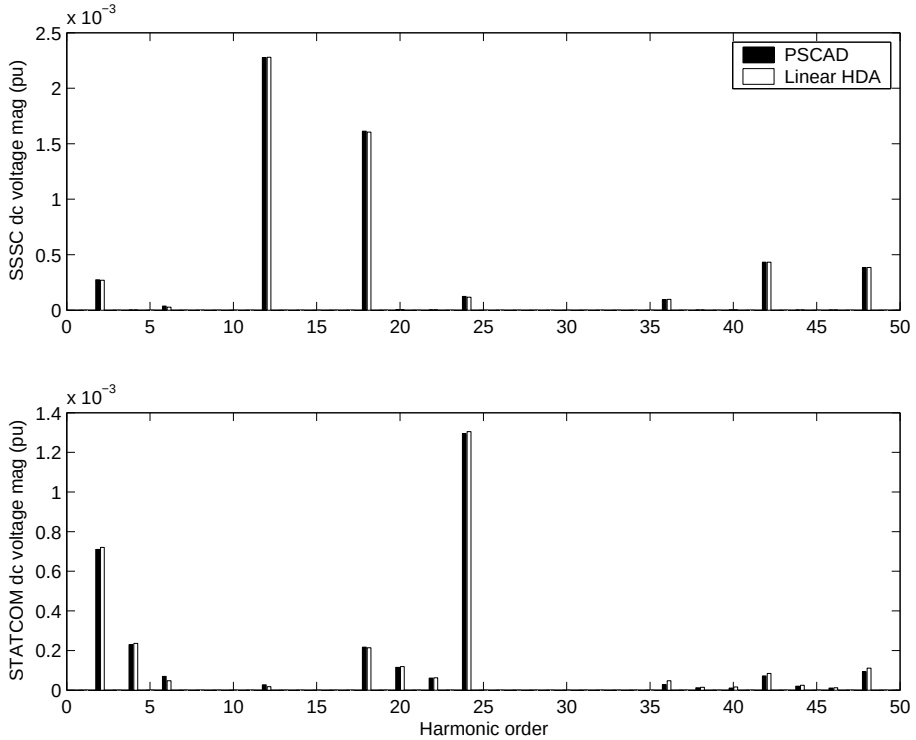

Figure 5.16 Illustration of the linearised techniques accuracy for idealised unbalanced cases with limited dc ripple

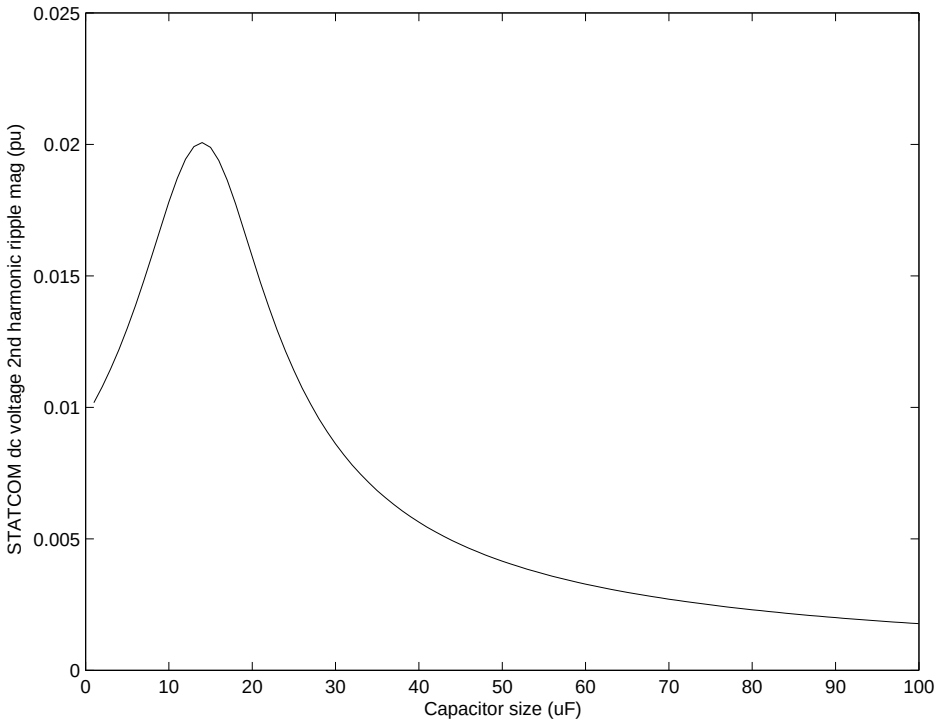

Figure 5.17 System resonance and the associated impact on second harmonic dc ripple

convergence was achieved using either a full Newton solution or with a fixed harmonic Jacobian. The second, fixed Jacobian option, being more efficient given appropriate initialisation.

System imbalance has been shown to increase the coupling between the harmonic solution and the operating point, of particular importance was the effect the dc capacitor has on the negative sequence impedance of the converter. This significant effect is not properly modelled by typical power-flow models, which assume no dc side distortion is present. The resultant error poses a problem for linearised models which neglect operating point variation, but justifies the use of an iterative solution in all but idealised situations.

By applying a fixed Jacobian to the iterative solution the efficiency loss compared to linear analysis techniques was minimised, the only difference being the use of repeated iterations. Since these iterations take such a small proportion of the time required to derive the Jacobian (or the practically identical linearised transfer matrix) the difference in solution speed is minimal. However since an iterative solution fully models the non-linear operating point and any associated harmonic interaction it provides a more generalised solution technique.

Chapter 6

FACTS DEVICE INTERACTION

6.1 INTRODUCTION

As converter systems become increasingly prevalent in power systems worldwide, the nature and impact of harmonic interaction between FACTS devices becomes increasingly important. Assessing this interaction has two critical components: first calculating the aggregate effect of multiple converters, and second quantifying the contribution of each converter. The first objective is primarily a computational problem, a compromise between system scale and solution speed, the second poses a more challenging problem.

Separating the contribution each converter makes to the aggregate distortion is complicated by each converter's dependence on the terminal conditions to which it is connected. This makes it difficult, if not impossible, to assign any particular harmonic to a single converter. Since the harmonic domain explicitly models this harmonic interdependence it offers a significant advantage over equivalent time domain methods for this type of analysis. This Chapter uses this advantage, in particular the solution Jacobian, to consider the ac and dc side interdependence of systems containing two PWM converters.

6.2 AC SIDE INTERACTION

The first aspect of FACTS device interaction considered is the amount of ac side interaction which occurs between individual FACTS devices. This is critical since accurately modelling the entirety of an ac power system is often not feasible, making it necessary to reduce the system beyond some boundary to an equivalent circuit. Determining where to place this boundary is dependent on the nature of the converters and interconnecting ac system. This Section considers three ac cases with varying amount of ac side interaction, outlining some determinants of ac side interaction.

6.2.1 Dominant low-pass interconnection

Simplistic test systems, like that used in Chapter 5 and innumerable papers, typically behave according to a low-pass characteristic. This is a result of fixed series impedances used to represent

transmission systems. The resultant attenuation at higher harmonic frequencies limits converter interdependence almost entirely to fundamental frequency, this is reflected in the system Jacobian which contains practically no off-diagonal block components (Figure 6.1(a)). As such the accuracy of the harmonic assessment for this case is not markedly affected by the assumption of converter independence at harmonic frequencies. This can be illustrated by setting the off-diagonal Jacobian blocks to zero, the resultant dc terminal voltages being practically identical (Figure 6.1(b)).

The similarity observed in the results reflects the near independent nature of the solution variables for each converter ($V_{dc_{1:nh}}$), as distinct from the lack of any interaction between the devices. In fact when the ac terminal current spectra are calculated (post-convergence) significant differences exist between the approximate harmonic domain solution and the full time domain representation (see Figure 6.2). The comparative independence of the dc side voltages is a function of two important mechanisms: the frequency and phase dependent impedance of each converter, and the low-pass ac system characteristic. In this case, the combination of these two effects isolates the solution variables (V_{dc}) somewhat unrealistically. Including a transmission line model increases the ac system sensitivity at some harmonic frequencies (due to resonances), thereby reducing this isolation.

6.2.2 Realistic transmission systems

In contrast to the idealised systems typically used to validate harmonic domain analysis techniques, actual transmission systems do not conform to a low-pass characteristic. Conductor geometry and the length of transmission lines leads to phase imbalance and harmonic resonances. Both these affect the harmonics generated by a convertor: imbalance causes the generation of non-characteristic harmonics, while the resonances lead to reduced interconnecting impedances.

These transmission line characteristics are incorporated using a three-phase equivalent-pi, initially derived from the model included in PSCAD/EMTDC. Then, after validation, the sensitivity of harmonic solution to small transmission line variations is illustrated by comparing these results with an analytic model based on line images and Carson's corrections for earth return (outlined in Appendix C).

Model validation with transmission system resonances

Including these phenomena has a dramatic effect on both the system Jacobian and the resultant electrical quantities. The transmission lines shunt capacitance (not modelled for the low-pass case) leads to a small shift in the fundamental frequency operating point, and a number of complex harmonic resonances. These resonances increase the solution's sensitivity to particular frequencies, contributing a large number of additional off-diagonal terms to the harmonic Jacobian (see Figure 6.3(a)). The increase in ac system complexity does not have a noticeable

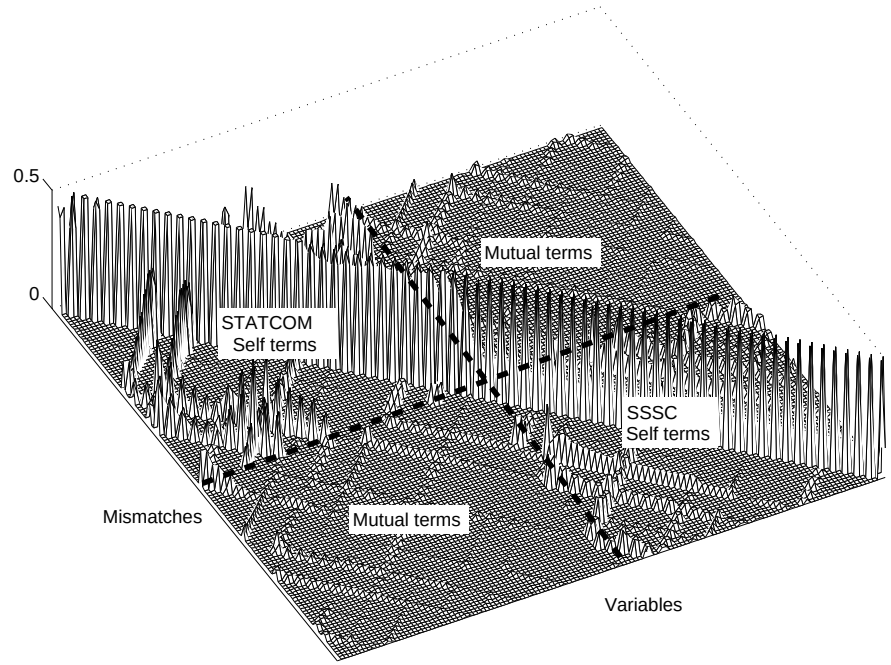

(a) Harmonic component of the system Jacobian with limited device interaction, $nh = 35$

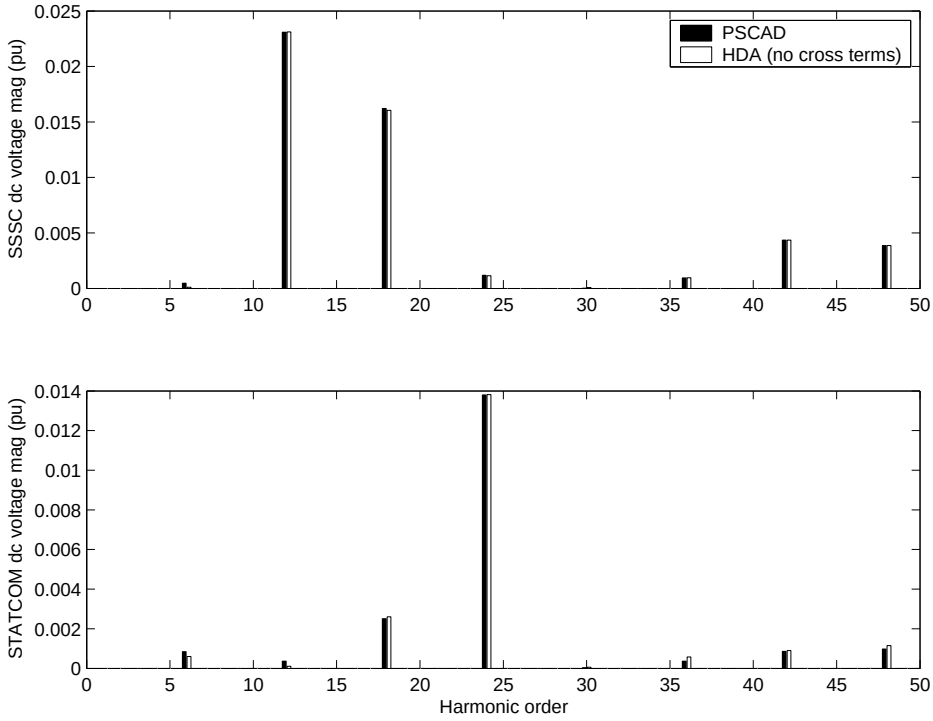

(b) Simulation results for the balanced 5-busbar test system without harmonic interaction

Figure 6.1 Illustration of the limited effect converter interaction has on the solution variables for dominant low-pass connections

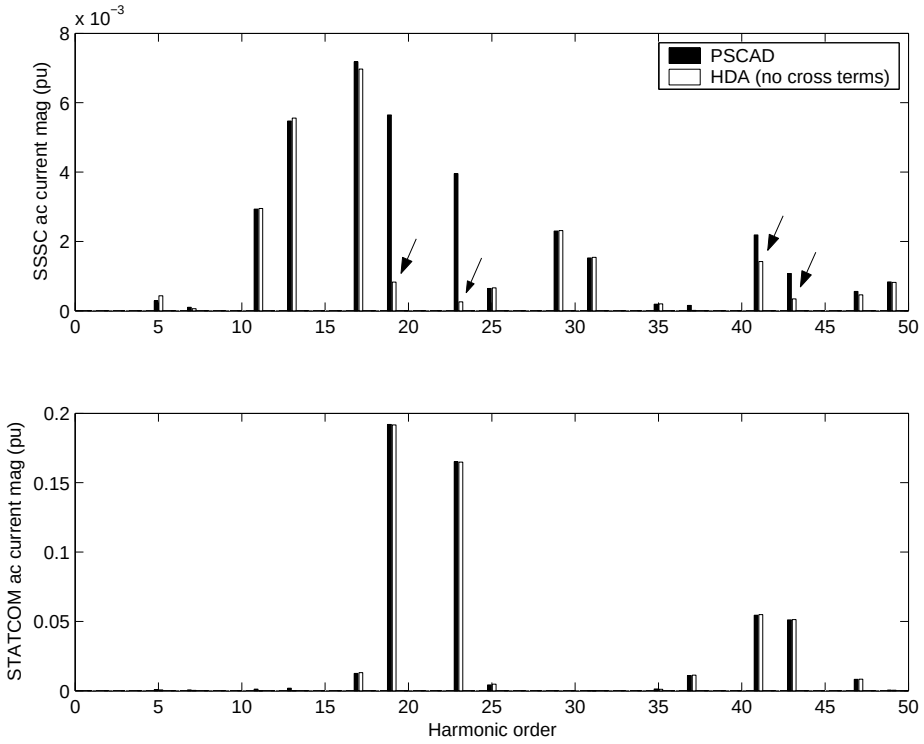

Figure 6.2 Accuracy degradation in the a-phase terminal currents for the low-pass case neglecting converter interaction

impact on the accuracy of the proposed technique, which still compares favourably with time domain simulation (see Figure 6.3(b)).

AC side interdependence

It is important to recognise that the large number of off-diagonal terms in the Jacobian does not necessarily imply a large amount of harmonic coupling between the converters. Instead it reflects the high sensitivity of certain harmonic mismatches to particular harmonic frequencies. Strong harmonic coupling is only present when one of the ac system resonances is excited, something not present in this test case. Nonetheless the Jacobian does help to visualise the effect of system resonance on PWM converter interaction, something which is difficult to picture in the time domain.

The mild interdependence in the solution variables is illustrated by the relatively small drop in accuracy in the solution variables when mutual terms are neglected. Here as an example the more sensitive SSSC dc voltage and a-phase ac terminal current are considered, Figure 6.4 [1]. The assumption of independence now causes a more significant reduction in the accuracy of the solution variables, visible errors being present in the dc voltage spectrum. Nonetheless the

[1]The SSSC is more sensitive in this case because of the relatively small magnitude of series injection relative to the shunt injection.

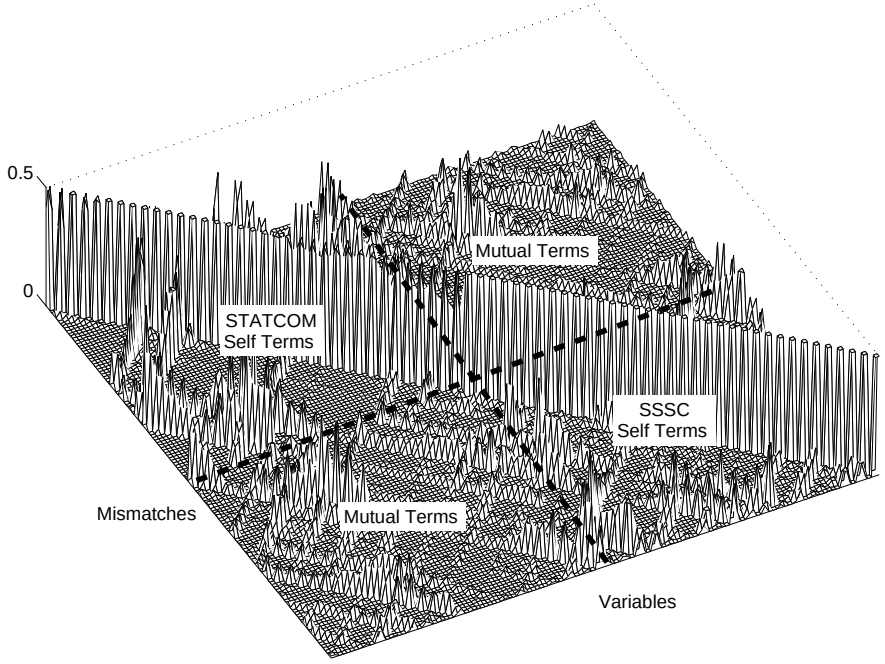

(a) Harmonic component of the system Jacobian, $nh = 35$

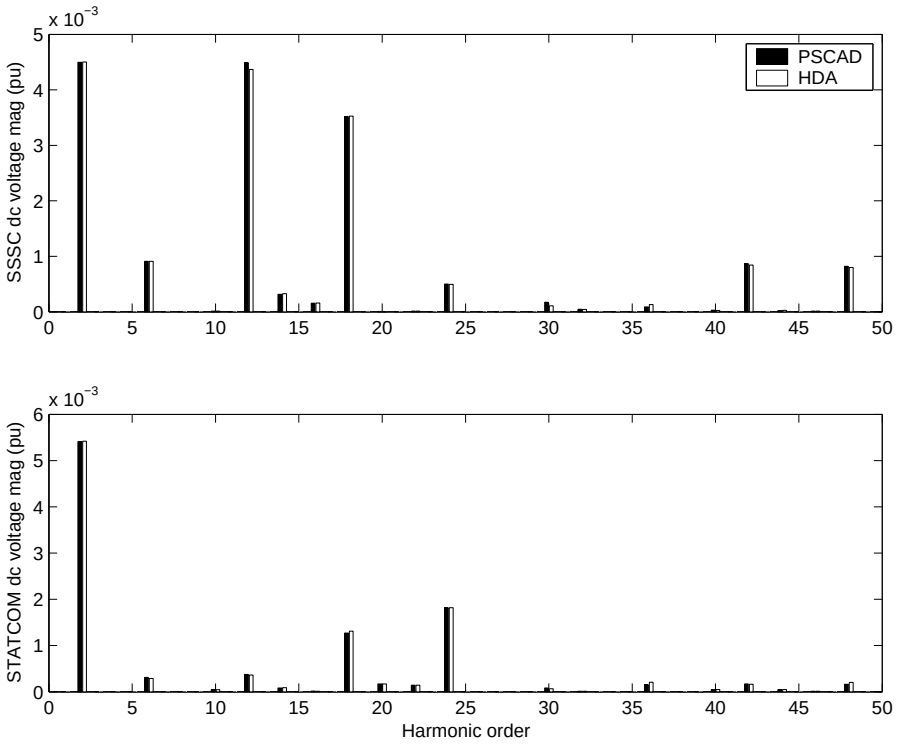

(b) Harmonic domain validation of the dc voltages

Figure 6.3 Illustration of the impact frequency dependent transmission lines have on the converter solution

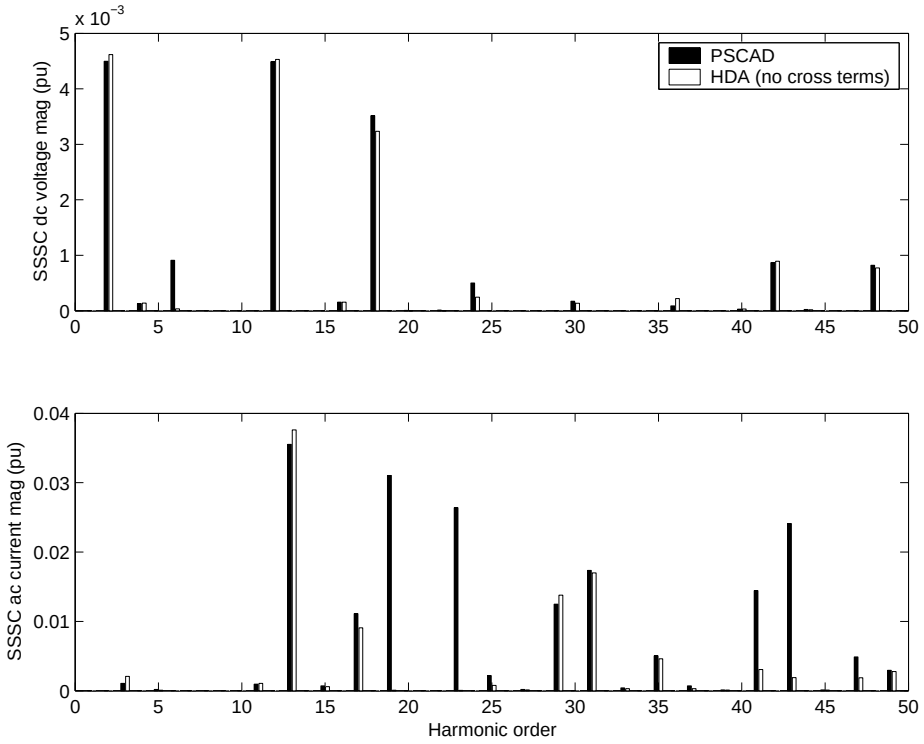

Figure 6.4 Illustration of the degraded solution accuracy for the SSSC when mutual coupling is neglected with transmission systems present

dc spectrum is still dominated by the characteristic terms which remain relatively unaffected, despite not modelling the mutual terms. Once again the similarity between the full and approximate solution is not observed in the ac side current spectra, which is clearly a function of harmonic distortion introduced by the STATCOM.

The contrasting effect this approximation has on the ac and dc side electrical quantities reinforces the blocking effect of the frequency and phase dependent impedance presented by a PWM converter. While ac terminal distortion is linearly dependent on all other ac distorting signals (i.e. no harmonic coupling), the dc side distortion is only a function of other distorting signals when these signals coincide with elements of the converter's PWM spectrum. As a result the two dc side voltages in the test system are all but independent since few of the STATCOM and SSSC PWM harmonics coincide. The only significant discrepancy occurs at the 6^{th} dc harmonic.

Lowering the switching frequency of the STATCOM to match the SSSC shifts the Jacobian peaks in the mutual blocks such that they align with the peaks in the self blocks, increasing the interdependence of the solution variables. The comparative magnitude of the two injected voltages leads to the STATCOM being relatively unaffected, while the smaller SSSC dc side spectrum is heavily affected by the distortion introduced by the STATCOM (Figure 6.5). All of the characteristic SSSC harmonics now show significant inaccuracy, the only exception is the 2^{nd} harmonic which is derived from the power-flow coupling which was still modelled. While this is an extreme example, it does illustrate the difficultly associated with accurately partitioning a

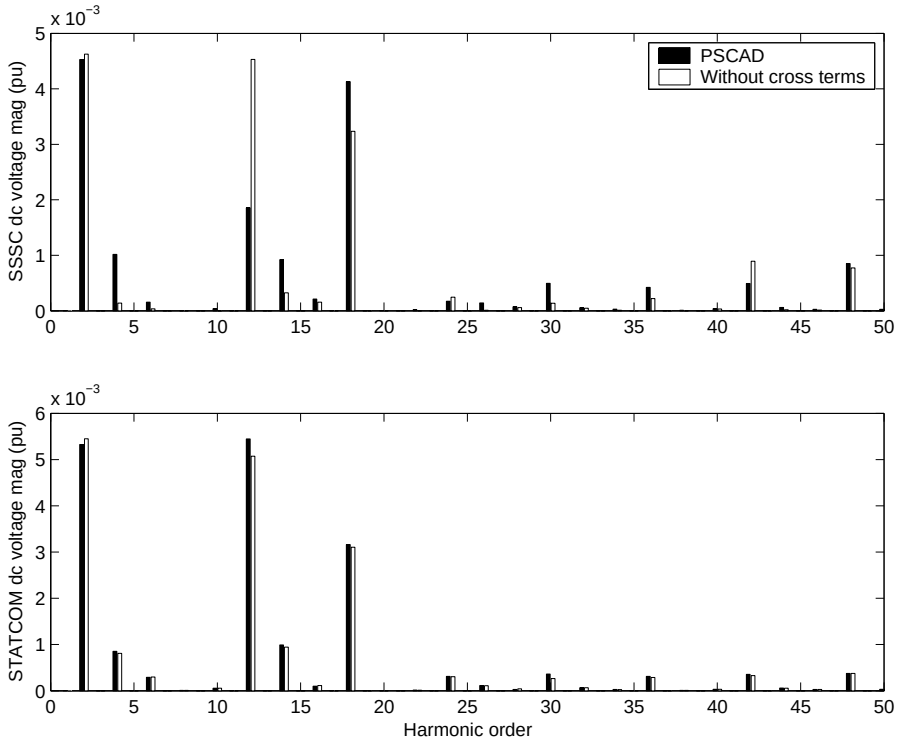

Figure 6.5 Additional solution degradation as a result of neglecting mutual coupling when both converters use an identical switching frequency

large system containing multiple PWM converters.

6.2.3 'High-pass' configurations

While a transmission system and the associated converters normally has a low-pass characteristic, the presence of system resonances and a lack of appropriate filtering can lead to unattenuated high frequency harmonic currents. These currents expose both the slight differences between the two transmission line models used within this thesis, and the effect of harmonic truncation. Both mechanisms affect solution accuracy and can be illustrated by removing the high-pass filter at busbar-5.

Transmission line model sensitivity

Inherent within any transmission system are a range of harmonic resonances. When these resonances coincide with elements of an unfiltered PWM spectrum the harmonic solution can become extremely sensitive to small changes in the resonant frequency. This is a result of how the harmonic domain samples the frequency profile of each transmission line at multiples of the fundamental frequency, these intervals do not necessarily correspond with the system resonances. As such two almost identical harmonic profiles can appear significantly different at frequencies

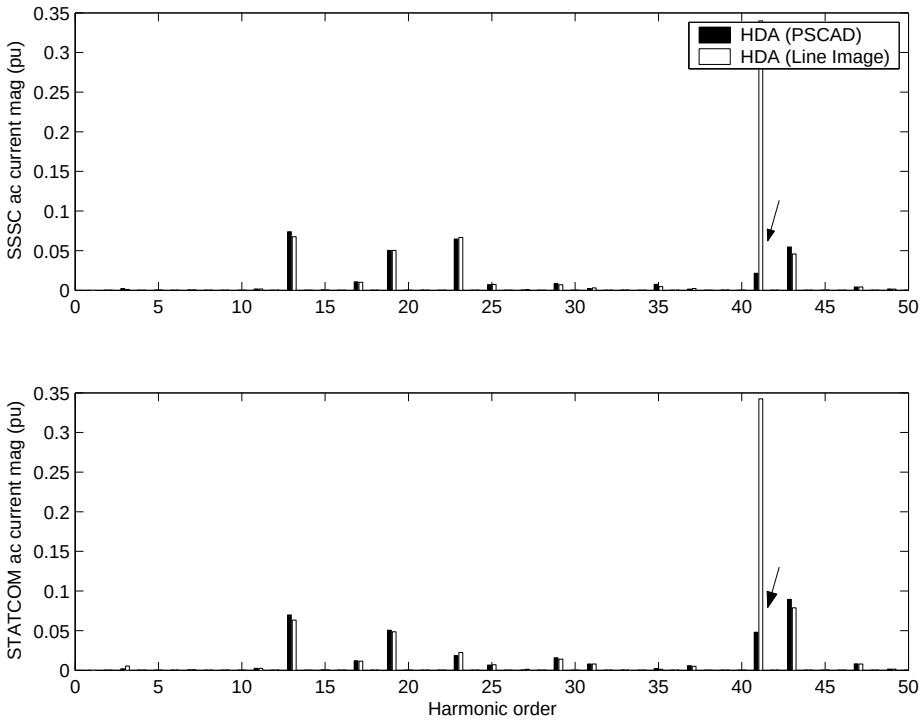

Figure 6.6 An illustration of the harmonic domains sensitivity to small variations in the transmission line model

near resonance. Appendix C illustrates this effect for the $100km$ transmission circuit used in the test system.

For the 5-busbar case (minus the HP filter) the half wave resonances occur at the 30^{th} and 40^{th} harmonics for $100km$ and $75km$ transmission lines respectively. These are both near elements of the PWM spectra, making the harmonic solution extremely sensitive to transmission line model accuracy. For the two models in question, a small $10Hz$ error in the resonant frequency leads to a massive error in the terminal currents at the 41^{st} harmonic (see Figure 6.6).

This extreme sensitivity, coupled with the inherent difficulties of modelling transmission systems [2] questions the point of reading too much into higher order results from unfiltered harmonic (or indeed time) domain simulations. The only exception would be situations where quality measured harmonic data exists for the transmission system being considered.

Harmonic truncation

Another limitation of the harmonic domain technique becomes apparent for the unfiltered case; the reliance on truncated harmonic spectra and transfers. In order to restrict the number of solution variables the harmonic bandwidth is limited, reducing the accuracy of the resultant time domain wave shapes in areas containing high frequency components. This loss of accuracy

[2]Typical transmission line modelling difficulties can include a non-homogeneous/variable earth resistivity and variable conductor geometry (e.g. the height above the ground in mountainous regions)

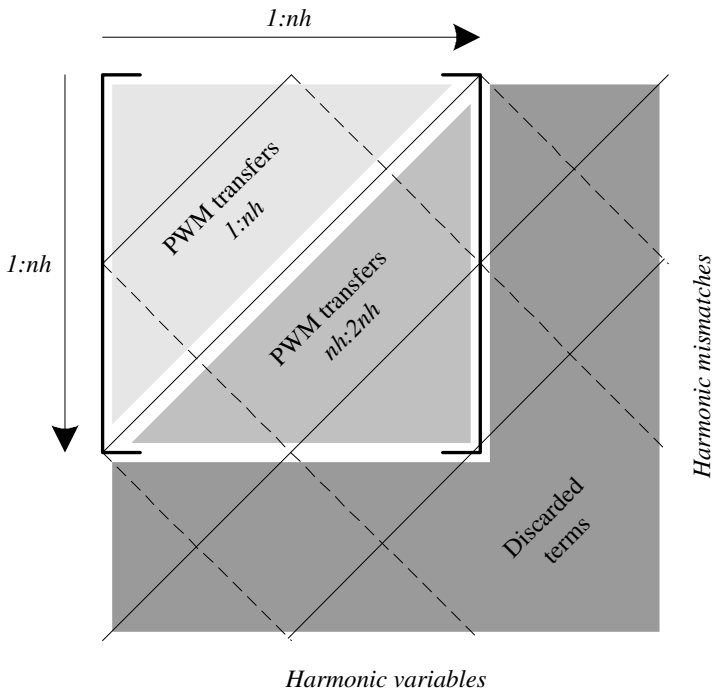

Figure 6.7 Discarded harmonic transfers in the system Jacobian

is predictable, however phasor truncation can also affect the accuracy at harmonics less than the highest harmonic of interest (nh). This comes about as a result of discarding the normally small transfers which can couple high order ($> nh$) harmonics to those less than the highest harmonic of interest (nh).

This is a function of the way the Jacobian is derived, incorporating all transfers between harmonics up to the highest harmonic of interest. The resultant Jacobian contains $nh \times nh$ tensor (2×2) transfers, the first half of which correspond to the PWM spectra up to harmonic nh (light grey area in Figure 6.7). The remainder of the Jacobian corresponds to PWM spectral transfers up to $2 \times nh$ which couple between harmonics less than nh (medium gray area in Figure 6.7). Any remaining terms which couple harmonics greater than nh are discarded, truncating any harmonic interaction beyond nh even though the PWM spectrum is evaluated up to $2 \times nh$. Figure 6.7 illustrates this composition for the harmonic component of a single converter Jacobian.

The harmonic truncation is not normally a significant issue for realistic systems dominated by low-pulse number converters which are filtered to limit high order interaction. However, when the higher switching frequencies associated with PWM modulation are combined with a system lacking harmonic filtering the effect can become apparent.

For example when the high-pass filter at busbar-5 is removed and the system is solved using the PSCAD/EMTDC transmission line model the accuracy of certain harmonics becomes a function

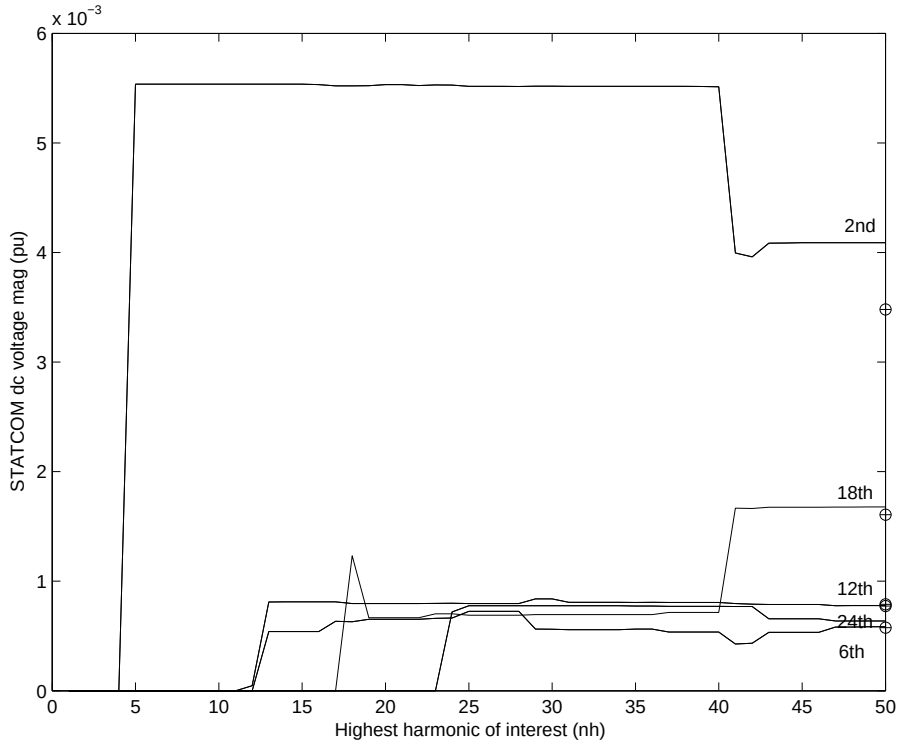

Figure 6.8 STATCOM dc voltage harmonics 2,6,12,18 & 24 as a function of nh

of the highest harmonic of interest. Figure 6.8 demonstrates how the magnitude of the five most significant STATCOM dc side harmonics 'evolve' as a function of nh. In this case reasonable accuracy (as compared with PSCAD/EMTDC, see marks on the RHS of the y-axis) is obtained when nh exceeds the 41^{st} harmonic. Even then a significant inconsistency still exists for the dc side 2^{nd} harmonic. This illustrates how transmission line resonance when combined with a lack of filtering can degrade the performance of harmonic domain solutions, even at low order harmonics.

6.3 DC SIDE INTERACTION

Harmonic interaction between converters is not limited to the ac terminal connections, the shared dc busbar in multi-converter FACTS devices providing a medium for harmonic interaction. While the scale and complexity of the dc system is limited in comparison to the ac system, the dc configuration plays an important role in multi-converter devices.

6.3.1 UPFC model validation

In order to illustrate this type of converter interaction the proposed technique has been applied to a distribution level UPFC. The UPFC model is formed by merging a STATCOM and an SSSC onto a shared dc busbar, capable of transmitting real power. This real power transfer

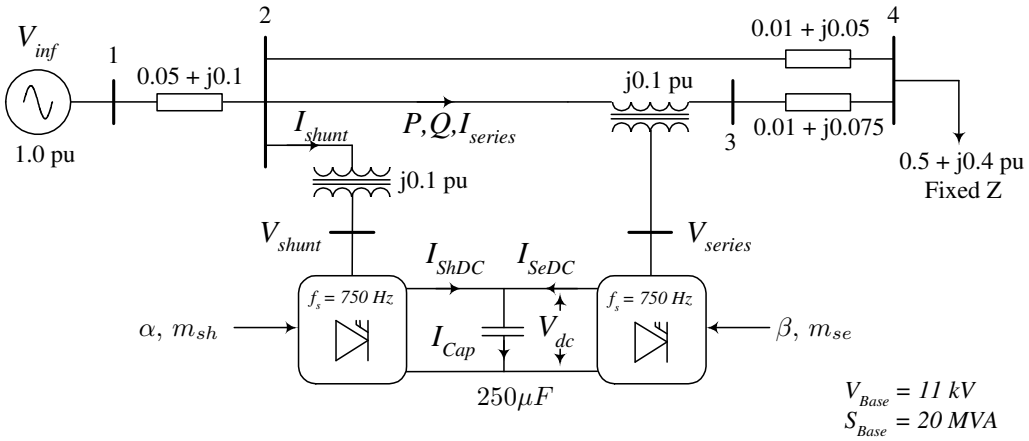

Figure 6.9 Single line diagram of the UPFC test system

between the two converters leads to a generalised series voltage source capable of real and reactive power-flow control. The test system (see Figure 6.9 and Appendix B.2) is composed of a single fixed impedance load fed through two parallel impedances, the power-flow through the larger impedance being regulated by the UPFC.

The UPFC control scheme implemented is based on that used by Dong [61], a schematic overview of which is included in Appendix B.2. It incorporates two PI loops which regulate the positive sequence real ($P_{Set} = 0.25pu$) and reactive ($Q_{Set} = 0.2pu$) power flows by adjusting the direct (E_d) and quadrature (E_q) components of the injected series voltage respectively. The shunt converter is controlled separately so as to regulate the dc side capacitor voltage ($V_{dc} = 1.0909pu$) and ac sending end voltage ($V_2 = 0.95pu$) via the shunt converter firing angle (α) and modulation index (m_{sh}) respectively.

When the test system is solved the model converges in four iterations to a solution consistent with time domain analysis. Figure 6.10 demonstrates this similarity in the time domain for both the dc busbar voltage and the ac terminal currents. In this case the harmonic solution for both converters is fully described by the single dc busbar voltage, the spectrum of which compares favourably with time domain solution (Figure 6.11(a)). Likewise, the ac side spectra (calculated post the main iterative solution) compare satisfactorily with the time domain solution (Figure 6.11(b)). Information regarding the operating point for the UPFC has been included in Appendix B.2.

6.3.2 Isolating dc side converter interaction

The combination of ac and dc side interaction makes assessing the amount of converter interaction for a UPFC less straightforward than the equivalent ac side converter analysis associated with single converter devices. Here a single vector of harmonic voltages defines both converters,

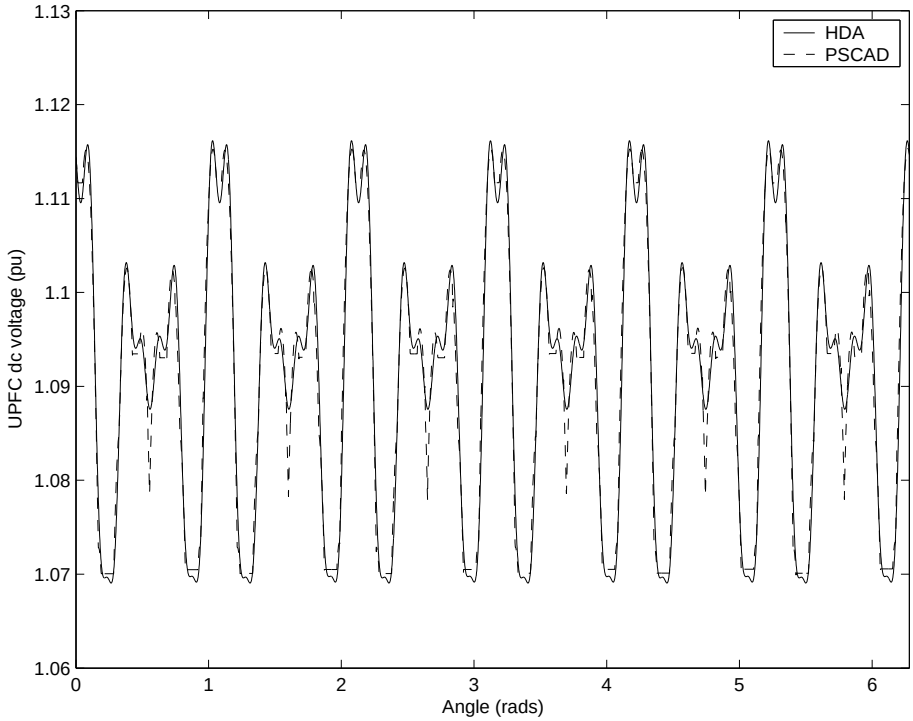

(a) dc voltage comparison

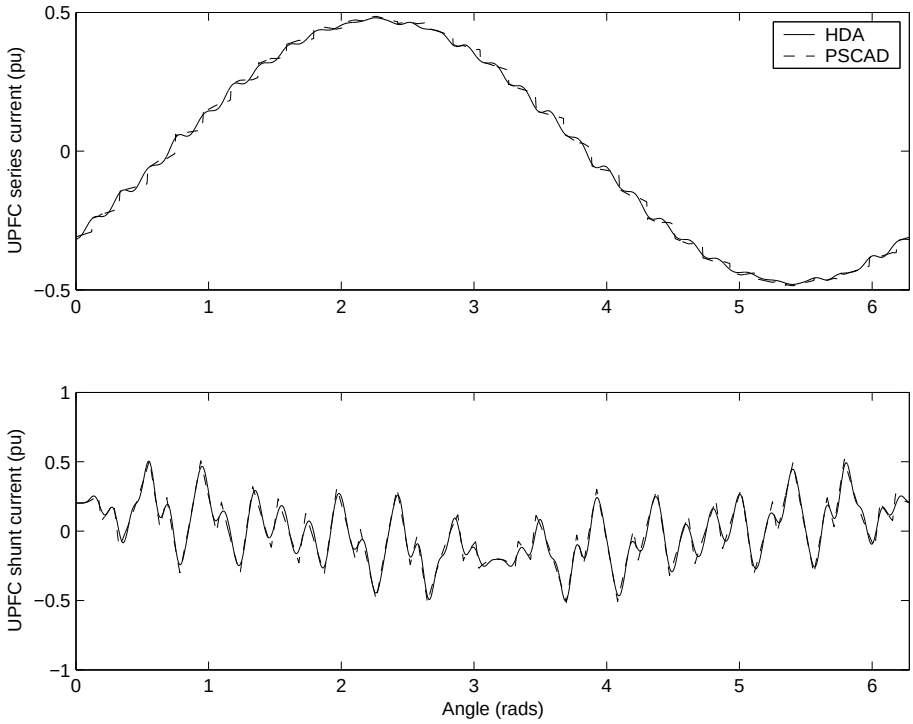

(b) a-phase current comparison

Figure 6.10 Time domain comparison of dc voltage and ac currents for the UPFC

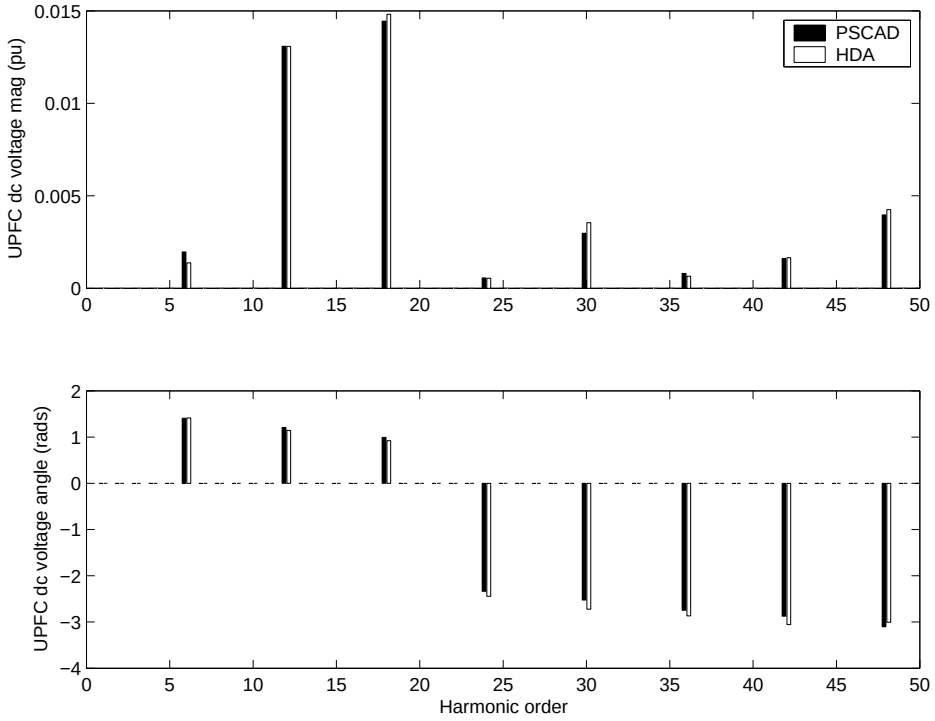

(a) dc voltage comparison

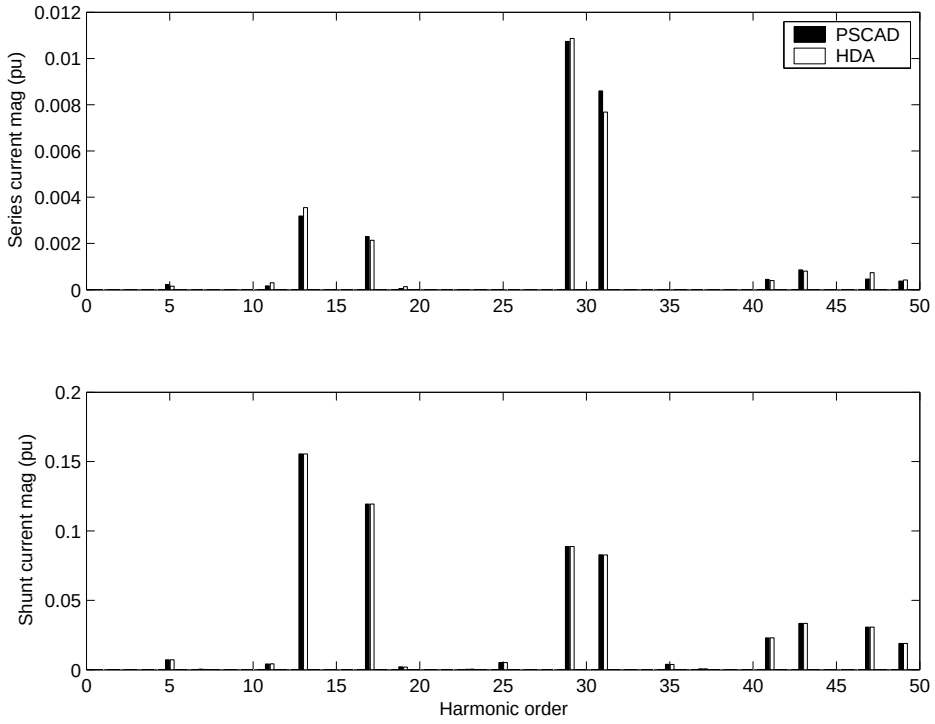

(b) a-phase current comparison

Figure 6.11 Harmonic domain comparison of dc voltage and ac currents for the UPFC

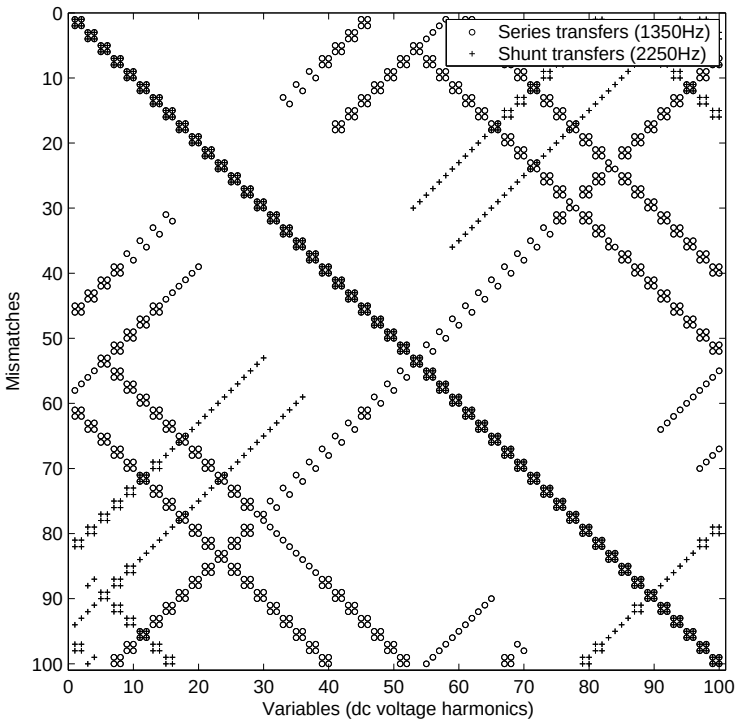

Figure 6.12 Series and shunt contributions to the harmonic Jacobian for the UPFC, $nh = 50$

effectively superimposing the ac and dc side interaction. In order to isolate the dc component of this interaction the ac cross-coupling terms are set to zero. Interestingly this has a negligible impact on either the solution variables or the system Jacobian for the test case (maximum change in a harmonic Jacobian element $< 2\%$), re-enforcing the isolating role played by each converters phase and frequency dependent impedance.

In contrast to ac interaction, dc side converter interaction actually forms the mismatches used to describe the UPFC (see Equation 4.20) and hence can have a significant impact on the solution variables. This dc side interaction is reflected in the Jacobian, which contains the sum of the shunt and series converter transfer terms. Figure 6.12 illustrates this principle for a UPFC using two different PWM switching frequencies. This type of interaction is difficult to visualise when both converters use the same switching frequency since the spectra overlap (e.g. the UPFC test system).

To illustrate how the two converters in the test system interact on the dc side it is necessary to decompose the dc side ripple into two separate components. This can be achieved by solving the full solution twice, once with the harmonic mismatch equation used for a STATCOM and once with the mismatch for an SSSC. The resulting dc harmonic spectra correspond to the shunt and series contributions respectively. For the test case this interaction is completely one-sided, the shunt converter completely dominating the dc ripple. This lack of interaction is primarily due to the large difference between the modulation index (m) of the two converters

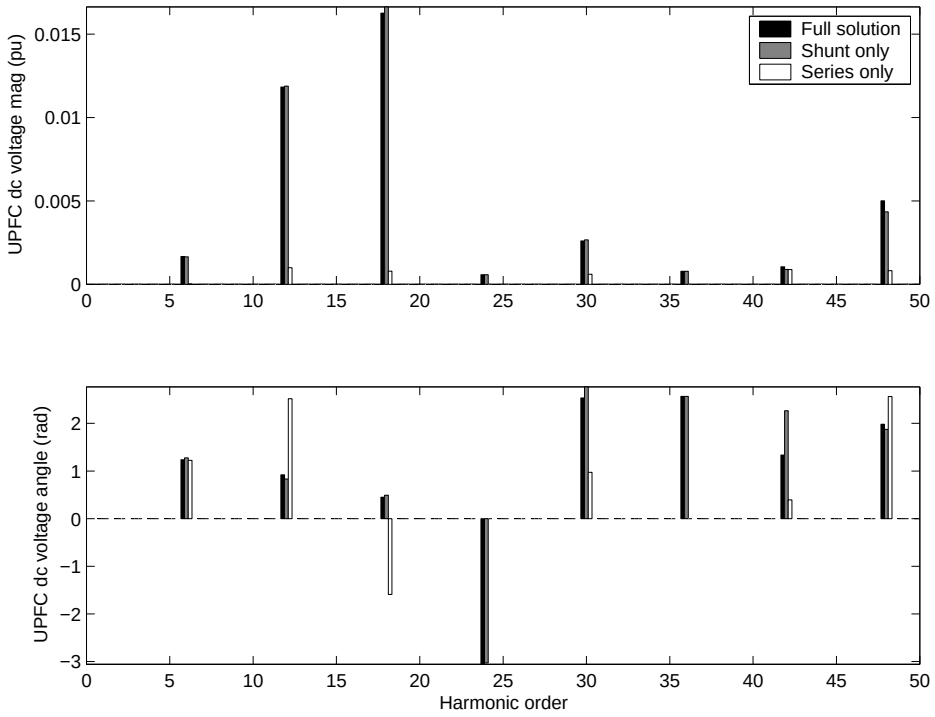

(a) Limited dc converter interaction, $m_{sh} = 0.8589$ & $m_{se} = 0.1505$

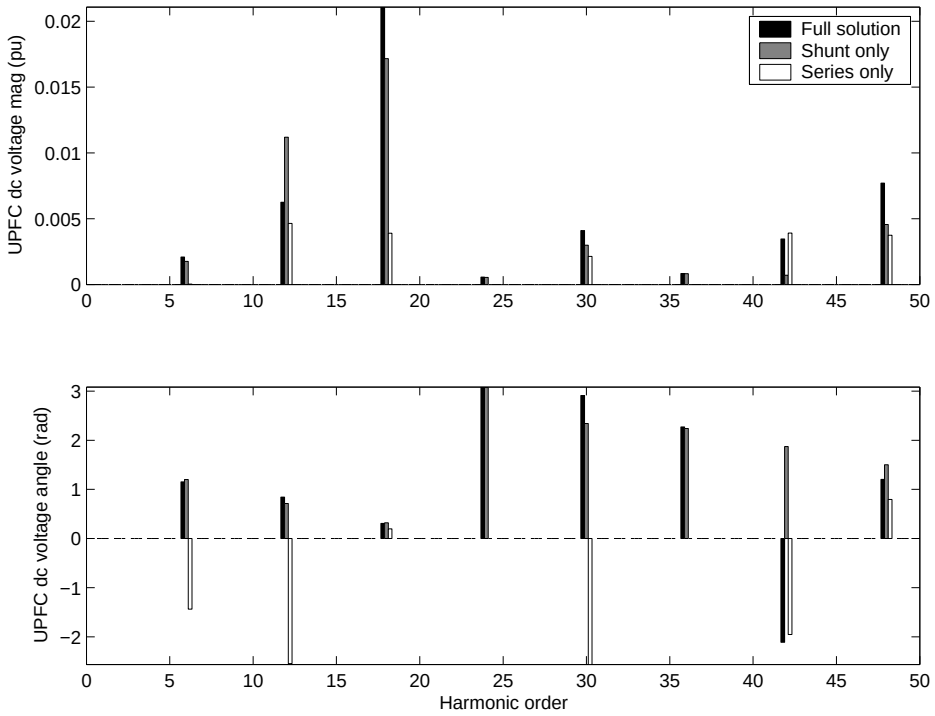

(b) Further increased dc converter interaction, $m_{sh} = 0.8599$ & $m_{se} = 0.2704$

Figure 6.13 UPFC dc ripple decomposed into shunt and series elements

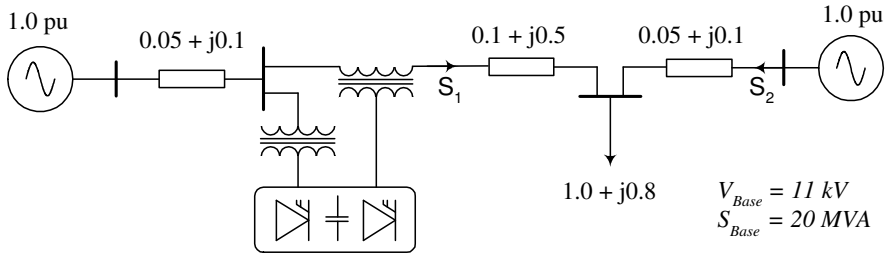

Figure 6.14 Single line diagram of the modified UPFC test system

($m_{sh} = 0.8275$ vs. $m_{se} = 0.0392$). If the system loading is increased (and the operating-point adjusted accordingly) this imbalance between the converter modulating indices can be reduced, making the linear interaction observable.

Figure 6.13 contains the decomposed dc voltage spectrum for two more heavily loaded cases. The increased series injection now contributes a noticeable proportion of dc voltage ripple. Interaction between these two contributions is linear in the sense that the sum of the shunt and series components equates with the full solution (assuming the ac side interaction is modelled). In this case, without ac side interaction, there is a small difference (1-norm of $0.016pu$) between the sum of the decomposed ripple components and the full solution. The tiny remainder reflects the negligible ac side converter interaction.

6.3.3 DC side harmonic cancellation

The dependence of the dc ripple on the operating point of both converters can lead to interesting situations where changes in the operating point result in the partial cancellation of certain dc side harmonics. This effect can be illustrated by considering the modified UPFC test system (see Figure 6.14), which supplies a fixed impedance load from two separate generators via vastly different impedances.

As the operating point for this system is shifted, increasing S_1 in Figure 6.14 from $0.05 + j0.04$ (5%) through to $1.0 + j0.8$ (100%), the magnitude of the series converter injection increases ($M_{se} = 0.0685$ vs. 0.6291), while the shunt injection magnitude remains comparatively unchanged ($M_{sh} = 0.8702$ vs. 0.9279). This increase in the modulation index of the series converter has a significant impact on the dc side harmonics present (Figure 6.15). Interaction clearly occurs between the two 750 Hz PWM spectra, which as a result of the operating point have different fundamental frequency phase angles. This phase angle variation is reflected in the less than intuitive nature of the dc side THD and harmonic ripple components.

In this case the steadily increasing magnitude of both the shunt and series injections are not necessarily accompanied by increasing dc side harmonic ripple. Take for example the $48th$

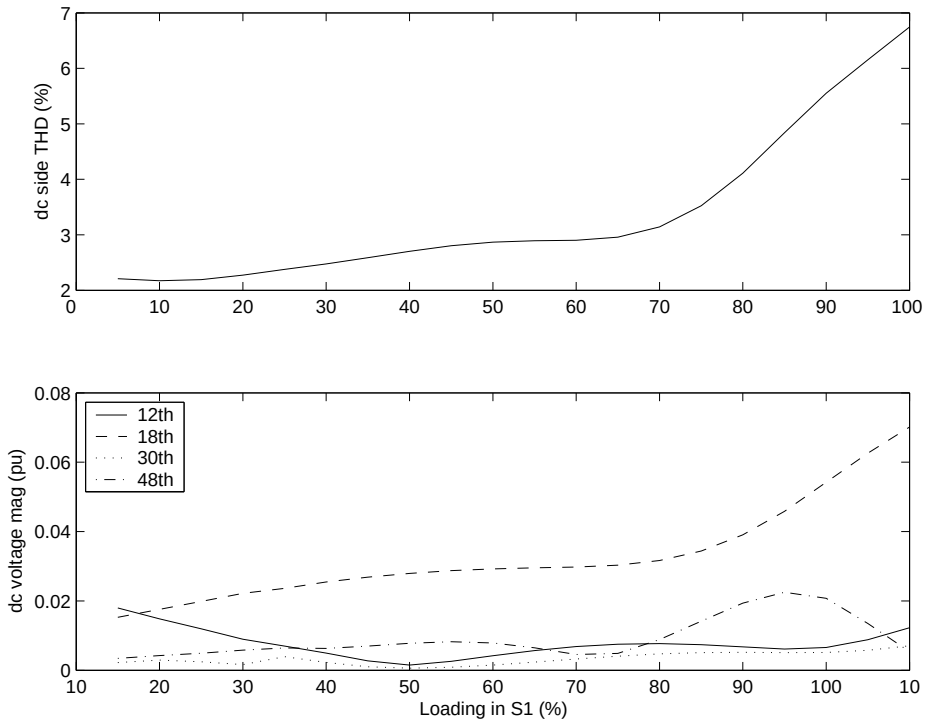

Figure 6.15 Illustration of how the dc side distortion is dependent on the operating point of the UPFC

harmonic which contains two definite peaks (at 45% and 85% loading) corresponding to points where the phase angle of each converters contribution at this harmonic align. Likewise the level area for the $18th$ harmonic ($45 - 65\%$ loading) is attributed to an anti-phase null, which offsets the increasing magnitude of each converters contribution at this harmonic.

6.4 IMPACT OF CONVERTER INTERACTION ON CONVERGENCE PROPERTIES

The predominantly independent nature of the solution variables leads to the solution being relatively insensitive to the amount of harmonic interaction in all but extreme unfiltered cases. This insensitivity is reflected in the convergence characteristics, both the solution time (Figure 6.16(a)) and rate of convergence (Figure 6.16(b)). These results correspond closely with those obtained for the basic fixed impedance test systems, the critical determinants of solution speed and convergence still being the dimensions of the Jacobian and the amount of system imbalance, respectively.

While the inclusion of transmission line resonances significantly reduces the sparsity of the Jacobian it does not increase the amount of computation required to derive the Jacobian. This is a result of how all Jacobian elements must be calculated in order to assess sparsity. The reduced sparsity will slightly slow each iteration, however this effect is negligible for the test cases. For example, the solution time for the case including transmission line resonances is practically identical to the unbalanced fixed impedance case (labelled TLines and Fixed Z in

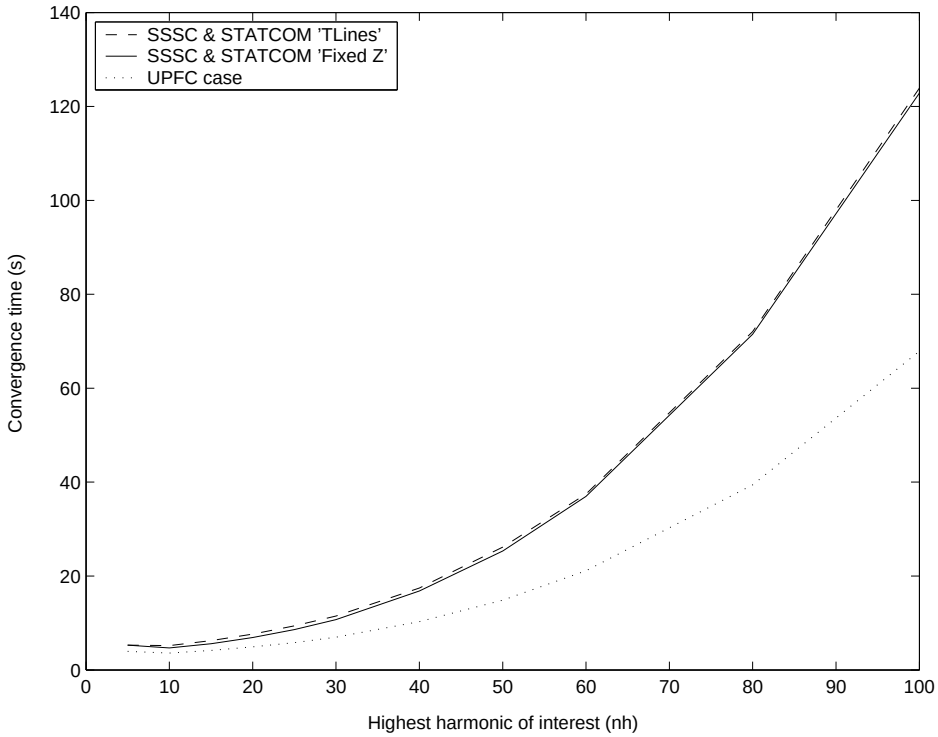

(a) Solution time, using a 2.2GHz PC

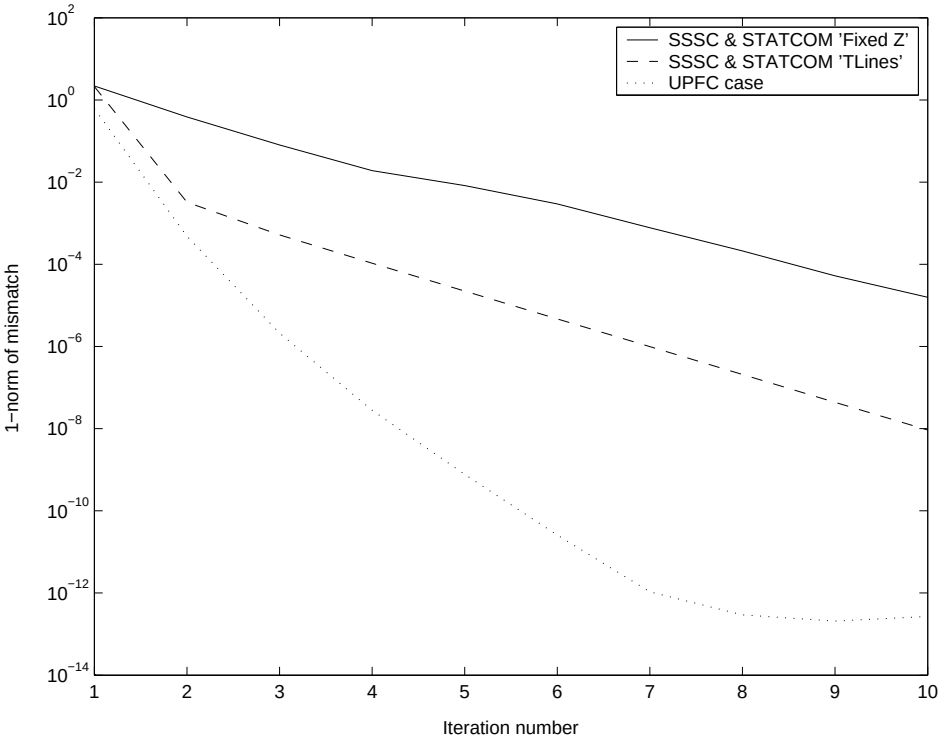

(b) Convergence characteristics with a fixed Jacobian

Figure 6.16 Solution convergence properties for the unbalanced fixed impedance, transmission line, and UPFC test systems

Figure 6.16(a)). Likewise the UPFC case requires approximately the same amount of time as a single converter fixed impedance case, illustrating how the number of isolated dc busbars is the major determinant of the Jacobian's size and hence the solution speed.

Similarly the rate of convergence using a fixed Jacobian is not significantly degraded in the presence of system resonances. In fact the rate of convergence for test systems containing ac or dc interaction (TLines and UPFC in Figure 6.16(b)) is superior to that obtained for the unbalanced fixed impedance case. This stems from how the transmission system considered within this Chapter has less unbalance than the unrealistic test case used in Chapter 5. Interestingly the balanced UPFC case converges faster than the balanced single converter case (Figure 5.9); the cause of this improved convergence has not been definitively identified, however it is likely that the different control schemes used by the respective FACTS devices contributes to this difference.

6.5 CONCLUSIONS

This chapter has investigated the impact converter interaction has on the proposed harmonic solution technique. It has demonstrated how increased harmonic interaction does not significantly degrade the models performance, either in terms of accuracy or convergence. Moreover the choice of the dc side voltage as a solution variable has been justified by the near independence of each devices' dc voltage spectrum. This independence in the solution variables does not necessarily imply a lack of linear ac side interaction, which was observed in ac terminal quantities. As such the amount of dc voltage interdependence is a useful guide as to whether and/or where in depth harmonic interaction analysis is required.

The magnitude of any interaction is shown to be dependent on both the operating point and the composition of the test system, in particular resonant components such as filters and transmission systems. While the Jacobian reflects these components and the resultant sensitivity in the harmonic solution, it is not necessarily a good measure of the magnitude of the interaction present since resonances are not necessarily excited.

Chapter 7

CONTROL SYSTEM LINEARITY

7.1 INTRODUCTION

Previous chapters have focused on the electrical aspects of FACTS device analysis in the harmonic domain, as such the associated test systems featured heavily filtered control networks and conservative operating points (i.e. no over-modulation). Both of these common assumptions improve system linearity by idealising the PWM process. This results in improved computational efficiency, something which is advantageous for multi-converter studies requiring a large system Jacobian. This chapter considers the impact these common assumptions have on both the accuracy and convergence of the proposed iterative solution, before discussing where these control assumptions are appropriate.

7.2 DISTORTED CONTROL FEEDBACK

While the PI controller and the associated filters are assumed within this thesis to behave in a linear fashion, the output from this block has a significant impact on the PWM process (a primary source of non-linearity). For heavily filtered control cases this non-linearity is limited to the switching spectrums dependence on the power-flow control variables α_{dc} and m_{dc}, leaving the harmonic transfers perfectly linear. Removing this isolation contributes additional non-linear harmonic transfers which complicate the solution by increasing the Jacobian size and reducing the rate of convergence. The resultant reduction in efficiency makes the assumption of a heavily filtered feedback network particularly attractive. In order to assess the accuracy of this common assumption this section presents the impact of introducing PWM distortion to an SSSC.

7.2.1 Feedback mechanism

The introduction of harmonic distortion to the PWM process leads to variation in the switching instants, which in turn generates non-characteristic ac side harmonics. Figure 7.1 illustrates this effect for the ac terminal current spectra of the SSSC test system (see Appendix B.3). In this case the sinusoidal modulating function has been heavily distorted by a second harmonic ripple (10%) in the control angle (α). Since the introduced distortion is modulated by the switching

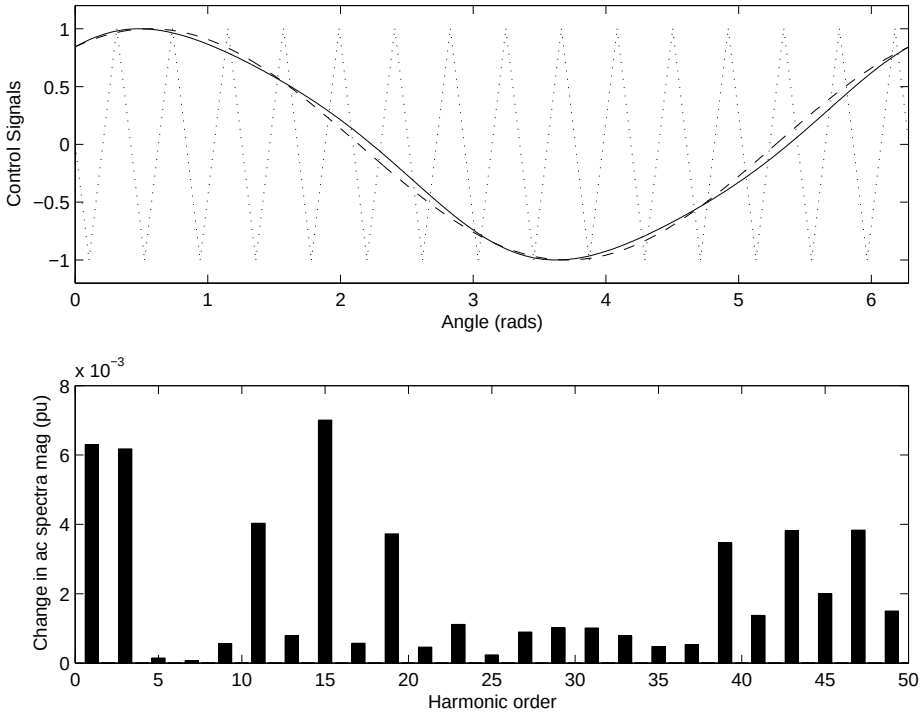

Figure 7.1 Impact of 2nd harmonic PWM distortion on the a-phase current spectra

process it leads to changes in the ac spectrum at the first and third harmonics. Likewise, the higher frequency PWM components are also modulated causing further changes in the ac spectra surrounding the dominant PWM harmonics.

These additional terms are reflected in the system Jacobian (Figure 7.2), which now contains four distinct blocks for the SSSC:

A The dc side harmonic transfers contributed by the SSSC remain relatively unchanged. While the main $ac \leftrightarrow dc$ transfers do now contain extra non-characteristic terms, these are negligible in comparison to the undistorted PWM terms.

B The very sensitive nature of the PWM process is mirrored in the large terms contained in block B. These terms correspond to the spectra of non-characteristic harmonics produced when harmonic distortion is introduced into the PWM modulation process. Typically the comparatively small magnitude of any control distortion leads to these terms having a minimal effect on the solution.

C In contrast block C is a better measure of the impact control distortion has on the full solution, primarily since it is a function of the more distorted system voltages. The sensitivity of this block is a function of the control systems frequency response, here it is shown with a unitary gain. When the transducer and notch filter frequency responses are included the magnitude of terms in this block are further reduced.

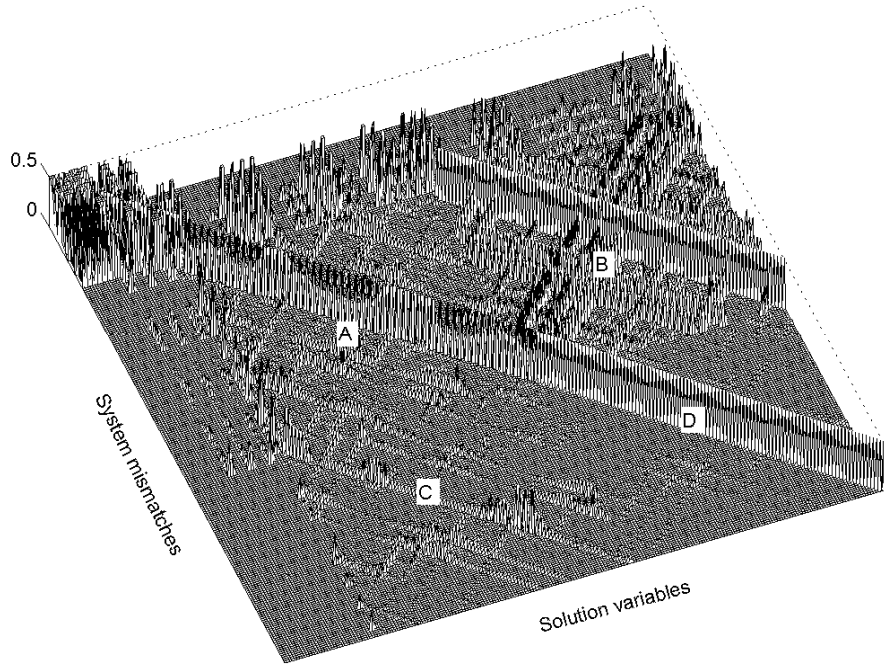

Figure 7.2 System Jacobian for the SSSC system with harmonic control feedback (Gain=1), variables arranged as per Figure 4.8(b)

D The control mismatch definition and near unitary gain of the PI controller at harmonic frequencies leads to block D (the transfers between control variable distortion and the control mismatches) being dominated by diagonal terms with a magnitude of approximately one.

7.2.2 Distorted feedback example

As an example of how these additional harmonic transfer blocks affect the full harmonic solution they have been applied to an SSSC regulating the positive sequence series current (see Appendix B.3). The switching converter and transmission network surrounding the FACTS device make this control quantity both distorted and unbalanced, as illustrated in Figure 7.3. As a result the un-filtered direct component of the current, which is used by the PI controller to adjust the modulating angle (α), contains a significant amount of harmonic distortion.

If this un-attenuated distortion is applied directly to the PWM switching process (Gain = 1) a tiny shift in the operating point (of the order of $0.001pu$) and a small shift in the harmonic solution is observed (see Figure 7.4). This shift includes both small changes in existing harmonics (e.g. 2^{nd} and 12^{th}) and the generation of small new harmonics (e.g. 6^{th}), however the magnitude of all these changes are very small.

The value of modelling control distortion is further reduced when a realistic control transfer function is included. Since controllers typically attenuate high order harmonics and often include

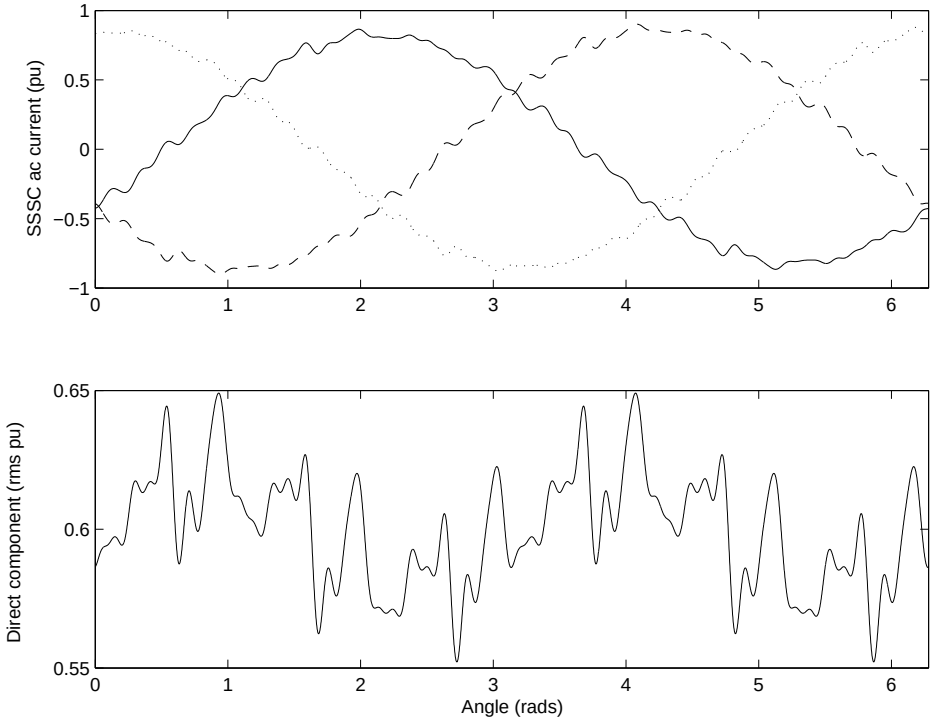

Figure 7.3 The distorted SSSC terminal current used for control feedback and the associated unfiltered direct component

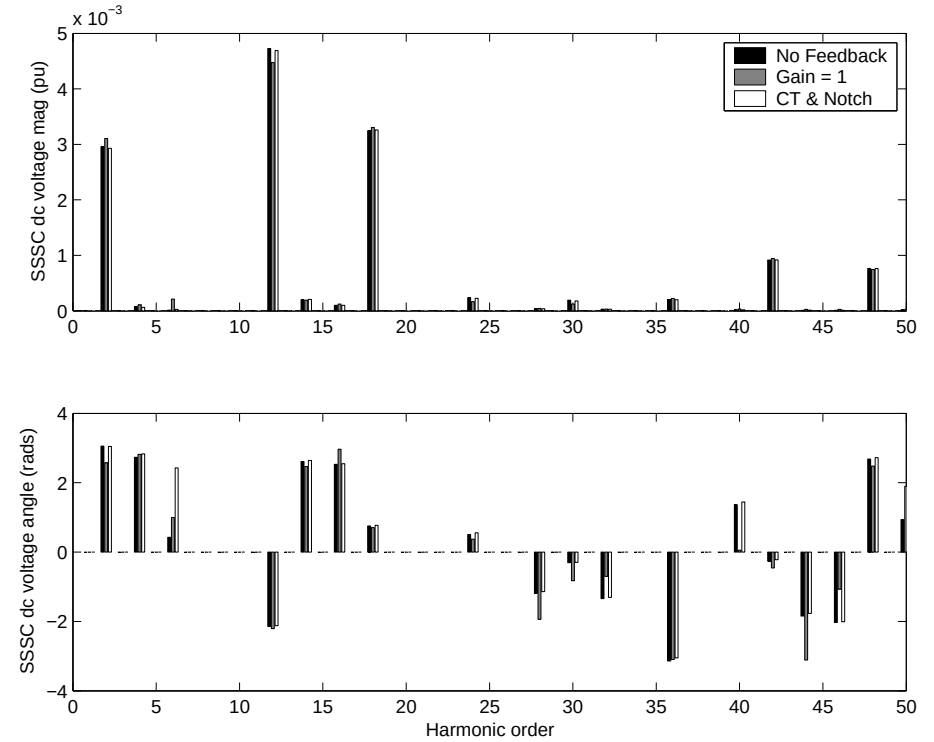

Figure 7.4 The impact of harmonic feedback through the controller on the dc voltage ripple

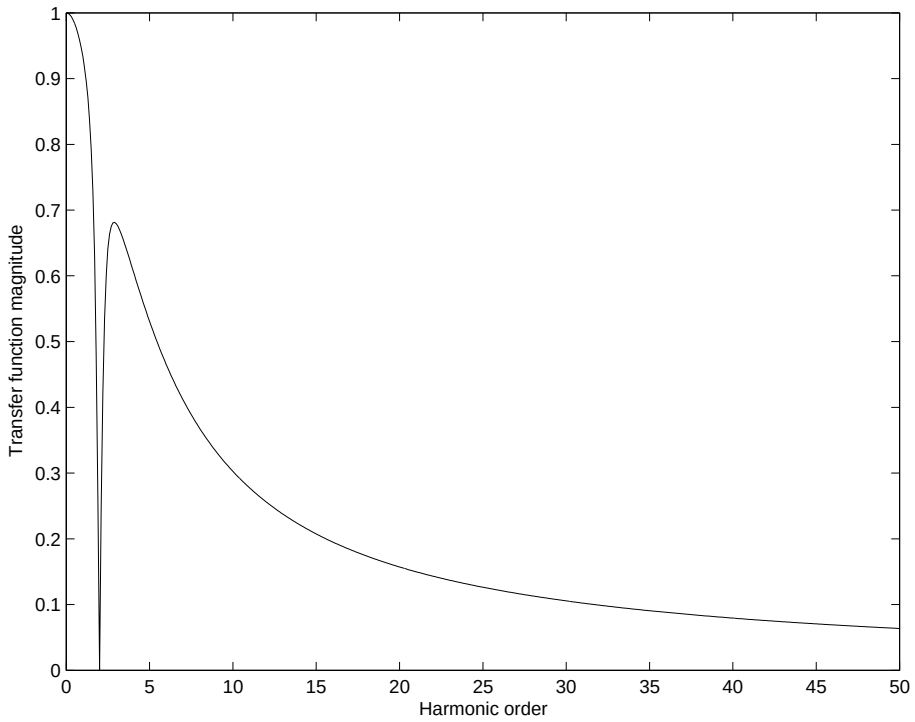

Figure 7.5 Control loop transfer function, including a 2^{nd} harmonic notch

low frequency notches, they increase the isolation between the distorted electrical system and the PWM process. In this case the control transfer (included in Figure 7.5) is composed of the current transducers high frequency attenuation (Gain = 1, Time constant = 0.001) and a second harmonic notch filter (Gain = 1, Damping factor = 0.16) [1].

The resultant harmonic attenuation in the control loop reduces the change observed in the full solution to negligible levels, bordering on unobservable (Figure 7.4). In addition Block C of the system Jacobian is now extremely sparse, questioning the value of calculating the additional Jacobian terms.

7.2.3 Impact on convergence and solution speed

While the inclusion of harmonic distortion in the PWM process only has a limited impact on the actual solution, it has a dramatic impact on the solution speed and a small impact on the rate of convergence. These changes are primarily a function of the increased size of the Jacobian and the extent to which the control system is isolated from harmonic distortion respectively.

Distortion in the PWM process requires the inclusion of non-linear transfers in the harmonic block of the solution, this of course reduces system linearity and the rate of convergence. The extent of this reduction in linearity is a function of the frequency response of the control block.

[1] It is interesting to note how the limited bandwidth of the PI controller (Gain = 1, Time constant = 0.01) leads to it not playing a significant role at harmonic frequencies.

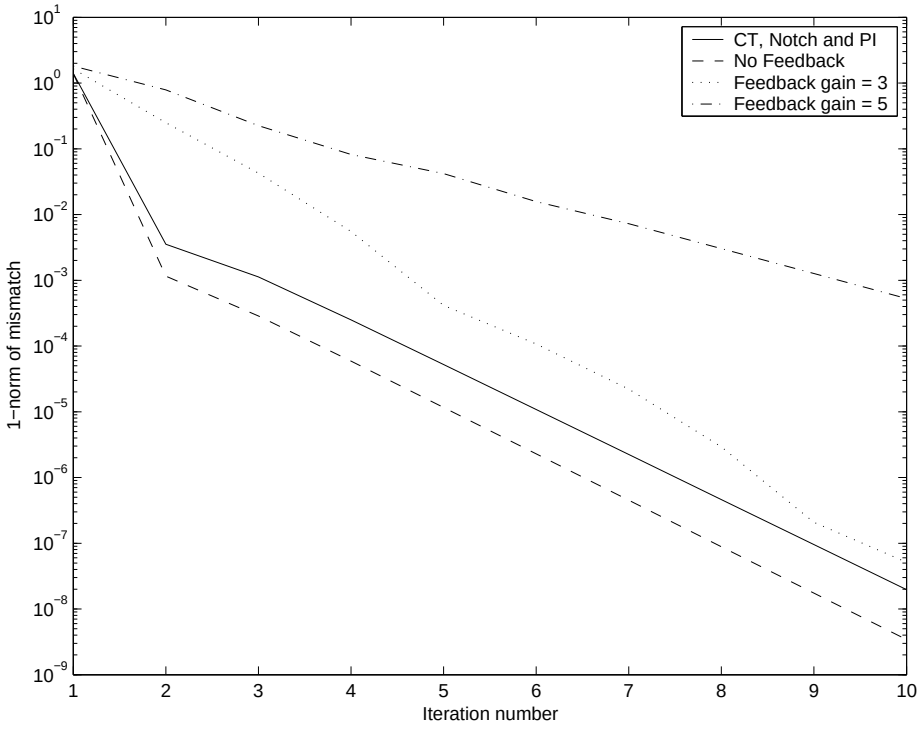

Figure 7.6 Illustration of the degraded solution convergence resulting from harmonic feedback through the controller

The rate of convergence improves as the amount of harmonic attenuation in the filter is increased. Figure 7.6 illustrates this for a range of cases solved using a fixed Jacobian. Note how the filtered case exhibits a similar convergence characteristic to the undistorted PWM case, this highlights the small impact realistically filtered feedback has on system linearity.

The additional computational expense required to calculate the extra Jacobian blocks dominates the increase in the solution time, which is approximately double the zero feedback case. Given the negligible effect properly filtered feedback has on the PWM converter, it is difficult to justify this massive reduction in efficiency for the majority of cases. This conclusion agrees with common PWM modelling practice which invariably assumes a sinusoidal modulating function. An important exception would be converters used for active harmonic filtering, where the controller gain at particular harmonic frequencies could result in both a reduced rate of convergence and a shift in the full solution.

7.3 PWM OVER-MODULATION

The linearity of a solution system can also be affected by the fundamental frequency operating point, a classic example being saturated transformers. PWM converters experience a similar phenomena when the modulation index (m) exceeds one. In this region the fundamental frequency ac output voltage is no longer linearly dependent on the modulation index. Further,

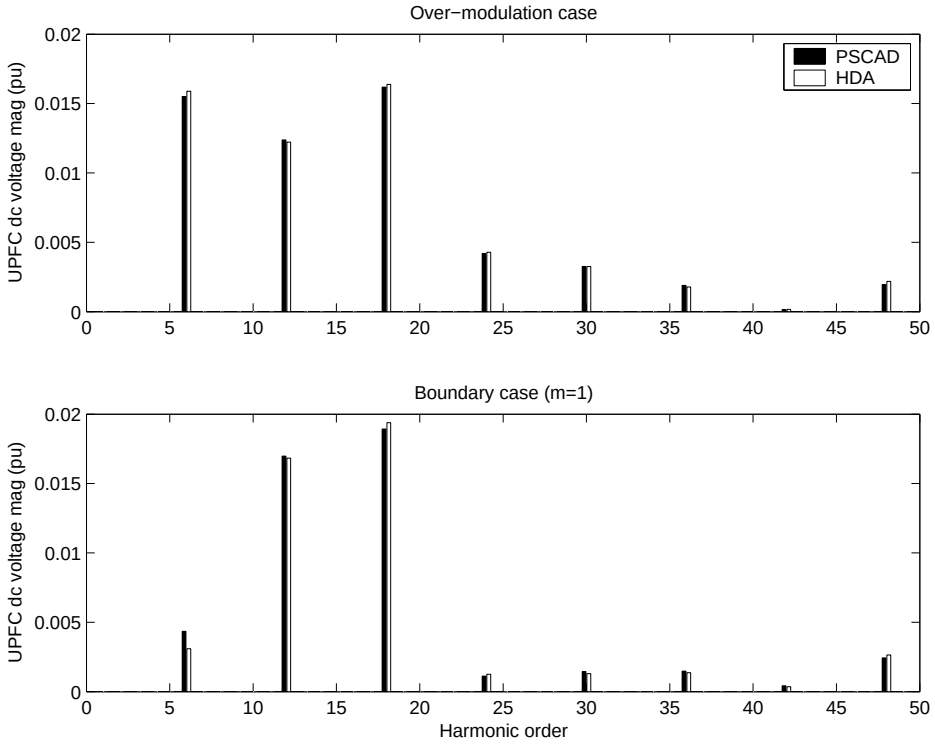

Figure 7.7 Model accuracy in the presence of over-modulation

over-modulation also causes a significant change in the harmonic solution with more sideband harmonics (and reduced dominant characteristic harmonics) being generated [3]. Both of these changes lead to a step change in the Jacobian, which in turn effects system convergence.

Previous chapters have avoided this issue by using either fixed modulation indices or an operating point well within the linear range. This section assesses the impact over-modulation has on the convergence properties of the model. By lowering the dc voltage set point used in the UPFC test system (see Appendix B.2) the magnitude of both PWM injections is reduced, leading to a corresponding increase in the shunt and series modulation indices (given that the remaining set points are unchanged). This approach forces the shunt converter into over-modulation, while the comparatively small series injection remains in the linear PWM range.

When over-modulation is applied to the proposed iterative solution the additional non-linearity does not have a significant impact on the solution accuracy (see Figure 7.7). This is primarily a result of the solution format, which uses a full Newton solution (i.e. the Jacobian is updated at each iteration) for the power-flow initialisation. This component of the solution is capable of dealing with the most significant non-linear element of over-modulation, the shift in the control variable (m_{dc}). Figure 7.8 illustrates both the increased power-flow non-linearity (see Fixed Jacobian) and the very slight impact this has on the full Newton solution used for initialisation (see Updated Jacobian).

Given this satisfactory estimate of the operating point it is possible to derive the full harmonic

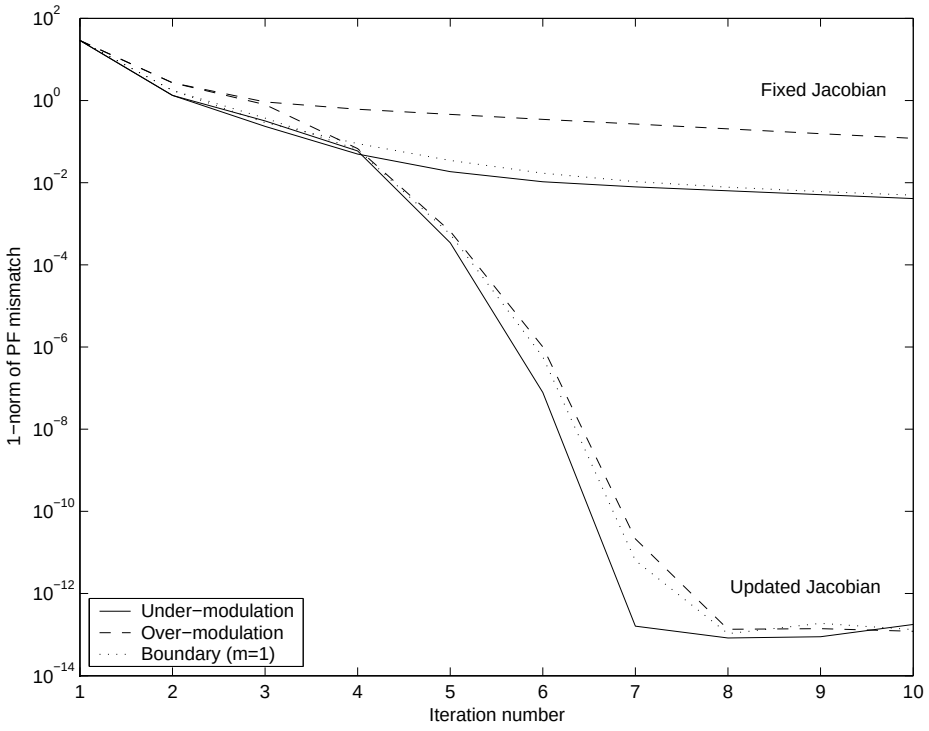

Figure 7.8 Power-flow initialisation convergence in the presence of over-modulation, the fixed Jacobian is included to illustrate increased non-linearity resulting from over-modulation

Jacobian. This linearisation inherently includes the impact of over-modulation, and provides satisfactory convergence (see Figure 7.9). Difficulty is only experienced when the operating point is near the boundary between under- and over-modulation. In this case the first estimate of the harmonic Jacobian will become a less accurate estimate of the linearisation if the operating point shifts into the over-modulation region. While this case still converges with a fixed Jacobian, it does so at approximately half the rate. The reduced convergence points to the discontinuity which exists in the switching spectra at the boundary of over-modulation.

This discontinuity is not typically a problem since the operating point rarely shifts enough to make the initial estimate of the Jacobian inadequate. However, this unlikely phenomena does highlight the limitations of either method of Jacobian derivation. The numerical method is too slow to allow recalculation after each discontinuity, while it is difficult to include this discontinuity using the analytic technique. Hybrid derivation of the Jacobian offers a compromise between these two extremes. The hybrid technique combines analytic derivation of the near linear harmonic transfers with numerical derivation for terms related to the operating point, maintaining generality with a significant gain in efficiency.

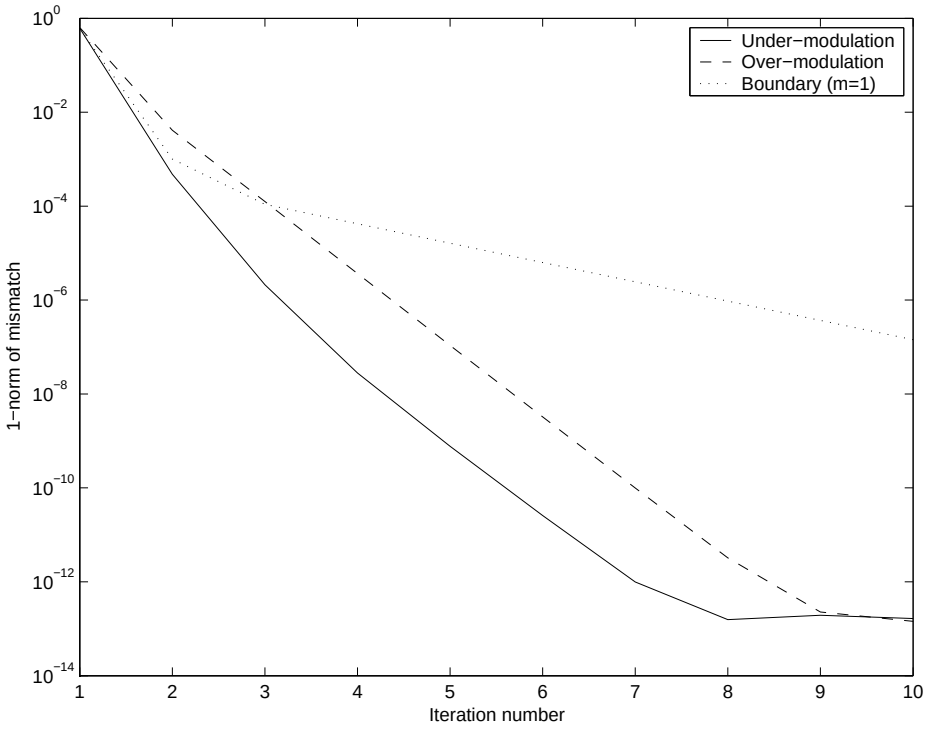

Figure 7.9 Model convergence in the presence of over-modulation

7.4 CONCLUSIONS

Investigation of the models performance in the presence of non-ideal PWM conditions has demonstrated both; the models reliable convergence, and the accuracy of assuming the PWM process is undistorted. While harmonic propagation through the controller and over-modulation both cause a reduction in system linearity, neither cause the proposed model to diverge. Further, the magnitude of any inaccuracy introduced by neglecting harmonic control transfers has been shown to be very small.

Both results are important in terms of maintaining computational efficiency. By neglecting the harmonic control transfers the number of harmonic solution variables can be halved, while the satisfactory convergence with an over-modulated operating point avoids unnecessary (and costly) Jacobian recalculation. Unusual cases which include control systems without harmonic attenuation (e.g. active filters) or operating points near the discontinuous point of $m_{dc} = 1$ do question these assumptions and result in reduced accuracy or convergence. However, the proposed model can (if it is deemed necessary) incorporate these characteristics, but only with a reduction in computational efficiency.

Chapter 8

CONCLUSIONS AND FUTURE WORK

8.1 CONCLUSIONS

The application of PWM switching to modern power system equipment has provided a wealth of control possibilities, it has not however lessened the requirement for accurate harmonic simulation tools. A review of existing harmonic analysis techniques revealed a bias toward older line commutated technologies and basic linearised PWM modelling. Using this review as a basis, a comprehensive Newton solution algorithm, tailored to PWM FACTS devices, has been proposed.

The format adopted allows multiple interconnected PWM converters, configured as FACTS devices, to be comprehensively characterised in the steady-state. To achieve this the proposed formulation incorporates both fundamental and harmonic frequency variables in a single solution set, the size of which is minimised by using a novel dc side harmonic formulation based on current mismatches. Nonetheless, both the power-flow and harmonic solutions reflect the full three-phase ac system and are capable of analyzing non-characteristic harmonic distortion resulting from system imbalance. The full harmonic solution, which is initialised using a three-phase power-flow, has been shown to reliably converge for a range of test systems incorporating transmission line resonance and multiple PWM converters. The results have subsequently been validated against time domain simulation; excellent agreement being obtained at both fundamental and harmonic frequencies.

The modular PWM converter block has been successfully applied to shunt, series and hybrid FACTS devices using a combination of harmonic current and voltage sources. These distorting sources interact across a linear ac system admittance leading to converter interdependence. This interdependence has a considerable impact on ac side quantities but, as a result of the converters phase and frequency dependent impedance, not on the dc side quantities used as the solution variables. This independence provides further justification for the use of dc side quantities as solution variables. Interestingly the Jacobian is not a good visual measure of this independence, but instead is dominated by small but sensitive resonances. DC side harmonic interaction has also been demonstrated for the UPFC. In this case the Jacobian better reflects the linear combination of each individual converters harmonic lattice, making it a useful measure of dc side harmonic interaction.

Both these harmonic interaction mechanisms are, in the absence of control distortion, perfectly linear. As such, an iterative solution is only required because of the non-linear interaction between the harmonic and fundamental frequency solutions. For idealised cases the magnitude of this harmonic induced operating point shift is small, however the presence of system imbalance leads to a noticeable shift. In these non-ideal cases (e.g. small dc side capacitor or large ac current imbalance) the operating point shift should be included in the solution, either with an iterative solution or with a linearised power-flow equivalent (small-signal cases only).

Investigation into the control network confirmed both the model's reliable convergence, and the accuracy of assuming the control system is immune to harmonic distortion. Both results improve the generality of the proposed model; the reliable convergence permits over-modulation to be considered, while the assumption of controller immunity greatly improves computational efficiency. This improved efficiency is particularly relevant to systems containing multiple distributed FACTS devices, where it is necessary to simulate many interconnected converters in order to assess the aggregate impact on the system.

8.2 FUTURE WORK

The research detailed in this thesis could be extended in a number of ways, both in terms of improving the proposed model and using the results to develop more efficient solution techniques.

8.2.1 Iterative model improvements

This thesis has described and validated a novel solution framework for PWM FACTS devices, as such the emphasis has been placed on investigating the characteristics of the proposed model, rather than an optimal implementation. While the MATLAB implementation developed is much faster than an equivalent time domain solution, there is still significant room for improvement. The following refinements are particularly important:

Coding environment The MATLAB environment has proved satisfactory for model evaluation, however it is not a very efficient modelling environment. This restriction becomes apparent when the model needs to handle the large amounts of data associated with system level studies (e.g. massive system matrices and variable vectors). It would therefore be advantageous to migrate the proposed technique into a more efficient coding environment.

Jacobian derivation In terms of efficiency the largest gains would be obtained by developing analytic expressions for the system Jacobian. Of particular importance are the large harmonic transfer blocks. These large blocks could be described relatively easily and provide a significant efficiency gain, without compromising generality. In contrast analytic derivation for the control blocks would not necessarily be as rewarding, since these complex very non-linear blocks only contribute a small proportion of the Jacobian. Thus a hybrid derivation could improve efficiency without compromising generality or modularity.

The extent to which each FACTS device and the surrounding network is modelled could be improved by considering the following aspects:

AC component models For validation purposes the solution technique has been implemented using basic power-flow and harmonic models (with the exception of transmission lines). Ideally the proposed dc mismatch technique should be interfaced with an existing power-flow program with more advanced component models (e.g. delta connections and off-tap transformers). Likewise, the harmonic frequency models and the associated system admittance formulation could easily be refined by incorporating existing direct harmonic analysis models and techniques.

Transformer saturation Saturated transformers, like FACTS devices, behave in a non-linear fashion which can be characterised using harmonic domain techniques. Complex conjugate models of this type already exist and there is no reason why these models could not be transferred to the positive frequency approach and integrated with the proposed solution.

Asynchronous PWM The assumption of an ideal PLL is very important in HDA since it generates both a constant frequency and angle reference. These references lead to a synchronous PWM process. While steady-state harmonic PLL distortion could be incorporated within this synchronous framework (in a similar fashion to PWM distortion), the applicability of harmonic domain techniques to asynchronous situations has yet to be investigated.

8.2.2 Extension to other PWM devices

Other FACTS devices

The modular formulation of the proposed model makes it relatively simple to extend the existing analysis to other FACTS devices which share the PWM converter block. A large range of ac and dc side combinations could be considered using the existing components. For example an Interline Power Flow Control (IPFC) could be modelled by combining two series PWM converters, which share a dc bus. This harmonic representation could then be combined with the appropriate power-flow and control mismatches (many of which could be derived from existing mismatches) to form the full steady-state solution.

The existing solution framework is however limited to hard switched converters which have one dc port and one three-phase ac port. The formulation is not presently capable of modelling the complex dc side configurations associated with multi-level converter systems. These systems have multiple dc ports corresponding to each voltage level and present an interesting extension to existing harmonic analysis techniques.

Active filters

Active harmonic filtering is based on the principle of varying a converters modulation scheme such that anti-phase harmonic currents are injected. These currents in turn mitigate existing distortion. This procedure makes the non-linear modulation process heavily dependent on harmonic variables (via the control loop), something which the proposed model is specifically designed to represent. Given the calculation of the switching angles (and the associated transfer function) is internalised, it would be relatively easy to substitute an appropriate modulation technique without effecting the main dc side harmonic transfers.

PWM motor drives

At lower voltage levels PWM converters are often used as part of motor drive systems. The PWM transfers described within this thesis are directly applicable to this situation. Indeed, the shared dc busbar configuration used to model the UPFC could easily be modified to represent the rectifier and inverter components of a variable speed motor drive system. Likewise this structure is also relevant to wind energy systems utilising either doubly-fed induction or variable frequency synchronous generators.

8.2.3 Large distributed system studies

It is important to view all these improvements in context of PWM devices, rather than HVdc equipment[1]. Whereas it may be appropriate to model large converters in an extremely detailed fashion (e.g. including transformer saturation and thorough control modelling) this is not necessarily important, or indeed feasible, for distributed PWM devices. It is important that the small accuracy improvements available are balanced against the associated loss in efficiency. Further these small accuracy improvements must be viewed in terms of the inherent difficulties involved in modelling the interconnecting transmission network. For most cases uncertainty regarding the harmonic impedance of loads and transmission circuits will question whether minor converter details are the limiting factor for harmonic simulation accuracy.

With this in mind a distinction should be drawn between modelling an isolated FACTS devices in minute detail, and modelling the aggregate effect of many converters. While harmonic domain techniques are capable of undertaking detailed studies, the harmonic domain's real strength remains with system level studies. Studies of this type require elegant solutions which take advantage of appropriate simplifying assumptions. The research described in this thesis has used a detailed PWM converter model to illustrate some of these critical assumptions. Looking forward, further investigation is required into efficient/approximate multi-converter modelling techniques which can be applied to large scale distributed networks.

[1]The vast majority of PWM devices are relatively small and widely distributed, in contrast HVdc systems are large but rare.

Appendix A

PUBLISHED PAPERS

The following papers have either been published or presented in conjunction with the work described within this thesis:

1. C.D. Collins, G.N. Bathurst, N.R. Watson, and A.R. Wood. Harmonic domain approach to STATCOM modelling. *IEE Proc.-Gener. Transm. Distrib.*, 152(2):194-200, Mar. 2005.

2. C. Collins, N. Watson, and A. Wood. UPFC modeling in the harmonic domain. *IEEE Transactions on Power Delivery*, 21(2):933-938, Apr. 2006.

3. C.D. Collins, A.R. Wood, and N.R. Watson. Unbalanced STATCOM analysis in the harmonic domain. *Proceedings of the 11th ICHQP*, 1:232-237, Lake Placid, 2004.

4. C.D. Collins, N.R. Watson, and A.R. Wood. FACTS device interaction in the harmonic domain. *Proceedings of AUPEC05*, 1:243-247, Hobart, 2005.

5. C.D. Collins, N.R. Watson, and A.R. Wood. Unbalanced SSSC Modelling in the Harmonic Domain. *Proceedings of IPEC05*, Singapore, 2005.

Appendix B

TEST SYSTEMS

B.1 STATCOM/SSSC 5-BUSBAR SYSTEM

The main test system, used for validation and interaction studies, incorporates two transmission level FACTS devices and a simplified transmission network. The test system is composed of an SSSC regulating the positive sequence current through two parallel transmission circuits, and a STATCOM providing voltage support to one of the two fixed impedance loads, Figure B.1. Passive filtering is included at the STATCOM busbar using a star connected second order high-pass filter ($f_0 = 500Hz$, $m = 1$) [62]. All loads are balanced and star grounded, the only exception is the transmission circuits which may contain imbalance and phase coupling.

The representation used for the transmission lines (labelled $TL1-3$) varies, but is based on the PSCAD/EMTDC type 3L1. This uses three single conductor ('chukar') circuits and a pair of half inch steel ground wires, as outlined in Figure B.2 and Table B.1. Initially a simplified balanced series equivalent is adopted for validation (Chapter 5), this is replaced by a three-phase frequency dependent equivalent-pi circuit for the ac interaction studies (Chapter 6).

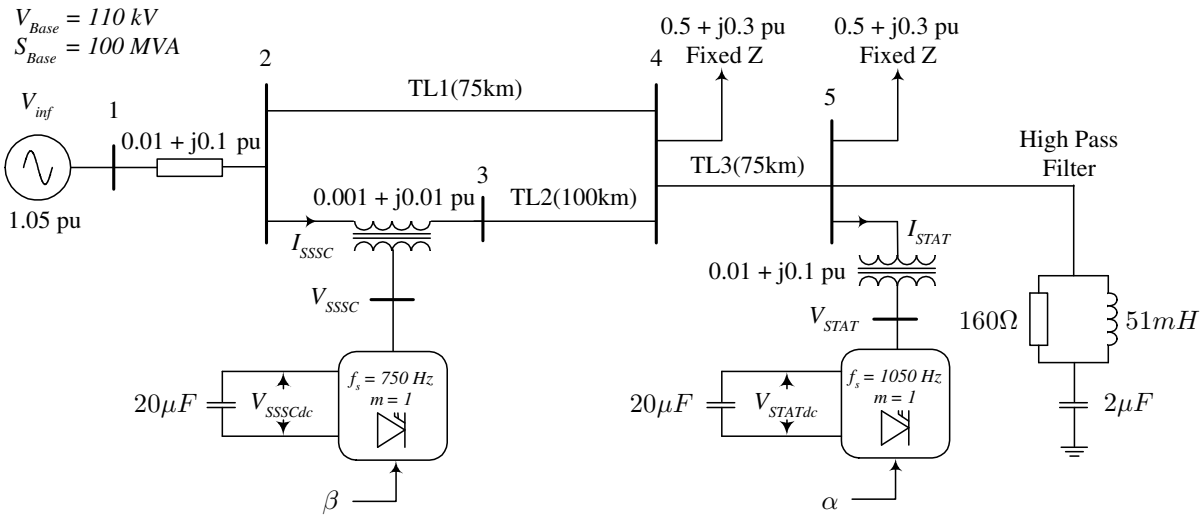

Figure B.1 Single line diagram of the 5-busbar test system

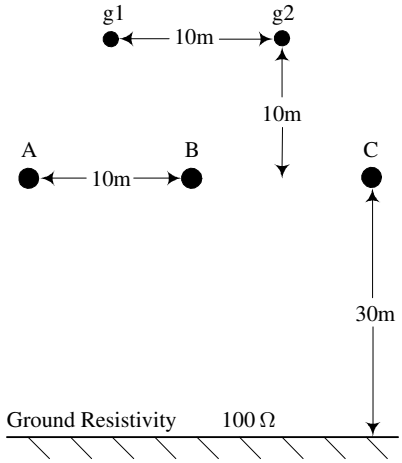

Figure B.2 Single circuit transmission lines used in the 5-busbar test system

Table B.1 Transmission line data

	ACSR Conductors			Ground Wires	
	$r_{outer}(mm)$	$r_{inner}(mm)$	$\rho(\Omega m)$	$r_{outer}(mm)$	$\rho(\Omega m)$
TL1-3	20.3454	5.55	38.7×10^{-9}	5.5245	275×10^{-9}

Table B.2 SSSC + UPFC system operating points

		STATCOM				
Section	V_5^+	I_{STAT}^+		m	α	$V_{dc(0)}$
5.3.1	$0.900\angle -27.43°$	$0.364\angle 55.29°$		1.0	$-27.97°$	0.8795
5.3.2	$0.900\angle -26.80°$	$0.356\angle 57.10°$		1.0	$-27.30°$	0.8854
6.2	$0.900\angle -17.56°$	$0.131\angle 54.94°$		1.0	$-17.88°$	0.8597
		SSSC				
	V_2^+	V_3^+	I_{SSSC}^+	m	α	$V_{dc(0)}$
5.3.1	$1.000\angle -4.856°$	$1.056\angle 2.988°$	$0.600\angle -23.23°$	1.0	66.74°	0.1498
5.3.2	$1.000\angle -4.807°$	$1.055\angle 0.968°$	$0.600\angle -22.75°$	1.0	67.82°	0.1551
6.2	$0.995\angle -4.706°$	$1.034\angle 0.864°$	$0.600\angle -26.36°$	1.0	65.95°	0.1056

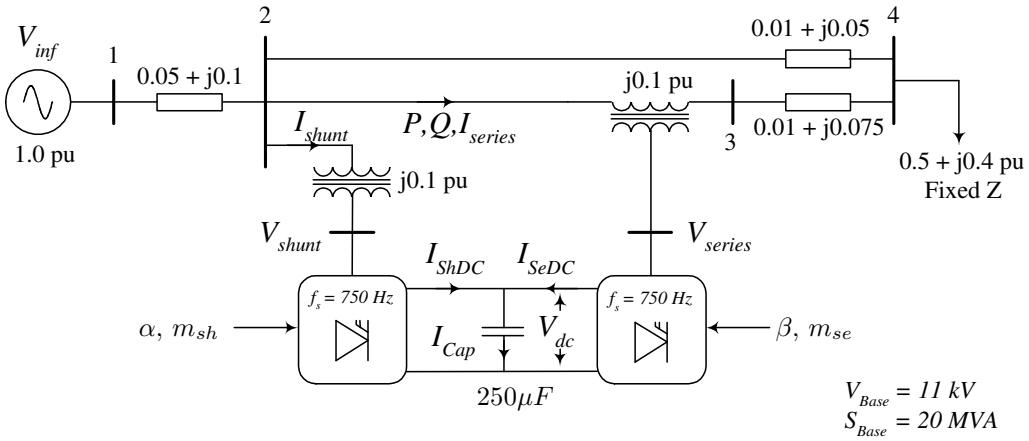

Figure B.3 Single line diagram of the UPFC test system

In both cases the STATCOM and SSSC use elementary single variable phase angle control to regulate the fundamental frequency positive sequence voltage ($V_5^+ = 0.9pu$) and current ($I_{SSSC}^+ = 0.6pu$) respectively (see Section 3.4.1). Both controllers are assumed to be immune to distorted electrical quantities. The resultant operating point varies depending on the specific version of the test system used, see Table B.2.

B.2 DISTRIBUTION LEVEL UPFC SYSTEM

A similar test system is used to illustrate dc side harmonic interaction. It is based around an unfiltered distribution level UPFC which regulates the sending end voltage ($V_2 = 0.95pu$), the dc busbar voltage ($V_{dc} = 1.0909pu$) and the transmitted power ($P + jQ = 0.25 + j0.2pu$). As illustrated in Figure B.3.

The control system is composed of two blocks, the shunt component regulating the ac and dc busbar voltages via two separate PI loops, and the series component which regulates the real and reactive power through the larger transmission impedance using two coupled PI loops. The series block is based on the controller used by Dong [61], it is included in Figure B.4. Both blocks are assumed to be immune to harmonic distortion. The resultant operating points are included in Table B.3.

B.3 SSSC SYSTEM: WITH DISTORTED CONTROL FEEDBACK

The final test system, used to investigate the impact harmonic distortion has on the PWM process, is based on the 5-busbar test system (see Appendix B.1). The only significant changes are the removal of the STATCOM at busbar 5 and the addition of a more detailed control representation. The frequency response of this single variable PI control loop is defined by the variables included in Table B.4.

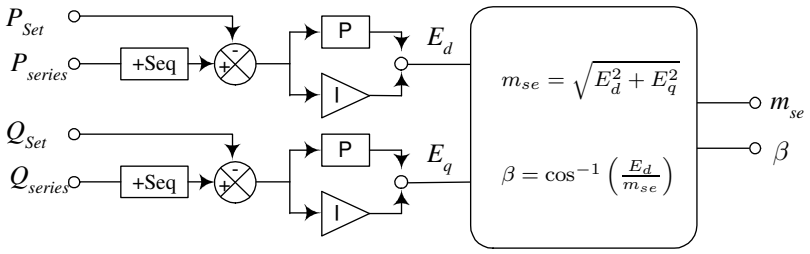

Figure B.4 Series converter control scheme for the UPFC

Table B.3 UPFC system operating points

	Electrical quantities				
	V_2^+	V_3^+	I_{sh}^+	I_{se}^+	
Validation	$0.950\angle -1.988°$	$0.957\angle -1.432°$	$0.124\angle 84.127°$	$0.334\angle -40.08°$	
Over-modulation	$0.950\angle -1.960°$	$0.957\angle -1.404°$	$0.122\angle 85.772°$	$0.334\angle -40.07°$	
$m_{sh} = 1$	$0.950\angle -1.965°$	$0.957\angle -1.415°$	$0.122\angle 85.336°$	$0.334\angle -40.07°$	
	Control quantities				
	α	m_{sh}	β	m_{se}	$V_{dc(0)}$
Validation	$-2.034°$	0.8275	$49.761°$	0.0392	1.0909
Over-modulation	$-1.988°$	1.1832	$49.790°$	0.0517	0.8250
$m_{sh} = 1$	$-2.000°$	1.0000	$49.784°$	0.0473	0.9019

Table B.4 SSSC control loop variables

Current transducer gain	1	Current transducer time constant	$0.001s$
Notch filter frequency	$100Hz$	Notch filter gain	1
Notch filter damping factor	0.16		
PI Loop proportional gain	1	PI Loop time constant	$0.01s$

Appendix C

TRANSMISSION LINE MODELLING

The phase to phase coupling, imbalance and harmonic resonances present in transmission systems play a critical role in the propagation of harmonic distortion. As such it is important that these transmission line phenomena are included in the harmonic solution. The range of modelling approaches available and the difficulties involved in validating these models makes including these phenomena anything but trivial. To a large extent this thesis avoids these problems by adopting the PSCAD/EMTDC frequency dependent line model (basically a distributed RLC travelling wave model) and assuming it to be correct. This is ideal for validating the converter models performance, but does not illustrate the difficulties associated with transmission line modelling at harmonic frequencies. To illustrate the sensitivity of the converter model to this issue an alternate transmission line modelling approach is included for comparison.

C.1 ALTERNATIVE APPROACH: LINE GEOMETRY AND CARSON'S CORRECTIONS

This common approach is based around using Carson's equations and correction factors to calculate the shunt admittance (Y) and series impedance (Z) matrices. These matrices are formed in terms of each individual conductor, which are subsequently reduced by bundling conductors together to form phases, reducing the size of the matrix. This process also removes the earth wires.

The shunt admittance (Y) is described by an n by n matrix (where n is the number of conductors) formed from Maxwell's potential coefficient matrix (P), which relates the line to ground voltage with the charge on each conductor. This is calculated from the geometry of the line,

$$P_{ii} = 18 \times 10^6 \times \ln\left(\frac{2h_i}{r_{ext_i}}\right) \tag{C.1}$$

$$P_{ik} = 18 \times 10^6 \times \ln\left(\frac{D_{ik}}{d_{ik}}\right) \tag{C.2}$$

where it is assumed that the conductor radius (r_{ext_i}) is much smaller than its vertical height (h_i) or inter-conductor spacing (d_{ik}). D_{ik} refers to the distance between conductor i and the image of conductor k. The capacitance between each wire and the ground, and the mutual capacitance between any two conductors are described by the inverse of P, leading to Y being described (per

unit length) by:

$$[Y] = j2\pi f \times [P]^{-1} \tag{C.3}$$

Likewise the series impedance of the line is described by an n by n matrix (Z) which contains the self and mutual inductances for each conductor. The self inductance terms (on the diagonal) describe the series impedance per unit length of each conductor, using the ground as a return path. The mutual inductance terms being the inductance between any two conductors. This leads to the series impedance (Z) being defined per unit length by:

$$Z_{ii} = (R_{ii} + \Delta R_{ii}) + j\left(2\omega \times 10^{-4} \times \ln\left(\frac{2h_i}{GMR_i}\right) + \Delta X_{ii}\right) \tag{C.4}$$

$$Z_{ik} = Z_{ki} = \Delta R_{ik} + j\left(2\omega \times 10^{-4} \times \ln\left(\frac{D_{ik}}{d_{ik}}\right) + \Delta X_{ik}\right) \tag{C.5}$$

The correction coefficients (ΔR & ΔX) are described using the infinite integral proposed by Carson [58]. GMR_i refers to the geometric mean radius of each conductor, while R_{ii} refers to the ac series resistance of each cable (including skin effect).

After reduction the Y and Z matrices are applied to a long line corrected equivalent-pi circuit. The multi-phase nature of Y and Z complicates this calculation, requiring the use of modal analysis to diagonalise both matrices. This process is well described by Acha [63].

C.2 MODEL COMPARISON

The two models produce very similar results, take for example the a-phase self admittance and impedance terms for the 100km line (Figure C.1). The only significant difference is the slight variation in the resonant frequency. However, when this continuous data is sampled at each harmonic frequency (the series impedance is also inverted for inclusion in the harmonic admittance matrix) these small differences get exaggerated (Figure C.2). The result is significant discrepancies between the two models at frequencies near resonance. The magnitude of the error introduced by this discrepancy being dependant on the amount of harmonic filtering present in the test system (see Section 6.2.3).

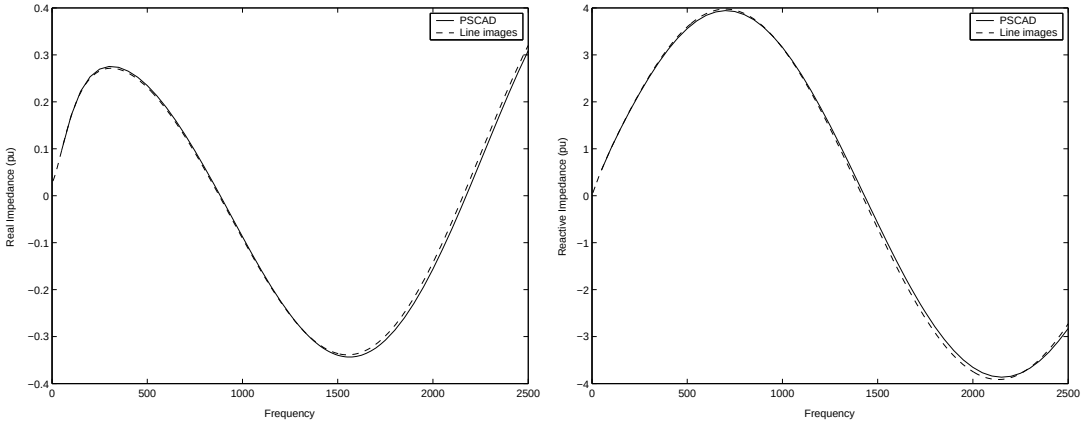

(a) Series Z11 (real component)

(b) Series Z11 (imaginary component)

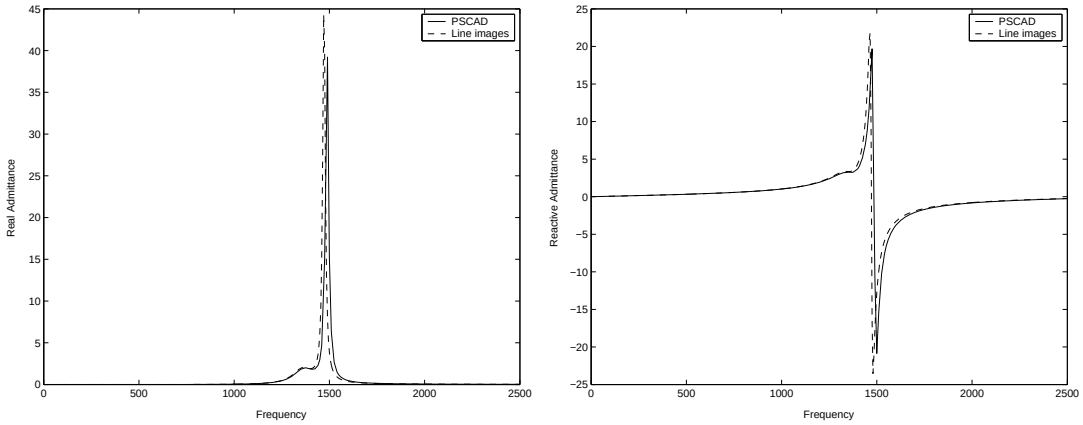

(c) Shunt Y11 (real component)

(d) Shunt Y11 (imaginary component)

Figure C.1 Continuous frequency comparison of the two transmission line representations used

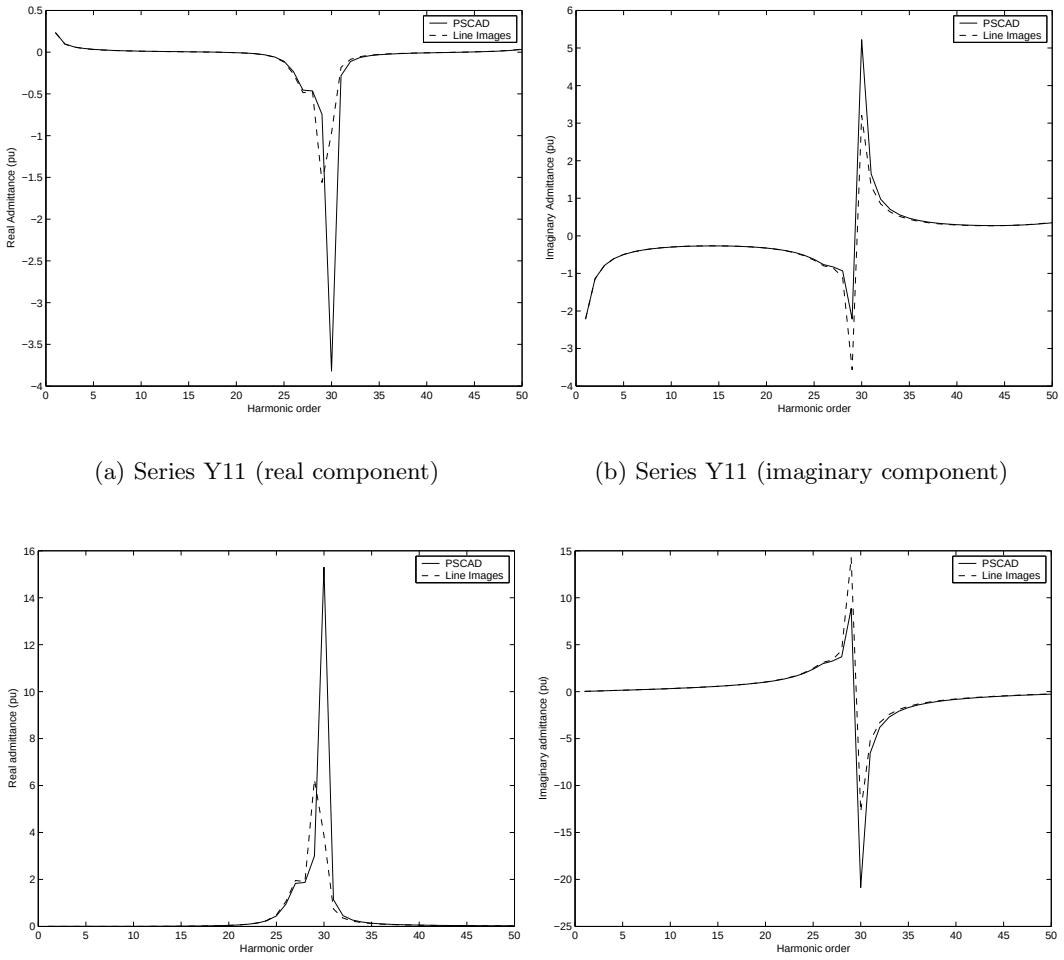

(a) Series Y11 (real component)

(b) Series Y11 (imaginary component)

(c) Shunt Y11 (real component)

(d) Shunt Y11 (imaginary component)

Figure C.2 Harmonic frequency comparison of the two transmission line representations used

REFERENCES

[1] E.W. Kimbark. *Direct Current Transmission*. Wiley Interscience, New York, 1971.

[2] J. Arrillaga, C.P. Arnold, and B.J. Harker. *Computer Modelling of Elecrical Power Systems*. John Wiley and Sons, 1983.

[3] N. Mohan, T.M. Undeland, and W.P. Robbins. *Power Electronics:Converters, Applications, and Design*. John Wiley and Sons, 2nd ed., 1995.

[4] H.W. Dommel. Digital computer simulation of electromagnetic transients in single and mutliphase networks. *IEEE Transactions on Power Apparatus and Systems*, 88(4):388-399, Apr. 1969.

[5] D. Woodford, A. Gole, and R. Menzies. Digital simulation of dc links and ac machines. *IEEE Transactions on Power Apparatus and Systems*, 102(6):1616-1623, Jun. 1983.

[6] T.J. Aprille and T.N. Trick. Steady-state analysis of non-linear circuits with periodic inputs. *Proceedings of the IEEE*, 60(1):108-114, Jan. 1972.

[7] Manitoba HVdc Research Centre. *PSCAD/EMTDC V3 users manual*. Manitoba HVdc Research Centre, Winnipeg, Canada, 1988.

[8] N. R. Watson. *Frequency dependent ac system equivalents for harmonic studies and transient converter simulation*. PhD thesis, Department of Electrical and Electronic Engineering, University of Canterbury, Christchurch, New Zealand, 1987.

[9] R. Carbone, D. Menniti, R.E. Morrison, and A. Testa. Harmonic and interharmonic distortion modeling in multiconverter systems. *IEEE Transactions on Power Delivery*, 10(3):1685-1692, Jul. 1995.

[10] B.C. Smith. *A harmonic domain model for the interaction of the HVdc converter with ac and dc systems*. PhD thesis, Department of Electrical and Electronic Engineering, University of Canterbury, Christchurch, New Zealand, 1996.

[11] E. Acha. *Modelling of power system transformers in the complex conjugate harmonic space*. PhD thesis, Department of Electrical and Electronic Engineering, University of Canterbury, Christchurch, New Zealand, 1988.

[12] A. Semlyen, E. Acha, and J. Arrillaga. Harmonic norton equivalent for the magnetising branch of a transformer. *IEE Proceedings*, Part C, 143(2):162-169, Mar. 1987.

[13] W.H. Press, S.A. Teukolsky, W.T. Vetterling, and B.P. Flannery. *Numerical Recipies in FORTRAN*. Cambridge University Press, 2nd ed., 1992.

[14] E.V. Larsen, D.H. Baker, and J.C. McIver. Low order harmonic interaction on ac/dc systems. *IEEE Transactions on Power Delivery*, 4(1):493-501, Jan. 1989.

[15] L. Hu and R. Yacamini. Harmonic transfer through convertors and hvdc links. *IEEE Transactions on Power Electronics*, 7(3):514-525, Jul. 1992.

[16] D.L. Dickmander, S.Y. Lee, G.L. Desilets, and M. Granger. AC/DC harmonic interactions in the presence of GIC for the Quebec-New England phase II HVdc transmission. *IEEE Transactions on Power Delivery*, 9(1):68-78, Jan. 1994.

[17] A.R. Wood. *An analysis of non-ideal HVdc converter behaviour in the frequency domain, and a new control proposal*. PhD thesis, Department of Electrical and Electronic Engineering, University of Canterbury, Christchurch, New Zealand, 1993.

[18] D.J. Hume. *Harmonic and interharmonic cross modulation in HVDC links*. PhD thesis, Department of Electrical and Computer Engineering, University of Canterbury, Christchurch, New Zealand, 2002.

[19] M. Madrigal and E. Acha. Modelling of custom power equipment using harmonic domain techniques. *Proceedings of the 9th ICHQP*, 1:264-269, 2000.

[20] C. Saniter, A.R. Wood, R. Hanitsch, and D. Schulz. Modelling the effects of AC system impedance unbalance on PWM converters using frequency coupling matrices. *Proceedings Power Tech*, IEEE Bologna, vol. 2, Jun. 2003.

[21] J. Reeve and J.A. Baron. Harmonic interaction between hvdc converters and ac power systems. *IEEE Transactions on Power Apparatus and Systems*, 90(6)2785-2793, 1971.

[22] R. Yacamini and J.C. de Oliveira. Harmonics in multiple converter systems: a generalised approach. *IEE Proceedings Pt. B*, 127:96-106, Mar. 1980.

[23] J.F. Eggleston. *Harmonic modelling of transmission systems containing synchronus machines and static converters*. PhD thesis, Department of Electrical and Electronic Engineering, University of Canterbury, Christchurch, New Zealand, 1985.

[24] C.D. Callaghan. *Three phase integrated load and harmonic flows*. PhD thesis, Department of Electrical and Electronic Engineering, University of Canterbury, Christchurch, New Zealand, 1989.

[25] R. Carbone, M. Fantauzzi, F. Gagliardi, and A. Testa. Some considerations on the iterative harmonic analysis convergence. *Proceedings of the 5th ICHQP*, pp. 49-55, Sep. 1992.

[26] G. Carpinelli, F. Gagliardi, M. Russo, and D. Villacci. Generalised converter models for iterative harmonic analysis in power systems. *IEE Proceedings on Generation, Transmission and Distribution*, 141(5):445-451, Sep. 1994.

[27] G.T. Heydt and D. Xia. Harmonic power flow studies parts 1 and 2. *IEEE Transactions on Power Apparatus and Systems*, 101(6):1257-1265, Jun. 1982.

[28] J.J. Rico, E. Acha, and T.J.E Miller. Harmonic domain modelling of three-phase thyristor-controlled reactors by means of switching vectors and discrete convolutions. *IEEE Transactions on Power Delivery*, 11(3):1678-1684, Jul. 1996.

[29] L.T.G. Lima, A. Semlyen, and M.R. Iravani. Harmonic domain periodic steady state modeling of power electronics apparatus: SVC and TCSC. *IEEE Transactions on Power Delivery*, 18(3):960-967, Jul. 2003.

[30] A. Medina and J. Arrillaga. Analysis of transformer-generator interaction in the harmonic domain. *IEE Proceedings on Generation, Transmission and Distribution*, 141(1):38-46, May 1994.

[31] J. Arrillaga, A. Medina, M.L.V. Lisboa, M.A. Cavia, and P. Sanchez. The harmonic domain. A frame of reference for power system harmonic analysis. *IEEE Transactions on Power Systems*, 10(1):433-440, Feb. 1995.

[32] M.L.V. Lisboa. *Three-phase three-limb transformer models in the Harmonic Domain*. PhD thesis, Department of Electrical and Electronic Engineering, University of Canterbury, Christchurch, New Zealand, 1996.

[33] M. Valcarcel and J.G. Mayordomo. Harmonic power flow for unbalanced systems. *IEEE Transactions on Power Delivery*, 8(4):2052-2059, Oct. 1993.

[34] G.N. Bathurst. *A Newton solution for the harmonic analysis of power systems with multiple non-linear devices*. PhD thesis, Department of Electrical and Electronic Engineering, University of Canterbury, Christchurch, New Zealand, 1999.

[35] N.Q. Dinh, J. Arrillaga, and B.C. Smith. A steady-state model of direct connected generator-HVdc converter units in the harmonic domain. *IEE Proceedings on Generation, Transmission and Distribution*, 145(5):559-565, Oct. 1998.

[36] S.R. Sanders, M.J. Noworolski, X.Z. Liu, and G.C. Verghese. Generalized Averaging Method for Power Conversion Circuits. *IEEE Transactions on Power Electronics*, 6(2):251-259, Apr. 1991.

[37] A.M. Stankovic, P. Mattavelli, V. Caliskan, and G.C. Verghese. Modeling and Analysis of FACTS Devices with Dynamic Phasors. *IEEE Power Engineering Society Winter Meeting*, 2:1440-1446, Jan. 2000.

[38] J.J. Rico, M. Madrigal, and E. Acha. Dynamic harmonic evolution using the extended harmonic domain. IEEE Transactions on Power Delivery, 18(2):587-594, Arp. 2003.

[39] N.G. Hingorani. High Power Electronics and flexible AC Transmission System. *IEEE Power Engineering Review*, pp. 3-4, Jul. 1988.

[40] N.G. Hingorani. Flexible AC transmission. *IEEE Spectrum*, 30:40-45, 1993.

[41] N.G. Hingorani, and L. Gyugyi. *Understanding FACTS Concepts and Technology of Flexible AC Transmission Systems*. IEEE Press, New York, 1999.

[42] P. Petitclair, Y. Besanger, S. Bacha, and N. Hadjsaid. Facts modelling and control: Applications to the insertion of a STATCOM on power system. *Proceedings of the 32nd IAS Annual Meeting*, Part 3,Oct. 1997.

[43] B.M.K. Han, G.G. Karady, J.K. Park, and S.I. Moon.Interaction analysis model for transmission static compensator with EMTP. *IEEE Transactions on Power Delivery*, 13(4):1297-1302, Oct. 1998.

[44] M.A. Madrigal, O. Anaya, E. Acha, J.G. Mayordomo, and R. Asensi. Single-phase PWM converters array for three-phase reactive power compensation. I. Time domain studies. *Proceedings of the 9th ICHQP*, 2:541-547, 2000.

[45] C.K.L. Sao, P.W. Lenh, M.R. Iravani, and J.A. Martinez. A benchmark system for digital time-domain simulation of a pulse-width-modulated D-STATCOM. *IEEE Transactions on Power Delivery*, 17(4):1113-1120, Oct. 2002.

[46] O. Anaya-Lara and E. Acha. Modeling and analysis of custom power systems by PSCAD/EMTDC. *IEEE Transactions on Power Delivery*, 17(1):266-272, Jan. 2002.

[47] W. Freitas and A. Morelato. A generalised current injection approach for modelling of facts in power system dynamic simulation. Presented at *7th International Conference on AC-DC Power Transmission*, London, 2001.

[48] F.W. Huang, B.S. Rigby, and R.G. Harley. A static synchronous series compensator model for EMTDC. Presented at *6th IEEE Africon Conference 2002*, 2002.

[49] H.F. Wang. Modelling multiple FACTS devices into multi-machine power systems and applications. *International Journal of Electrical Power & Energy Systems*, 25:227-237, 2003.

[50] A.R. Wood, and C.M. Osauskas. A Linear Frequency-Domain Model of a STATCOM. *IEEE Transactions on Power Delivery*, 19(3):1410-1418, Jul. 2004.

[51] C.Saniter, R. Hanitsch, C. Osauskas, and H. Laird. A small signal frequency domain model of a controlled PWM converter. *Proceedings IEEE Postgraduate Power Conference*, Budapest, 2002.

[52] G.N. Bathurst, N.R. Watson, and J. Arrillaga. Adaptive frequency-selection method for a Newton solution of harmonics and interharmonics. *IEE Proceedings on Generation, Transmission and Distribution*, 147(2):126-130, Mar. 2000.

[53] B.C. Smith, N.R. Watson, A.R. Wood, and J. Arrillaga. Steady state model of the AC/DC converter in the harmonic domain. *IEE Proceedings on Generation, Transmission and Distribution*, 142(2):109-118, Mar. 1995.

[54] Z. Yang, C.Shen, M.L. Crow, and L. Zhang. An improved StatCom model for power flow analysis. *IEEE Power Engineering Society Summer Meeting*, 2:1121-1126, Jul. 2000.

[55] W. Freitas, and A. Morelato. A generalised current injection approach for modelling of FACTS in power system dynamic simulation. *Seventh International Conference on AC-DC Power Transmission*, pp. 175-180, Nov. 2001.

[56] T.J. Densem. *Three phase power system harmonic penetration.* PhD thesis, Department of Electrical and Electronic Engineering, University of Canterbury, Christchurch, New Zealand, 1983.

[57] J. Arrillaga, E. Acha, T.J. Densem, and P.S. Bodger. Ineffectiveness of Transmission Line Transpositions at Harmonic Frequencies. *IEE Proceedings*, Part C, 133:99-104, Mar. 1986.

[58] J.R. Carson. Wave propagation in overhead wires with ground return. *Bell System Technical Journal*, 5:539-54, 1926.

[59] C.A. Canizares. Power flow and transient stability models of FACTS controllers for voltage and angle stability studies. *IEEE Power Engineering Society Winter Meeting*, 2:1447-1454, 2000.

[60] D.A. Woodford, A.M. Gole, and R.W. Menzies. Validation of digital simulation of hvdc transients by field tests. *IEE conf. publ. on AC and DC power transmission*, (255):377-381, 1985

[61] L. Dong, M.L. Crow, Z. Yang, C. Shen, L. Zhang, and S. Atcitty. A reconfigurable FACTS system for university laboratories. *IEEE Transactions on Power Systems*, 19:120-128, Feb. 2004.

[62] J. Arrillaga, D.A. Bradley, and P.S. Bodger. *Power System Harmonics.* John Wiley and Sons, 1nd ed., 1985.

[63] E. Acha, C. Fuerte-Esquivel, H. Ambriz-Perez, and C. Angeles-Camacho. *FACTS Modelling and Simulation in Power Networks.* John Wiley and Sons, 1st ed., 2004.